

**Biochemical analysis of the N28F mutant of human class Pi
glutathione S-transferase.**

Chien Yu Chen

**A dissertation submitted in fulfilment of the requirements for the degree of
Master of Science at the University of the Witwatersrand.**

**Johannesburg
October 1996**

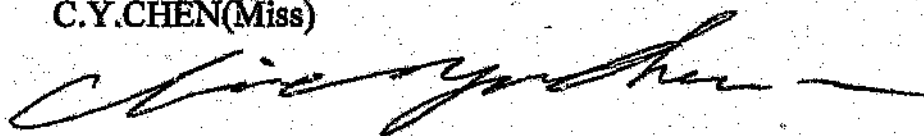
**Biochemical analysis of the W28F mutant of
human class Pi glutathione S-transferase**

Chien Yu Chen

DECLARATION

I declare that this dissertation is my own, unaided work. It is being submitted for the degree of Master of Science in the University of Witwatersrand, Johannesburg. It has not been submitted before for any degree or examination in any other University.

C.Y.CHEN(Miss)

A handwritten signature in cursive script, appearing to read 'C.Y. Chen', with a long horizontal flourish extending to the right.

...day of ... 1996

Abstract

Glutathione S-transferase (GST) class Pi has two tryptophan residues which are conserved within domain one. Trp38 plays a functional role in sequestering glutathione at the active site, whereas Trp28 plays a structural role. The effects of the sterically-conservative substitution of Trp28 to Phe were investigated. When the W28F mutant was compared with the wild-type enzyme, mutation of Trp28 to Phe was not well tolerated and resulted in a dimeric protein with impaired catalytic function and conformational stability. The quality of purified enzyme was determined by SDS-PAGE, size-exclusion HPLC, IEF and western blot. The enzyme's specific enzyme activity and catalytic efficiency were halved. Interaction of glutathione with its binding site (the G-site) did not seem to be affected, as suggested by the unchanged K_m for glutathione and unchanged I_{50} values for the competitive inhibitors, the S-hexylglutathione and glutathione sulphonate. The topography of hydrophobic binding site (the H-site) for the electrophilic substrate (1-chloro-2,4-dinitrobenzene) was affected, as reflected in the two-fold increase in the substrate's K_m value. Thermal inactivation and equilibrium unfolding experiments showed the Trp28 → Phe mutant to be thermodynamically less stable than the wild-type enzyme. Equilibrium unfolding and urea-gradient gel electrophoresis experiments suggested that the folding/unfolding of human GSTP1-1 is a two-state process involving folded native dimer and unfolded monomer. Its stability was also shown to be dependent on protein concentration. A mutant structure was constructed by homology modelling and the relationship between Phe28 and its neighbouring environment was inspected. These results suggest an essential structural role for Trp28 in maintaining a functional H-site and a stable class Pi enzyme structure. Its indole side chain is involved in the network of polar interactions buried in the protein matrix below the H-site.

DEDICATION

I would like to dedicate this to my parents and my sister, Pei-Yu.

ACKNOWLEDGEMENTS

I would like to thank the following people: Prof. H.W. Dirr, my supervisor for his constant encouragement and advise; J. Erhardt, W. Kaplan and L. Wallace for their valuable academic suggestions and discussions; the members of Department of Biochemistry, University of Witwatersrand.

<u>TABLE OF CONTENTS</u>	<u>Page</u>
DECLARATION	i
ABSTRACT	ii
DEDICATION	iii
ACKNOWLEDGEMENTS	iv
LIST OF FIGURES	viii
LIST OF TABLES	x
LIST OF ABBREVIATIONS	xi
CHAPTER ONE - INTRODUCTION	
1.1 Historical Perspective	1
1.2 Families of GST isoenzymes	1
1.3 Nomenclature and classification	3
1.4 Functions of GSTs	7
1.4.1 GST's involvement in the detoxification pathway	7
1.4.2 The ATP dependent glutathione conjugate pump	10
1.4.3 Degradation of glutathione S-conjugates	10
1.4.4 Binding and intracellular transport of non-substrate ligands	12
1.5 Structure and conformational stability of GSTs	14
1.5.1 Structural comparisons of GST family	14
1.6 Catalysis	17
1.6.1 Basis of catalysis by GSTs	17
1.6.2 Recognition of GSH at G-site	22
1.6.3 Substrate specificity of GSTs	23

1.7	GST and its association with health and diseases	24
1.8	Application of GSTs	27
1.8.1	Environmental bioremediation	27
1.8.2	Gene therapy involving GSTs	28
1.9	Structural aspects of class Pi GSTs	29
1.9.1	General description of class Pi GSTs	29
1.9.2	Domain interface	34
1.9.3	Association of subunits	36
1.9.4	Active site	38
1.9.4.1	The glutathione-binding site	39
1.9.4.2	The binding site for hydrophobic substrates	43
1.10	Site-directed mutagenesis of class Pi GSTs	45
1.11	Tryptophan residues	45
1.12	Conformational stability of class Pi GSTs	49
1.13	Objectives	49

CHAPTER TWO - MATERIAL AND EXPERIMENTAL METHODS

2.1	Materials	50
2.2	Over-expression and purification of recombinant protein	50
2.2.1	Culture growth and over-expression	50
2.2.2	S-hexylglutathione affinity chromatography	51
2.3	Protein concentration determination	52
2.4	Homogeneity determinations	53
2.4.1	SDS-PAGE	53
2.4.2	Isoelectric focusing	53
2.4.3	Size-exclusion HPLC	55
2.4.4	Western blot	55
2.5	Steady-state kinetic studies	58
2.5.1	Routine enzyme assay	58
2.5.2	V_{max} and K_m	59
2.5.3	Catalytic efficiency	59
2.5.4	Inhibition by glutathione analogues	60

2.6	Thermal-inactivation studies	61
2.7	Steady-state fluorescence spectroscopy	61
2.7.1	Steady-state fluorescence emission	64
2.7.2	Quantum yields	64
2.7.3	Acrylamide quenching	65
2.8	Solvent-induced unfolding equilibrium	67
2.8.1	Urea-induced unfolding equilibrium	68
2.8.2	Graphical analysis of denaturation curves	68
2.9	Urea-gradient gel electrophoresis	70
2.10	Homology modelling	74

CHAPTER THREE - RESULTS AND DISCUSSION

3.1	Purification and yield	77
3.2	Homogeneity	78
3.2.1	SDS-PAGE	78
3.2.2	Isoelectric focusing	78
3.2.3	Size-exclusion HPLC	81
3.2.4	Western blot	81
3.3	Steady-state enzyme kinetics	84
3.4	Heat-inactivation studies	89
3.5	Fluorescence spectroscopy	92
3.5.1	Fluorescence emission spectra	92
3.5.2	Quantum yield	92
3.5.3	Acrylamide quenching studies	94
3.6	Urea-induced equilibrium unfolding studies	96
3.7	Urea-gradient gel electrophoresis	106
3.8	Structural basis for destabilization	108
3.9	Homology modelling	112
3.10	Conclusions	117

CHAPTER FOUR - REFERENCES	118
----------------------------------	------------

LIST OF FIGURES

	<u>Pages</u>
Fig.1 The proposed evolutionary scheme for GSTs	4
Fig.2 The three-phase pathway of detoxification of xenobiotics	9
Fig.3 The degradation pathway of S-glutathione-conjugates	11
Fig.4 The conjugation of CDNB with GSH by GSTs	19
Fig.5 Sequence alignment of species of class Pi GSTs	31
Fig.6 Dimeric structure of hGSTP1-1 viewed down the 2-fold axis	32
Fig.7 Subunit structure of hGSTP1-1 viewed perpendicular to the 2-fold axis	35
Fig.8 Dimeric structure of hGSTP1-1 viewed perpendicular to the 2-fold axis	37
Fig.9 Western blot apparatus	57
Fig.10 Photophysical events of the emission of fluorescence of fluorophores	62
Fig.11 Apparatus for preparing urea-gradient gels	73
Fig.12 SDS-PAGE of wild-type and W28F mutant enzymes	79
Fig.13 IEF of wild-type and W28F mutant enzymes	80
Fig.14 Size-exclusion of wild-type and W28F mutant enzymes	82
Fig.15 Western blot of wild-type enzyme	83
Fig.16 Inhibition of enzyme activity by S-hexylglutathione	87
Fig.17 Inhibition of enzyme activity by glutathione sulphonate	88
Fig.18 Thermal inactivation of wild-type and W28F mutant enzymes	90
Fig.19 Time-dependence of thermal inactivation of wild-type and W28F mutant enzymes	91
Fig.20 Corrected fluorescence emission spectra of native wild-type and W28F mutant enzymes	93
Fig.21 Stern-Volmer plot for acrylamide quenching of wild-type and W28F mutant enzymes	95

Fig.22	Raw data of the concentration-dependence experiment of wild-type hGSTP1-1	99
Fig.23	Concentration-dependence of wild-type hGSTP1-1	100
Fig.24	Urea-unfolding of wild-type and W28F mutant enzymes	104
Fig.25	ΔG as a function of urea concentration	105
Fig.26	Urea-gradient gel electrophoretograms of native and denatured wild-type hGSTP1-1	107
Fig.27	Subunit structure of the constructed W28F mutant model by homology modelling	114
Fig.28	Stereoview of the local environment of Trp28 of wild-type enzyme and Phe28 of W28F mutant enzyme	115
Fig.29	Local environment of Trp28 of wild-type enzyme and Phe28 of W28F mutant enzyme	116

LIST OF TABLES

	<u>Pages</u>
Table.1 Research development of GSTs	2
Table.2 Example of nomenclature of GSTs	6
Table.3 Structure of GSH and the amino acids involved in the specific polar interaction with GSH at the G-site of GST	42
Table.4 A summary of site-directed mutagenesis on class Pi GST	47
Table.5 Kinetic parameters of wild-type and W28F mutant GSTP1-1	86

LIST OF ABBREVIATIONS

CDNB	1-chloro-2,4-dinitrobenzene
GSH	glutathione
GST	glutathione S-transferase
G-site	glutathione binding site
H-site	electrophilic substrate binding site
IPTG	isopropyl-β-D-thiogalactopyranoside
kDa	kilodalton
Kd	dissociation constant
M	molar
Mr	relative molecular mass
O.D.₆₀₀	optical density at 600 nm
pI	isoelectric point
r.p.m.	rotations per minute
TEMED	N,N,N',N'-tetramethylethylenediamine
TNB	1,3,5-trinitrobenzene
vs	versus
3D	three-dimensional

The IUPAC-IUBMB three letter codes for amino acid are used.

Chapter 1

Introduction

1.1 Historical perspective

Glutathione S-transferases (EC2.5.1.18) (GST) were initially identified in 1961 as a liver enzyme that catalyses the conjugation of 1-chloro-2,4-dinitro-benzene (CDNB) with reduced glutathione (Booth et al., 1961; Coombs and Stakelum., 1961). GSTs are a family of multi-functional proteins that function both as eminent enzymes of detoxification and intracellular binding proteins. These exceptional functions are of interest to investigators in biochemical, toxicological, pharmacological, cell biological and physiological fields and interests in the GST superfamily continue to proliferate. The chronological order of the major advances in GST research are presented in Table.1.

1.2 Families of GST isoenzymes

GSTs exist in multiple forms and cytosolic GSTs can be grouped into five evolutionary classes, designated Alpha, Mu, Pi, Theta and Sigma (Mannervik et al., 1985; Mannervik and Danielson., 1988; Meyer et al., 1991; Hiratsuka et al., 1990; Buetler and Eaton., 1992; Ji et al., 1995). A new class of GST, Sigma, has recently been isolated from squid digestive gland (Ji et al., 1995). The microsomal glutathione S-transferase is a membrane-bound member of an important detoxification system consisting of a number of enzymes that catalyze the conjugation of glutathione to a wide range of electrophilic compounds (Mannervik and Danielson., 1988; Morgenstern and DePierre., 1988; Pickett and Lu., 1989; Armstrong., 1991). Microsomal GST is abundant in liver microsomes and in the

-
- 1961 Demonstration of GST activity.
- 1973 First purification schemes for GST.
- 1974 Ligandin (Y protein) identified as a GST.
- 1976 Selenium-independent glutathione peroxidase is a GST.
- 1977 Use of SDS-PAGE to identify Ya, Yb and Yc GST.
- 1979 Ligandin activity attributed to the Ya-type subunit.
- 1981 Proof that distinct GST subunits can hybridize, forming heterodimers.
Demonstration of polymorphic expression of GST in humans.
- 1982 Isolation of a unique microsomal GST.
- 1984 First full-length cDNAs encoding GST described.
Expression of pi-class GST in hepatic preneoplastic nodules.
- 1985 Overexpression of GST in drug-resistant cells lines.
Alpha-, Mu-, and Pi-class GST families defined.
- 1986 Association between absence of mu-class GST and susceptibility to lung cancer.
- 1988 Identification of a bacterial GST responsible for resistance to antibiotic fosfomycin.
- 1990 Identification of novel cis-acting elements in flanking regions of GST genes that respond to xenobiotics.
- 1991 Theta-class GST characterized.
X-ray crystallography of GST.
Three-dimensional structure of class Pi GST determined.
- 1992 Crystal structure of class Mu GST determined.
GSTs were involved in the elimination of Phase II conjugation products as the third phase of detoxification.
Class Sigma GST was proposed.
- 1993 Crystal structure of class Alpha GST determined.
- 1994 GSTs can activate compound to form alkylating agents.
Crystal structure of class Mu GST determined.
- 1995 Sigma-class GST characterized and Theta-class was proposed as the evolutionary forerunner of cytosolic GST isoenzymes.
Crystal structures of blowfly class Theta and class Sigma GSTs determined.
The projection structure of microsomal GST obtained by two-dimensional crystallography shown to be a trimer.
- 1996 The first crystal structure of plant GST from *Arabidopsis thaliana* determined.
-

Table.1 Historical overview of GST research (adopted and modified from Beckett and Hayes., 1993).

outer mitochondrial membrane (Morgenstern and DePierre., 1988), but cells of the other tissues also express the enzyme at a lower level. The microsomal isoenzyme has the ability to protect cells against lipid peroxidation (Morgenstern and DePierre., 1988). Pemble and Taylor (Pemble and Taylor., 1992) suggested that Alpha, Mu and Pi classes isoenzyme originated from duplication of a Theta-like gene. The Mu class GST diverged from the common Alpha/Mu/Pi gene before the divergence of Alpha and Pi classes. When Ji et al (Ji et al., 1995) compared the primary structure, gene structure and three-dimensional structure of different classes of GSTs, they proposed that the Sigma class isoenzyme diverged from the ancestral precursor before the divergence of the precursor gene for Alpha, Mu, Pi and Theta classes. The proposed evolutionary scheme for GST family is shown in Fig.1.

1.3 Nomenclature and classification

The earliest reported attempt to classify the different forms of glutathione S-transferase was made by Boyland and Chasseaud (Boyland and Chasseaud., 1969). They classified the GSTs into five groups: GSH-S-aryltransferase, GSH-S-epoxidetransferase, GSH-S-alkyltransferase, GSH-S-aralkyltransferase and GSH-S-alkenetransferase. Classification was based on GST's substrate specificity towards electrophilic substrates. Comparison of the specific activities of isolated isoenzymes with more diverse substrates displayed overlapping substrate specificities, and their activities were proved not to be linked to a single functional group. For example, the purified epoxidetransferase was active with alkyl and aralkylhalides in the conjugative process (Pabst et al., 1973). In 1975, Kamisaka et al (Kamisaka et al., 1975) grouped the five basic (class Alpha) forms of GST isolated from human liver; these were assigned in Greek alphabetical symbols, namely α , β , γ , δ and ϵ . The neutral form (class Mu) GST in liver and the

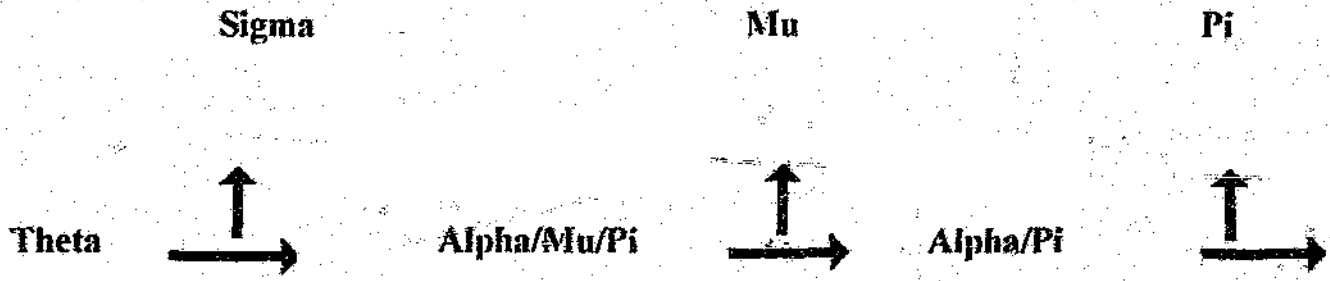


Fig.1 The proposed evolutionary scheme for GSTs. It explains the early divergence of Sigma class Theta ancestor followed by the divergence of Mu class GSTs from the common Alpha/Mu/Pi ancestor. GST diverged from the common Alpha/Pi ancestor (adopted from Ji et al., 1995).

placental acidic form (Pi) were also designated as μ , ψ , ϕ and π (Pi) (Guthenberg et al., 1979; Warholm et al., 1981; Singh et al., 1987; Hayes et al., 1989). Stockman et al (Stockman et al., 1985) developed a system based on the quaternary structure of proteins. This particular system described the three enzymes (B_1B_1 , B_1B_2 and B_2B_2) formed by the combination of two distinct subunits called B_1 and B_2 (Stockman et al., 1987). An alternate approach to the classification of the GST was to number the enzymes according to their gene loci, using evidence obtained from zymogram analysis (Board., 1981b; Strange., 1984). It gave rise to the designation of GST1, GST2, GST3, which were the loci encoding Mu, Alpha and Pi classes isoenzymes, respectively. Jakoby and co-workers suggested that the six forms of GST, which they had identified in rat liver, namely E, D, C, B, A, AA, in the order of their elution from a carboxymethylcellulose ion-exchange matrix (Mannervik and Danielson., 1988). One of the nomenclature systems was developed according to the isoenzymes' relative mobilities in sodium dodecyl sulphate polyacrylamide gel electrophoresis. Subunits started with Y and were followed by Roman letters in subscript that designated the appropriate subunits (Mannervik., 1985; Mannervik and Danielson., 1988). An obstacle arose as the relative mobility was dependent on the degree of crosslinking of SDS-PAGE gel and the true molecular mass values were not reflected from the SDS-PAGE (Hayes and Mantle., 1986). A unified system was finally introduced in 1992 by Mannervik et al (Mannervik et al., 1992) and the guidelines for the nomenclature of human GST were described in detail.

Examples of different GST nomenclature are shown in Table.2. In the example of human GST P1-1(hGST P1-1), h represented the species origin of the enzyme, P was designated to the Pi class isoenzyme with Arabic number 1-1 displayed the association of identical type -1 subunits.

Previous designation as GST	Class
B ₁ B ₁ , GST2-type 1, Ha(Subunit 1), $\alpha_x\alpha_x$, GSTe	Alpha
B ₂ B ₂ , GST2-type 2, Ha(subunit 2), $\alpha_y\alpha_y$, GST γ	Alpha
GST1-type 2, H _b (subunit 4), GSTM ₁	Mu
GST1-type1, GSTM ₂	Mu
GST3, π,ρ	Pi
GST θ	Theta
Microsomal GST	Microsomal

Table.2 Example of human GST isozyme nomenclature.
(adopted from Mannervik et al., 1992).

1.4 Functions of GSTs

1.4.1 GST's involvement in the detoxification pathway

Toxic compounds are produced by micro-organisms, plants and animals as a form of self protection enabling successful evolutionary adaptation against predators. Toxins are also produced by humans as a consequence of modern industrialised processes.

The detoxification of structurally diverse toxins was classified into two distinctive pathways:

(a) P-glycoprotein system: xenobiotics are exported by P-glycoprotein, a 170 kDa plasma membrane glycoprotein that mediates the efflux of drugs and xenobiotics (Endicott and Ling., 1989).

(b) Three phase detoxification pathway (see Fig.2): Phase I of the metabolism of xenobiotics of the three phase detoxification pathways involves the activation of xenobiotics by oxidation, reduction or hydrolysis. An example is the oxidation of xenobiotics by the cytochrome P450 superfamily which resulted in the formation of reactive groups in the xenobiotics and provided a reactive group for phase II system. Variations in the order of product release and the intermediates utilized can result in a variety of products, including mono-oxygenase products, reduction products, epoxides and peroxides (Guengerich., 1991; Porter and Coon., 1991). The second phase generates genotoxic electrophiles, activated xenobiotics, including the products of phase I, which is deactivated via conjugation of the activated functional group with glucuronyl, sulphuryl and glutathionyl moiety, and transformed into

more hydrophilic forms (Hayes and Wolf, 1990). Phase II enzymes include glutathione S-transferase, UDP-glucuronosyltransferase and epoxide hydrolase. The hydrolysed epoxide by-product can react readily with proteins by Schiff-base formation or bind to DNA (Ishikawa., 1992). In the example of glutathione conjugation by GSTs, the risks of exposing the cellular environment to carcinogenic epoxides and its hydrolysed product are reduced.

Phase III involves the cellular elimination of inactive and water soluble conjugates via an ATP dependant pump located in the plasma membrane. This is because the intracellular accumulation of glutathione-conjugates can lead to a decrease in the detoxification ability of phase II enzyme (Ishikawa., 1992). The GS-X pump, which was proposed by Ishikawa et al (Ishikawa et al., 1986), exhibited high affinities toward glutathione S-conjugates that carried a long aliphatic carbon chain and suggested another role in transporting naturally occurring glutathione conjugates, e.g. leukotrienes C₄ (Samuelsson et al., 1987; Ishikawa et al., 1989a).

Three phase detoxification pathway was not only involved in the metabolism of xenobiotics but was also involved in the synthesis and release of biologically active endogenous compounds, e.g. prostaglandin (Chang et al., 1987b) and LC₄. Arachidonic acid was oxidised via the lipoxygenase pathway and conjugated with GSH, which leads to the formation of LC₄ from LA₄ (Chang et al., 1987a).

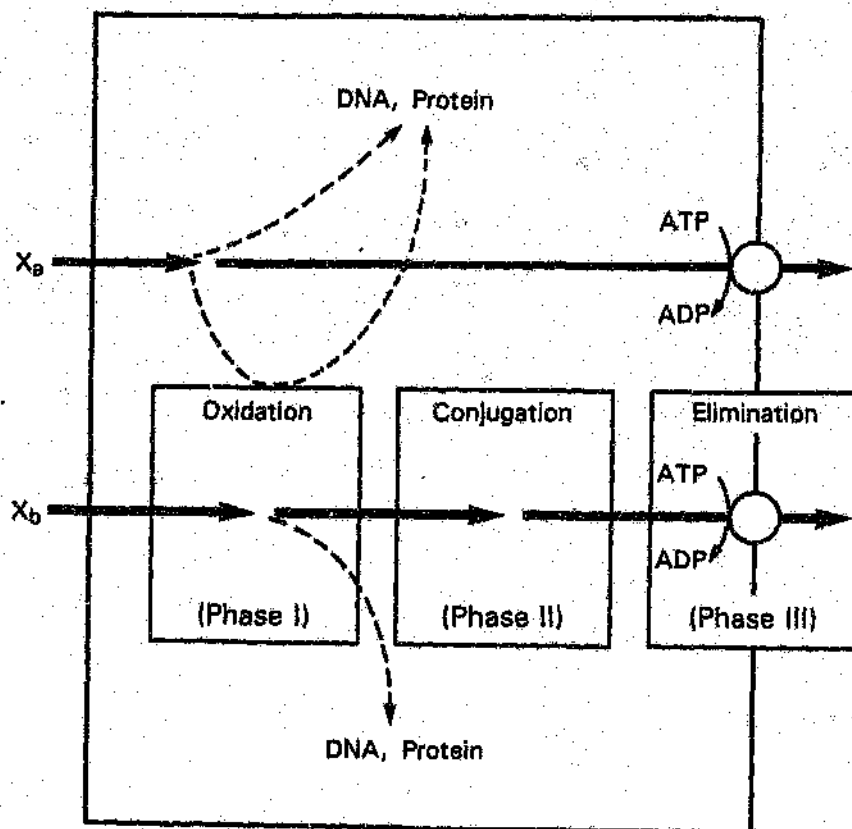


Fig.2 The three-phase pathway of detoxification of xenobiotics. X_a: xenobiotics that are exported by P-glycoprotein. X_b: xenobiotics that are bioactivated by monooxygenase in phase I and conjugated with glutathione in the phase II system. The metabolites bioactivated in the phase I can react with cellular protein or DNA. The glutathione S-conjugates formed in the phase II system are eliminated from the cell by the GS-X pump (phase III) (adopted from Ishikawa., 1992).

1.4.2 The ATP dependant glutathione conjugate pump

The ATP dependant glutathione S-conjugate pump was initially proposed by several investigators (Board., 1981a; Akerboom et al., 1982; Ishikawa., 1986) and was confirmed later from experiments using plasma membrane vesicles prepared from erythrocytes, rat heart and liver (Kando et al., 1982; Ishikawa., 1989b; Kobayashi et al., 1989; Kitamura et al., 1990). Kinetic studies showed that ATP was essential for the transport function of the glutathione S-conjugates (Ishikawa., 1989b). The ATP dependant pump serves two functions: it facilitates the degradation of glutathione S-conjugate by exporting the conjugates out of the cell, which is then transport to the kidneys by blood plasma. This occurs as it is vital to maintain the efficiency of the detoxification enzyme system in the cell. The pump consisted of the P, C and G domains where the P domain was responsible for the phosphorylation, and the C and G domains were involved in the recognition of glutathione S-conjugates (Ishikawa., 1993). The GS-X pump also exhibits a broad spectrum of substrate specificity towards different types of glutathione S-conjugates.

1.4.3 Degradation of glutathione S-conjugates

The degradation of glutathione S-conjugate starts with the removal of γ -glutamyl moiety and is followed by the cleavage of Cys-Gly peptide bond by a peptidase. The remaining S-(substituent)-cysteine derivative can be metabolised further upon acetylation of the cysteine conjugate by acetyl-coenzyme A to produce a final product called mercapturic acid, which is excreted via the kidney. Alternatively, the cysteine moiety can be cleaved at the C-S bond with the elimination of pyruvate and ammonia, resulting in the production of mercaptan. The thiol group of mercaptan can be further glucuronosylated with uridinediphosphoglucuronate or methylated

with S-adenosyl methionine to form methyl-thiol conjugate, and this can be further oxidised to form methylsulfinyl derivative which may be oxidised to form the last product which was a methylsulfonyl derivative. Thioglucuronide or methylthio derivative of xenobiotics, together with mercapturic acid, are excreted by kidneys (Mannervik., 1985). Details of the degradation pathway can be seen in Fig.3.

1.4.4 Binding and intracellular transport of non-substrate ligands

The GSTs were concurrently characterized based on their non-substrate binding ability. These enzymes were originally called Y- protein or ligandin before Kaplowitz et al (Kaplowitz et al., 1973) observed the glutathione S-transferase activity from them. GSTs bind to a diverse variety of large hydrophobic and amphipathic non-substrate ligands such as steroid hormones, thyroid hormones, bilirubin, heme, bile acid, fatty acids, leukotrienes, prostaglandins and neurotransmitters (Boyer., 1989; Listowsky., 1993). This protein also has the capacity to bind various exogenous substances such as drugs, dyes and xenobiotics, including mut. gens and carcinogens (Listowsky et al., 1988).

Non-substrate ligands can act as non-competitive inhibitors. Evidence for this includes: (1) covalent labelling of the non-substrate ligand binding site in rGST A1-2 does not result in complete loss of activity (Boyer., 1986); (2) the degree of inhibition by non-substrate ligands is pH dependant, (i.e. due to the formation of a kinetically active enzyme-substrate-inhibitor complex) (Van der Jagt et al., 1982; Boyer et al., 1984; Boyer and Vessey., 1987); (3) some forms of GST still retain full activity at 100% ligand saturation (Boyer et al., 1984); (4) Certain non-substrate ligands (phenoxyherbicides) have stimulatory effects instead of inhibitory effects (Vessey and Boyer., 1984; Vessey and Boyer., 1988) and (5) SJ26CST

retained 100% enzyme activity when the enzyme was assayed at the presence of 500 μM concentration of non-substrate ligand, Praziquantel (Walker et al., 1993). Praziquantel occupied the solvent accessible cleft created by the association of subunits was observed from the 3D structure of SJ26GST (McTigue et al., 1995).

Cytotoxic effects occur within the cells when the cellular concentrations of non-substrate ligands exceed the capacity of their specific receptors or if there is no specific receptor for the potentially toxic compound. Tipping and Ketterer (Tipping and Ketterer., 1981) observed GSTs' involvement in the transport of substrates for cytochrome P450, and subsequently the product of cytochrome P450 system will be used by GST as H-site substrates. GST can regulate the metabolism of toxic compounds by binding the toxin and rendering it more water-soluble and, therefore, facilitating the metabolism of toxins and protecting the cells against cytotoxic effect (Listowsky., 1993).

A negative effect arises when the metabolites formed become mutagenic or carcinogenic and induce an over-expression of GSTs, resulting in an increased cellular resistance to toxic compound. However, this can be controlled by GST itself. For steroid and thyroid hormones, the dissociation rate of hormones at high affinity receptor sites allows an efficient transfer of non-substrate ligands or alternatively, when the GST level is high, the enzyme will divert the bound hormone to another site to be metabolized (Listowsky., 1993). The high capacity of GST-thyroid hormone (T_3 or T_4) binding allows the regulation of action and metabolism of the thyroid hormone by controlling their intracellular transfer to receptors and components involved in thyroid hormone metabolism (Ishigaki et al., 1989). Chang et al (Chang et al., 1987) also suggest GSTs are potentially involved in the control of cellular concentration of androgen-dependent growth hormone.

1.5 Structure and conformational stability of GSTs

1.5.1 Structural comparisons of GST family

Cytosolic GST exists as homo- or hetero- dimer according to the dimerization of monomers within same class of isoenzyme. Members within the same classes share a high amino acid sequence identity and similar subunit sizes (24-28 kDa) (Dirr et al., 1994b; Wilce and Parker., 1994). Unlike the cytosolic GSTs, microsomal GSTs exist as trimeric protein with molecular mass of 17.3 kDa per monomer (Hebert et al., 1995). The folding topology of membrane-bound microsomal GSTs is different from cytosolic GSTs as each monomer contains an inner core of six parallel α -helices delineating a central low density region and the helical bundle is partly surrounded by elongated domains (Hebert et al., 1995).

Sequence identity between the different gene classes displays little identity (Pi-Mu 30%; Pi-Alpha 32%; Alpha-Mu 20%; Sinning et al., 1993). Class Pi isoenzyme shares the highest sequence identity with class Alpha, and moreover they also shared a high degree of structural similarity when the superimposed structures of the two classes are compared (Dirr et al., 1994b). However, class Pi and class Mu do share a higher degree of overall structural similarity when the superimposed backbone conformations are compared (Sinning et al., 1993). The plant class Theta GST of *A. thaliana* shared less than 20% of sequence identity with class Alpha, Mu and Pi GSTs (Reinemer et al., 1996). The blowfly class Theta GST also shared a very low sequence identity with Alpha, Mu and Pi GSTs, just below 21% (Wilce et al., 1995). The class Sigma GST isolated from squid digestive gland, shared 19-34% sequence identity with the other four principle vertebrate classes GSTs (Ji et al., 1995). The class Sigma GST shared highest identity with class Pi GST; 38,7%

for domain 1 and 31.2% for the entire molecule (Reinemer et al., 1996).

Classes of GSTs share 26 invariant amino acid residues, with many relatively conservative substitution changes that are accommodated without any major structural adjustments (Dirr et al., 1994b).

Many of these residues are located at the active site and contribute towards substrates binding, catalysis and conformational stability (Dirr et al., 1994b). The invariant amino acid residues are as follows: Tyr7(Pi)/Tyr6(Mu)/Tyr8(Alpha), Arg11(Pi)/Arg10(Mu)/Arg12(Alpha), Gly12(Pi)/Gly11(Mu)/Gly13(Alpha), Arg18(Pi)/Arg17(Mu)/Arg19(Alpha), Leu20(Pi)/Leu19(Mu)/Leu21(Alpha), Leu21(Pi)/Leu20(Mu)/Leu22(Alpha), Glu30(Pi)/Glu29(Mu)/Glu30(Alpha), Phe47(Pi)/Phe56(Mu)/Phe51(Alpha), Pro51(Pi)/Pro60(Mu)/Pro55(Alpha), Gln62(Pi)/Gln71(Mu)/Gln66(Alpha), Ile66(Pi)/Ile75(Mu)/Ile70(Alpha), Leu76(Pi)/Leu85(Mu)/Leu80(Alpha), Gly78(Pi)/Gly87(Mu)/Gly82(Alpha), Glu83(Pi)/Glu92(Mu)/Glu87(Alpha), Asp88(Pi)/Asp97(Mu)/Asp92(Alpha), Asp96(Pi)/Asp105(Mu)/Asp100(Alpha), Leu104(Pi)/Leu100(Mu)/Leu108(Alpha), Leu131(Pi)/Leu141(Mu)/Leu139(Alpha), Gly143(Pi)/Gly149(Mu)/Gly149(Alpha), Asp150(Pi)/Asp156(Mu)/Asp156(Alpha), Leu157(Pi)/Leu163(Mu)/Leu163(Alpha), Phe171(Pi)/Phe177(Mu)/Phe177(Alpha), Pro172(Pi)/Pro178(Mu)/Pro178(Alpha), Leu174(Pi)/Leu180(Mu)/Leu180(Alpha), Arg180(Pi)/Arg186(Mu)/Arg186(Alpha), Pro200(Pi)/Pro206(Mu)/Pro206(Alpha) (Dirr et al., 1994b).

Each subunit polypeptide chain folds into two structurally distinct domains that have a total secondary structure content about 48-59 % α -helix and 8-10 % β -strands (Dirr et al., 1994b). The smaller N-terminal domain has the topological arrangement for the secondary structure elements folded into the $\beta\alpha\beta\alpha\beta\alpha$ motif (Dirr et al.,

1994b). The superimposed subunit structure showed a high degree of backbone structural similarity between Alpha, Mu, Pi and Sigma classes of GSTs (Sinning et al., 1993; Dirr et al., 1994b; Ji et al., 1995). Each class has specific structural characteristics. For example, class Mu GST has an extended and mobile Mu loop connecting strand $\beta 2$ and helix $\alpha 2$ (Ji et al., 1992). The folding and frame work of class Mu GSTs was, therefore, not affected by the insertion of the Mu loop (Dirr et al., 1994b). Domain 1 of class Alpha subunit is folded from two separate polypeptide segments. This domain has an additional amphipathic α -helix, helix $\alpha 9$, which is created by the folding of the C-terminal region of the class Alpha polypeptide chain (Sinning et al., 1993). Blowfly class Theta GST did not have the loop found in class Mu GSTs or the C-terminal helix characteristic of class Alpha GST (Wilce et al., 1995). Helix 5 of blowfly Theta class GST is shorter and not bent. The conformation of the loop connecting helix 4 and 5 of blowfly Theta class GST together with the absence of helix 8 are unique features (Wilce et al., 1995).

Domain 2 is composed of five amphipathic α -helices (Dirr et al., 1994b; Wilce and Parker., 1994; Ji et al., 1995). The variations in sequences (due to substitution, insertion or deletion) have led to some overall structural readjustments between gene classes, such as the rotation of structural domains (Sinning et al., 1993). Class Pi and Mu shared higher degrees of structural similarity of domain 2 where class Alpha has a longer $\alpha 5$ helix and a shorter three-residue β -strand near the C-terminal segment which forms a structural part of the domain I of class Alpha (Dirr et al., 1994b). The folding topology of class Sigma GST was similar to other known GST except for a significant difference at the position of the $\alpha 4$ -turn- $\alpha 5$ (residues 102-126) (Ji et al., 1995).

A distinguishing feature between GST classes is the interactions involved at the dimer interface. A lock- and -key type of hydrophobic interaction is established in Alpha, Mu, Pi and SJGST (which belongs to the class Mu of GST family) by the wedging of a hydrophobic side chain of a Phe residue (Phe52/Alpha; Phe56/Mu; Phe 47/Pi; Phe51/SJGST) from one subunit into a pocket between $\alpha 4$ and $\alpha 5$ in the other subunit (Ji et al., 1995). This particular type of lock- and -key interaction is not present in squid class Sigma GST due to the absence of Phe and the loop on which the Phe resides. The two residues out of five residues (of lock) form electrostatic interactions rather than hydrophobic interactions and the hole of the lock is blocked by the side chain of Glu89 and Phe129. The decrease in hydrophobic interaction is compensated by the increase of electrostatic interactions (Ji et al., 1995). The subunit recognition of enzyme classes that have the hydrophobic lock (Alpha, Mu, Pi, SJ GST) are controlled primarily by the relative orientation of the N- and C-terminal domains (Sinning et al., 1993) which alters the distance between the key of subunit 1 and the lock of the subunit 2. This fits well into the hypothesis of the earliest divergence of class Sigma from the common ancestor (Ji et al., 1995) and the dimer interface of GSTs evolved from hydrophilic to more hydrophobic.

1.6 Catalysis

1.6.1 Basis of catalysis by GSTs

Glutathione S-transferase catalyses a variety of reactions, including nucleophilic aromatic substitution (S_NAr) between reduced glutathione (bound to the G-site as the activated thiolate) and a broad spectrum of electrophiles. The most common method to study the ability of GST to conjugate GSH with electrophilic substrates

is the spectrophotometric assay developed by Habig and Jakoby (Habig and Jakoby, 1981). 1-chloro-2,4-dinitrobenzene (CDNB) was used as an electrophilic substrate to observe the GST's catalytic activity (Habig et al., 1974). See the illustration in Fig.4, for the catalysis by GST. Most biomolecular aromatic nucleophilic substitution reactions on activated substrates are thought to proceed through an unstable Meisenheimer or σ - complex intermediate which represents the rate limiting step in this type of chemical catalysis. Graminski and co-workers (Graminski et al., 1989b) observed that the ability of rat liver class Mu isoenzyme 3-3 and 4-4 to stabilize the Meisenheimer complex intermediate. These works use 1,3,5-trinitrobenzene (TNB), an activated arene lacking a good leaving group. The electron deficient aromatic ring of TNB, did not favour the removal of hydrogen atom and the substitution reaction, it reversibly forms the dead-end Meisenheimer complex intermediate at the active site of GST (Graminski et al., 1989b). Studies on the class Pi and Mu isozymes suggest a positive correlation between catalytic efficiencies for the nucleophilic aromatic substitution reaction with the enzyme's ability to stabilise the Meisenheimer complex (Graminski et al., 1989b; Bico et al., 1994).

Proposed steady-state kinetic mechanisms for GSTs include ping-pong, sequential and random mechanisms (Wilce and Parker., 1994). Most of the studies support the idea of the random addition of glutathione and electrophilic substrates. However, under physiological conditions, the intracellular concentration of reduced glutathione is in the 1-10 mM range, whereas the dissociation constant of the enzyme varies between 10 -200 μ M. This is much higher than the K_d of GST, allowing the glutathione to bind to GST first as that will drive the initially proposed random

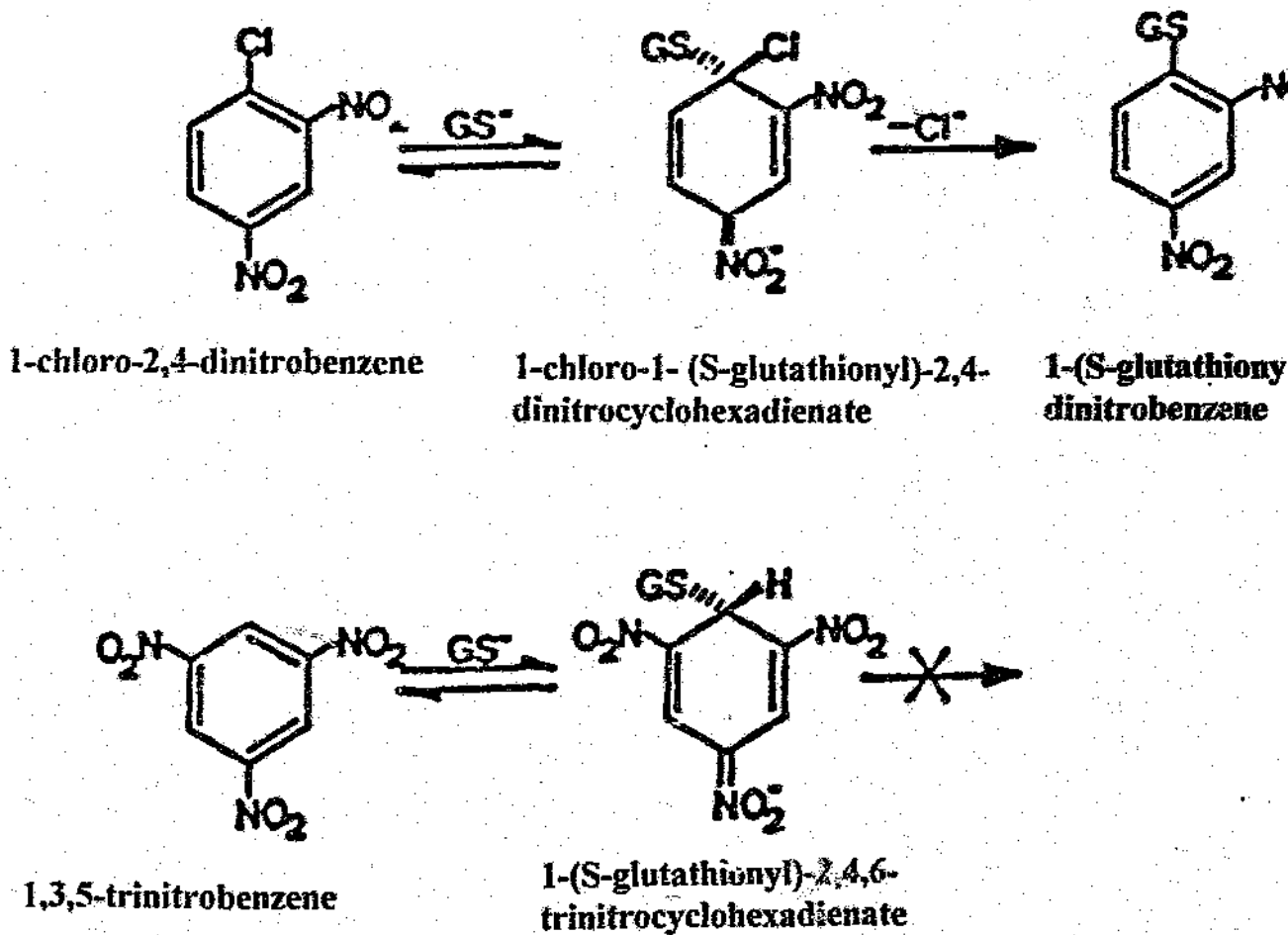


Fig.4 (a) The conjugation of 1-chloro-2,4-dinitrobenzene (CDNB) with reduced glutathione (GS⁻) to form 1-(S-glutathionyl)-2,4-dinitrobenzene. (b) The formation of Meisenheimer complex with 1,3,5-trinitrobenzene (TNB). GS⁻ represents the thiolate anion. Fig.4(b) represents the formation of product did not proceed (adopted from Bico et al., 1994).

addition to a sequential addition of substrates.

Roberts and co-workers (Roberts et al., 1986) estimated that the small thiolate anion was 10^9 times more reactive than its conjugate acid when comparing relative reactivity in aqueous solution. A central aspect of the catalytic mechanism is the ability of the enzyme to lower the kinetically determined pKa of the sulfhydryl group of reduced GSH from 8.9-9.0 in aqueous solution to values of 6-7 (spectrophotometrically determined) when the thiol group of glutathione bound at G-site (Chen et al., 1988; Graminski et al., 1989b). The estimated pKa for the bound thiol group is 5.7-6.9 for class Mu (Graminski et al., 1989a,b; Liu et al., 1992), 6.7-7 for class Alpha (Huskey et al., 1991; Wang et al., 1992) and 6.3 for class Pi (Kong et al., 1992b).

An evolutionary conserved Tyr (class Pi) /Tyr6(Mu)/Tyr8 (Alpha)/ Tyr7 (Sigma) is directly involved in the catalytic activation of glutathione which is supported by evidence from crystallographic, kinetic and spectroscopic studies of wild-type and Tyr \rightarrow Phe mutant GSTs (Graminski et al., 1989a,b; Reinemer et al., 1991; Stenberg et al., 1991; Ji et al., 1992; Reinemer et al., 1992; Kolm et al., 1992; Wang et al., 1992; Liu et al., 1992; Manoharan et al., 1992a,b; Kong et al., 1992a,b; Penington and Rule., 1992; Sinning et al., 1993; Raghunathan et al., 1994; Ji et al., 1995). It was found in Theta class GST, a conserved serine residue took over the catalytic tyrosine's role (Ser9 of *L.cuprina* GST and Ser11 of *A.Thaliana* GST) (Wilce et al., 1995; Reinemer et al., 1996).

Tyr 7 is in close proximity to the sulphonic group of glutathione sulphonate, the hydroxyl group of Tyr and one of the oxygen atoms of sulphonate, which is situated within hydrogen bonding distance (Reinemer et al., 1991; Dirr et al., 1994a). This

is further supported by comparing crystallographic structures of GST in complex with various GSH analogues (Reinemer et al., 1991; Reinemer et al., 1992; Garcia-Saez et al., 1994; Ji et al., 1992).

The replacement of tyrosine residue with phenylalanine by site-directed mutagenesis resulted in a very low turnover rate at pH 6.5. However, the enzyme still retained glutathione binding affinity which implies that the Tyr residue is primarily involved in the activation of the thiol group of glutathione (Stenberg et al., 1991; Liu et al., 1992; Manoharan et al., 1992a).

The close proximity of Tyr to the sulphur atom of GSH suggests a positive influence by Tyr on the pKa values of the thiol in the enzyme-glutathione complex. The pKa of enzyme bound thiol group is approximately 2 pH units below the pKa of free thiol of glutathione (Graminski et al., 1989a). The Y6F mutant of isoenzyme 3-3 has a higher pKa value ($pK_a > 8$) than wild type in the bound enzyme-thiol complex, implying that the hydrogen bond between them is involved in the stabilization of the thiolate anion at the G-site (Liu et al., 1992). An alternative role for the tyrosine at the active site has been proposed by Karshikoff et al (Karshikoff et al., 1994). In this proposal, the deprotonation of the hydroxyl group of Tyr is influenced by protein charge constellation, and in particular by the high positive potential generated by peptide dipoles of Gly12, Arg13 and Cys14, which belong to the N-terminus of helix αA of domain 1 (Karshikoff et al., 1993). This significant α -helix dipole moment activated the hydroxyl group of Tyr7 and resulted in a considerable reduction of pKa of Tyr7. Thus, at physiological pH, it can act as a general base and promote proton abstraction from the GSH thiol by creating a thiolate anion with high nucleophilic reactivity (Karshikoff et al., 1993).

The active sites in the crystal structure of GSTs are open to bulk solvent (Dirr et al., 1994b) and the solvation of the active site can result in a diminished catalytic function (Adams et al., 1989). However, the exclusion of water from the active site following the substrate binding could contribute to the destabilization of glutathione and thus, the catalytic potential. In the class Mu GST crystal structure, one hemisphere of the sulphur atom of glutathione was found to be completely shielded from solvent (Ji et al., 1992) and the desolvation of thiolate anion at the active site would, therefore, lead to enhanced nucleophilic reactivity of glutathione (Huskey et al., 1991).

The conjugation of GSH also involves the biosynthesis and release of biologically active endogenous substances, such as prostaglandin (Chang et al., 1987b). Arachidonic acid is oxidised via the lipoxygenase pathway and is conjugated with GSH, which leads to the formation of leukotriene C₄ from A₄ (Chang et al., 1987a). This in turn, regulates the allergic and anaphylactic reaction, resulting in smooth muscle contraction; the release of luteinizing hormone; and modulation of the G-protein gated potassium channels (Ishikawa., 1992).

1. 6. 2 Recognition of GSH at G-site

The G-site of GST is highly specific towards the thiol substrate GSH bound to the G site and it assumes an extended conformation. Variants of thiols, such as N-Ac-L-Cys, L-cysteine, 2-mercaptoethanol and the tetrapeptide γ -L-Glu- γ -L-Glu-L-Cys-Gly are not recognised by GST as substrates (Habig et al., 1974; Abbott et al., 1986). They also have a very low affinity towards the retro-inverse isomer of GSH, as the GST cannot recognise the reversed order of glutathione peptides (Chen et al., 1988).

The γ -glutamyl moiety is the major binding determinant, which allows the thiol group to align properly at the G-site (Adang et al., 1988; Adang et al., 1989; Adang et al., 1990). It interacts extensively with a hydrophilic complementary pocket found near the subunit interface. This is formed by the conserved and conservatively replaced residues in the domain 1 of one subunit and domain 2 of the adjacent subunits (Dirr et al., 1994b). The α -carboxylate group of the γ -glutamyl site chain is the most important recognition site as it is obligatory for enzyme activity (Adang et al., 1990). The α C-helix dipole could function as an electrostatic anchor for the γ -glutamyl moiety and it would assist in the binding and orientating of the γ -glutamyl moiety of GST (Dirr et al., 1994b). Mu 3-3 GST is also able to recognise non- γ -glutamyl-carboxylate groups, e.g. analogues of GSH with α -L-glutamyl or α -D-glutamyl residues. The amino group of γ -glutamyl is not the major determinant, as GST is still able to catalyse the analogue which has the amino group of γ -glutamyl moiety omitted. Crystallographic works on class Pi isoenzyme with glutathione sulphonate demonstrates that the amino group of γ -glutamyl moiety is also important for recognition at the G-site (Dirr et al., 1994b).

The position of cysteinyl residue is critical for the conjugation with the thiol group. The Glycyl-modified analogues showed that the Glycyl residue is the least restrictive moiety and not essential for the recognition of GSH at the G-site.

1. 6. 3 Substrate specificity of GSTs

GSTs are able to react with a large number of structurally diverse substrates, including alkyl- and arylhalides, lactones, epoxides, quinones, ester and activated alkenes (Mannervik and Danielson., 1988). These all share the common feature of being mostly hydrophobic and bearing an electrophilic centre. The specificity of

GSTs toward certain substrates has proved useful in classifying new classes of GSTs. For example, class Alpha GSTs are highly reactive towards cumene hydroperoxide (Beckett and Hayes., 1993; Wilce and Parker., 1994), and Δ^5 -Androstene - 3,17- dione will distinguish subunit type 1 from type 2 of class Alpha GST (Beckett and Hayes., 1993). Class Mu GSTs has a preference for epoxides, and class Pi GSTs are highly reactive with ethacrynic acid (Beckett and Hayes., 1993; Wilce and Parker, 1994), whereas Class Sigma GSTs are highly reactive with CDNB (Ji et al., 1995). Type 1 subunit of class Theta GST is identified by 1,2 - Epoxy-3- (*p*-nitrophenoxy) propane, and type 2 subunit is identified by menaphthyl sulphate (Beckett and Hayes., 1993).

1.7 Glutathione S-transferase and its association with health and diseases

The distribution of GST across human tissue is said to be heterogenous and tissue specific (Tsuchida and Sato., 1992). The difference in tissue distribution can be explained by distinct tissue function: GSTs act either as carrier proteins (ligandin function of GST), or be metabolically active and detoxify the potentially harmful xenobiotics. Wild-type subjects display dominate amount of Alpha GST together with small quantities of class Mu and microsomal GST present in the liver (Hayes et al., 1991). The class Alpha GST is expressed in the liver, kidney, small intestine and adrenal glands (Tsuchida and Sato., 1992; Listowsky., 1993), while in most hepatocellular carcinoma, class Alpha GSTs are expressed in the liver (Coles and Ketterer., 1990; Hayes et al., 1991). The class Pi GST is expressed and uniformly distributed in extrahepatic tissues (Pemble et al., 1986; McLellan and Hayes., 1987) and found mainly in normal cell types, such as erythrocytes, platelets, placenta, and in the thyroid gland and lungs, whereas in the kidney, heart, testis, ovary and uterus, multiple forms of GSTs are expressed (Listowsky., 1993).

Investigators have paid attention to the use of rat or human class Pi GST as a reliable preneoplastic or neoplastic marker enzyme, indicating that the detection of elevated levels of Pi class GST would provide a simpler pathway to identify malignancy of tissues than the conventional method used (Tsuchida and Sato., 1992; Listowsky., 1993). The class Pi GST is normally expressed in minimal levels in adult hepatocytes and thus the increase of class Pi GST levels is due to the increased transcription of the Pi gene in the malignant cells (Suguoka et al., 1985). This isoenzyme (class Pi) has been variably reported to be normal or increased in human hepatocellular carcinoma (Soma et al., 1986; Kano et al., 1987), increased in both dysplastic and neoplastic lesions of uterine cervix (Shiratori et al., 1987), colon adenomas (Kodate et al., 1986) and cancers in the lungs, brain and skin (Tsuchida and Sato., 1992).

The class Mu GST is subjected to polymorphism and the expression of Mu class is population specific. It is expressed in approximately half of the population studied by Hussey and co-workers (Hussey et al., 1987). In humans, there are three autosomal alleles at the GST M-1 locus (Type 1, Type 2 and Type 0 or null), and hence four possible phenotypes may be expressed in the liver (genotype 1,0 or 1,1; genotype 1,2; genotype 2,0 or 2,2; genotype 0). The frequency of these four phenotypes in the European population were 18, 6, 35 and 41 %, respectively (Strange et al., 1984). Therefore, 40 % of the population studied lacked the class Mu GST (genotype 0 or null). It was later found that the hereditary differences in the expression of class Mu GST is due to the deletion of the gene (Seidegard et al., 1988). Strange et al (Strange et al., 1991) suggested that individuals lacking the expression of class Mu GST have a greater risk of developing adenocarcinoma of the stomach or colon than those with class Mu GST. The class Mu GST was suggested as a possible marker for greater susceptibility to human lung cancer

among smokers. Experiments have shown the diminished GST (class Mu) in mononuclear leucocytes from lung cancer patients toward trans-stilbene oxide when compared with a matched control group of smokers (Seidegard et al., 1986; Seidegard et al., 1990).

There are two ways to explain the over-expression of a particular isoenzyme in malignancy. Firstly, the over-expression of a particular isoenzyme is due to the clonal expansion of cells expressing particular GST or, alternatively, the selective over-expression which offers replicative advantage to differentiated cells, as in the case of developed drug resistance. The over-expression of GST in tumours produces resistance in the neoplasm to certain anticancer drugs (Hayes et al., 1991; Beckett and Hayes., 1993; Gulick and Fahl., 1995). Elevated levels of GST have been observed in human and animal tumours (Charmichael et al., 1988; Shea et al., 1988; Lewis et al., 1989; Di Ilio et al., 1988 a, b; Howie et al., 1990; Moorghen et al., 1991). The decreased drug-binding membrane bound protein and decreased activity of cytochrome P450 system would result a slower rate of anti-cancer drug metabolism (Hayes et al., 1991).

Labelled antibody immunoassay is able to distinguish classes of cytosolic GSTs (Hussey et al., 1987; Howie et al., 1988; Tsuchida et al., 1989) and hetero-dimers from homo-dimers (Beckett et al., 1984; Stockman et al., 1985). The advantage of the immunoassay allows us to exclude the artifacts created by problems such as bound ligands (bile, bilirubin), which decrease the enzyme activity and cause errors in the kinetic test. The class Alpha enzyme is the primary enzyme measured in liver diseases, e.g. paracetamol poisoning, acute alcohol ingestion, acute liver damage, hypoglycaemia, and anaesthesia with halothane (which causes liver injury) (Beckett and Hayes., 1993). The class Alpha GSTs are also used in the detection of chronic

liver diseases, such as autoimmune chronic active hepatitis, alcoholic cirrhosis and thyroid hormone associated diseases (hyperthyroidism and monitoring the thyroxine replacement therapy) (Beckett and Hayes., 1993). This class of GST (Alpha class) can also be used to detect renal damage and to predict the cadaver kidney function prior to transplantation (Cho et al., 1981). The class Mu enzyme is mainly used to differentiate chronic hepatitis, as 94 % of patients with chronic hepatitis were found to express the class Mu enzyme (Harada et al., 1987). It has also been found that patients lacking the class Mu GST are more susceptible to the adenocarcinoma of the stomach or colon. The elevated class Pi GST expression is associated with gastrointestinal malignant growth and can be use as a tumour marker for hepatobiliary and gastrointestinal malignant tumours.

1.8 Application of GSTs

1.8.1 Environmental bioremediation

Dichloromethane is a widely used industrial solvent and known carcinogen (Anders and Pohl., 1985). Dichloromethane-dehalogenase from *Methylophilus* sp. DM11 is a GSH-dependent enzyme which catalyses the hydrolytic dehalogenation of dichloromethane to formaldehyde for biosynthesis purposes, as well as inorganic chloride (Wackett et al., 1992). The formaldehyde is then oxidized to carbon dioxide for energy, or assimilated into cellular organic molecules (Scholtz et al., 1988). Sequence analysis of the bacterial (*Methylophilus* sp. DM11) dichloromethane dehalogenase has shown the enzyme to be a GST homologue and a member of the Theta class (Blocki et al., 1994). The utilization of dichloromethane as the carbon and energy source by methylotrophic bacteria can be applied in the bioremediation of a polluted environment. The use of the microbial

system to treat dichloromethane will limit its exposure to mammals and thus protect the environment against pollution by discharging more water soluble formaldehyde into the environment (as unsupported hypothesis) (Wackett., 1994).

1.8.2 Gene therapy involving GSTs

Chemotherapy is generally limited in its effectiveness by the toxicity of the chemotherapeutic drug being used in healthy tissue, for example, the bone marrow. It was suggested by several authors that an appropriate vector system be used to introduce the resistance-conferring gene into the bone marrow which would be able to increase the concentration of chemotherapeutic agents in cells and which would then selectively kill a larger number of tumour cells, thus providing transient resistance and protection for healthy cells during the course of chemotherapy treatment (Dolan et al., 1991; Sorrentino et al., 1992; Deisseroth., 1993). Gulick and Fahl (Gulick and Fahl., 1995) speculated that GST mutants with which confer greater resistance against specific drugs would be more efficient at protecting the bone marrow during chemotherapy.

Another possible application of GST is to design a GST specifically to activate prodrugs which can be introduced into solid tumours. Introduction of the activating GST into the tumour population may result in an increase in toxicity for that population of cells only, which means that the drug can then treat a localized region of solid tumours (Gulick and Fahl., 1995).

1.9 Structural aspects of class Pi GSTs

1.9.1 General description of class Pi GSTs

The first Pi class GST to be crystallized was from bovine placenta (Schaffer et al., 1988). However, the crystallization conditions were not reproducible between protein batches and, in addition to this they did not acquire coincident diffraction patterns between crystals. Porcine class Pi GST from lung tissue was biochemically characterized and crystallized by Dirr et al (Dirr et al., 1991), who also produced the first three-dimensional structure of the GST supergene family (Reinemer et al., 1991; Dirr et al., 1994a). The porcine enzyme was co-crystallized with its competitive inhibitor, glutathione sulphonate (Reinemer et al., 1991; Dirr et al., 1994a). Other three-dimensional structures of class Pi GSTs have been resolved. Such an example is the human placental class Pi GST in complex with the competitive inhibitor, S-hexylglutathione (Reinemer et al., 1992). Class Pi isoenzyme from mouse liver complexed with competitive inhibitors such as S-(p-nitrobenzyl) glutathione, glutathione sulphonate and S-hexylglutathione (Garcia-Saez et al., 1994).

Class Pi isoenzymes from different species share primary sequence identities ranging from 82 to 86%. Pair-wise identities are as follows: human-porcine: 82%; human-mouse: 85%; human-rat: 85%; and human-bovine: 86%. The secondary structure content of GST is about 48-59 % α helix, and 8-10 % β sheets (Dirr et al., 1994b). See sequence alignment of class Pi GSTs in Fig .5.

The three-dimensional structure of human placental class Pi GST was solved in complex with S-hexylglutathione at 2.8 Å resolution (Reinemer et al., 1992).

Human class Pi GST is a homo-dimeric protein which consists of two identical subunits (see Fig.6); this phenomenon can be observed throughout the human, bovine, pig, rat and mouse species of class Pi GST isoenzyme. Each subunit of human and murine class Pi isoenzyme consists of 209 amino acids, as well as sharing a common insertion of two extra amino acids when compared with the porcine isoenzyme (Reinemer et al., 1992; Garcia-Saez et al., 1994).

The subunit of human class Pi isoenzyme is characterized by two structurally distinct domains (see Fig.7): a smaller N-terminal domain which is designated as domain 1 (residues 1-76), and a larger C-terminal domain which is designated as domain 2 (residues 81-209). These two domains are connected covalently by a 6 residue linker. Domain 1 consists of a four-stranded β -sheet ($\beta 1$ to $\beta 4$). $\beta 1$ is parallel to $\beta 2$ which is parallel with $\beta 3$ and $\beta 4$ running anti-parallel to each other. αA and αC helices lie packed against the β -sheets with their axes running parallel to the four stranded β sheets. They are flanked on one side by the β -sheet, which forms part of the non-solvent contact area. αB is highly mobile as it faces and is exposed to the solvent (it also exhibits elevated temperature factors) (Reinemer et al., 1992).

Porcine and murine class Pi GSTs have an αB - 3_{10} helix in the same position. The αB region of porcine class Pi GST is bent due to the presence of the two proline residues (Pro39 and Pro40) (Reinemer et al., 1991; Dirr et al., 1994a; Garcia-Saez et al., 1994). The murine class Pi GST has a salt bridge formed between the carbonyl oxygen atom at the C-terminus of αB and the amide nitrogen at the N-

1

porcine	hGSTP1-1	PPYTTITYFPVGRGRCEAMRMLLADQDQSWKEEVVTMETWPF--PLKPSCLFRQLPKFQDGD
bovine	hGSTP1-1	PPYTTIVYFPVQGRCEAMRMLLADQDQSWKEEVVAMQSWLQGLKASCLYGQLPKFQDGD
murine	hGSTP1-1	PPYTTIVYFPVGRGRCEAMRMLLADQDQSWKEEVVTIDTWMOGLLKPTCLYGQLPKFEDGDL
rat	hGSTP1-1	PPYTTIVYFPVGRGRCEATRMLLADQDQSWKEEVVTIDVWLQGLKSTCLYGQLPKFEDGDL
human	hGSTP1-1	LPTVVYFPVGRGCAALRMLLADQDQSWKEEVVTVETWQEGSLKASCLYGQLPKFQDGD

****, ****, *** * ***** *****., * ** ,** , ***** ,****

TLYQSNAILRHLGRSFGLYGKDQKEAALVDMVNDGVEDLRCKYATLIYTNYEAGKEKYVK
 TLYQSNAILRHLGRTLGLYGKDQEEAALVDMVNDGVEDLRCKYVSLIYTNYEAGKEDYVK
 TLYQSNAILRHLGRSLGLYGKINQREAAQMDMVNDGVEDLRGKYVTLIYTNYENKNDYVK
 TLYQSNAILRHLGRSLGLYGKDQKEAALVDMVNDGVEDLRCKYGTLIYTNYENKDDYVK
 TLYQSNAILRHLGRTLGLYGKDQEEAALVDMVNDGVEDLRCKYISLIYTNYEAGKDDYVK
 ***** ,***** , ***** ,*** ,***** ***** ** ,***** ** ***

ELPEHLKPFETLLSQNGGQAFVVGSIQSFADYNLLDLLRIHQVLPNSCLDAFPLLSAYV
 ALPQHLKPFETLLSQNGGQAFIVGDQISFADYNLLDLLRIHQVLPNSCLDSFLLSAYV
 ALPGHLKPFETLLSQNGGKAFIVGDQISFADYNLLDLLRIHQVLPAGCLDNFPLLSAYV
 ALPGHLKPFETLLSQNGGKAFIVGNQISFADYNLLDLLRIHQVLPAGCLDNFPLLSAYV
 ALPGQLKPFETLLSQNGGKAFIVGDQISFADYNLLDLLRIHQVLPAGCLDAFPLLSAYV
 ** ,***** ,** ,** ,** ***** ,** ,** * ** * *****

ARLSARPKIKAFLLSPEHVNRPINGNGKN	207
ARLNSRPKIKAFLLSPEHMNRPINGNGKQ	209
ARLSARPKIKAFLLSPEHVNRPINGNGKQ	209
ARLSARPKIKAFLLSPEHNLNRPINGNGKQ	209
GRLSARPKIKAFLLSPEVNLNRPINGNGKQ	209

** ,*** ,**** ,** ,* ***** ,

Fig.5 Sequence alignment of human, porcine, rat, bovine and murine GST P1-1. Asterisks indicates conserved amino acids. The deletion in the porcine sequence creates two gaps between residues 39 and 40. All sequences are extracted from SWISS-PROT. The accession codes are as follows: P80031 (porcine GST P1-1); P19157 (murine GST P1-1); P28801 (bovine GST P1-1); P04906 (rat GST P1-1) and P09211 (human GST P1-1).



Fig. 6. (a) A ribbon representation of the backbone of human GST P1-1 (Remmer et al., 1992). The dimeric structure is viewed down the crystallographic 2-fold axis. Parameters are generated using the graphic viewing programme RASPRO (Savio and Miller-White, 1995).

terminus of the following 3_{10} -helix. It was proposed that the secondary structural similarity between murine and porcine enzyme at this region was maintained in this way (Garcia-Saez et al., 1994). The human enzyme has an insertion of two amino acids (Glu40 and Gly41) which causes a break in the region of α B and results in α B1 and α B2 (Reinemer et al., 1992), instead of α -helix followed by the 3_{10} -helix observed in the murine and porcine structure (Reinemer et al., 1991; Dirr et al., 1994a; Garcia-Saez et al., 1994). Porcine, human and murine class Pi GST shared a similar overall folded protein structure despite the minute structural difference (Reinemer et al., 1992; Garcia-Saez et al., 1994).

Domain 2 consists of a right-handed bundle of six α -helices (α D - α I). Helices α D and α E are connected by a short S-shaped loop and packed in an anti-parallel fashion, while α E has a distinct crescent-shaped appearance. This special bent feature in the α E can be explain as a contribution made by the two proline residues (Pro123, Pro128) of the α E helix which disrupted the main chain hydrogen bonding. It is interesting to note that the Pro123 and Pro128 are specifically conserved in Pi class isoenzyme which contributed to this special bend characteristic of class Pi GSTs. One small left handed 3_{10} -helix connects the α E and α F, while α F and α G run perpendicular toward each other. α H possess a sharp bend as a result of the Pro187 and Pro196. A small 3_{10} -helix is found between helices F and G. It was proposed initially that the 3_{10} -helix situated between helices F and G, helix I was a special feature of human class Pi GST (Reinemer et al., 1992), however, it has subsequently been found that these two features are also presented in the porcine and murine class Pi GST (Dirr et al., 1994a; Garcia-Saez et al., 1994).

Three helices, α G, α H and α I, follow with sharp bends between them, due to the Pi class isoenzyme conserved proline residues (Pro174, Pro187, Pro196 and

Pro202) and this results in the special U-shaped spatial disposition in the known three-dimensional structure of porcine, murine and human class Pi GST. Helices α D, α E, α F and α G, together with their connecting loops, packed together form the main body of domain 2. Helices α H and α I are separated from the main body of domain 2 and are highly exposed to solvent. The above-average main-chain thermal factors of porcine class Pi GST, which correspond to the human counter part, indicate that they are highly mobile (Dirr et al., 1994a). The C-terminus polypeptide turns back to the main body of domain 2 and associates with the C-terminal region of α D and the N-terminal of α E, respectively. The polypeptide chain ends at the hydrophobic region of the active site.

1.9.2 Domain interface

Several forces participate in the association of the two domains. The non-covalent main-chain and side-chain contacts are mediated by polar interactions (which include hydrogen bonding and salt bridges) and hydrophobic interactions with hydrophobic elements in α A, the loop between α A and β 1, and the α C region of domain 1 with α D, α F, α H, α I and C-terminus region of domain 2. Residues of human class Pi GST involved in the polar interactions between the two domains and which are within 3.5 Å are: Arg11 - Tyr198, Arg11 - Leu201, Arg11 - Pro202, Arg11 - Ile203, Gly12 - Ile203, Arg¹³ - Glu97, Asp23 - Tyr153, Asp23 - Arg186, Asn66 - Asn93, Arg70 - Asp94 and Gly73 - Leu78 (Reinemer et al., 1992). There are also polar interactions only observed in one subunit. Asp23 - Leu189, Arg70 - Asp90 and Arg70 - Asn93 are observed in subunit 1, Asp23 - Lys188 and Gln24 - Tyr153 are present in the subunit 2, respectively (Reinemer et al., 1992).

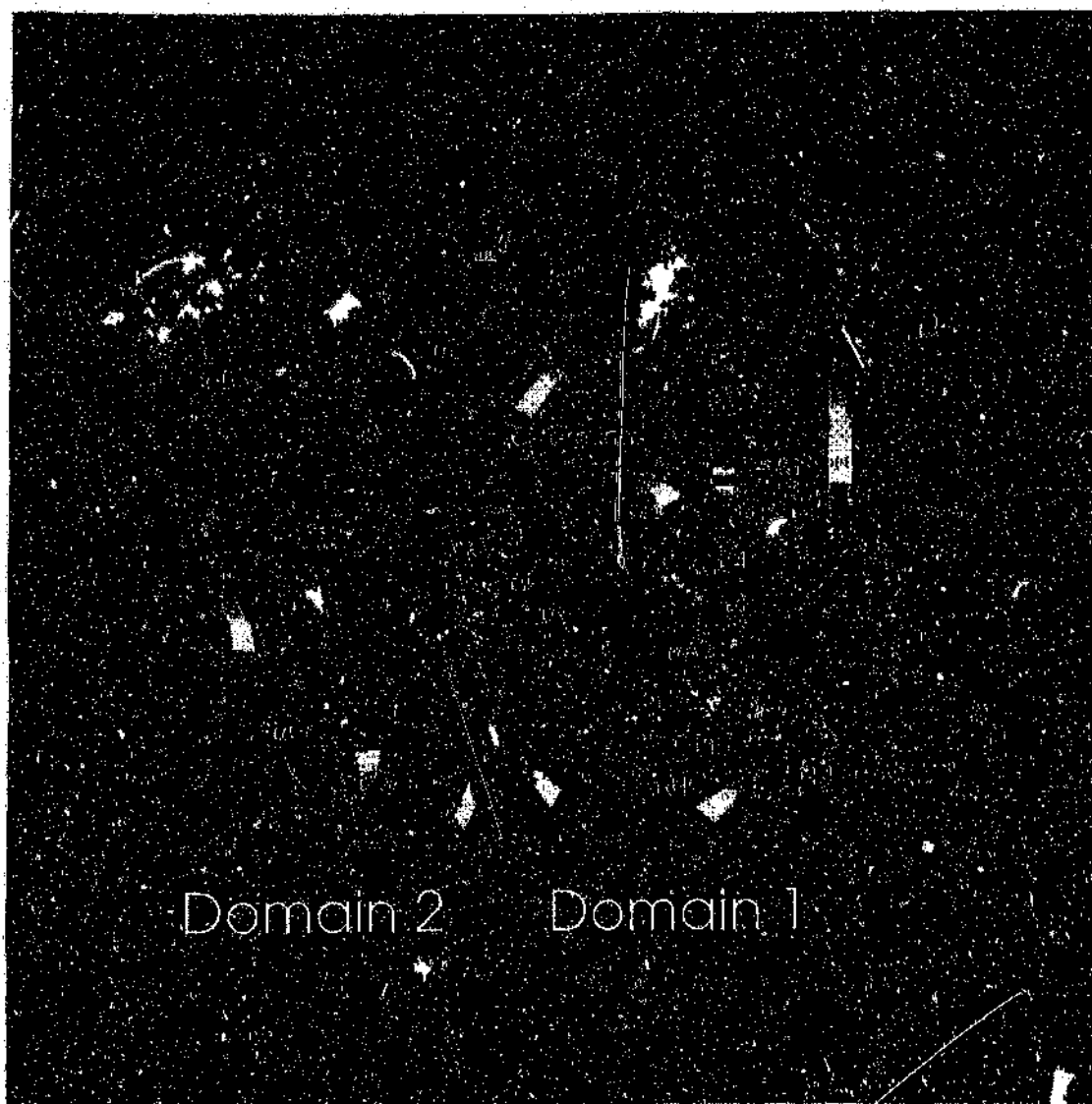


Fig.7 Subunit structure of hGST P1-1 showing domain 1 and domain 2 (Reinemer et al., 1992). The structure is viewed perpendicular to the crystallographic 2-fold axis. The diagramme is generated using the viewing programme RASMOL (Sayle and Miller-White., 1995).

Hydrophobic interactions within 4 Å are: between α A (residues Ala15, Met19 and Leu20) and α F (Phe150, Tyr153, Leu156 and Asp157); between α A (Arg18, Met19 and Ala22) and α H (Leu189, Phe192 and Leu193); between Trp28 and Phe192; and between α C (Leu69 and Arg70) and α F (Phe150 and Asn154 (Reinemer et al., 1992). It is very interesting to note that most of the amino acids involved in the polar and hydrophobic interactions at the domain interface are conserved within the Pi class isoenzyme (see Fig.5 for aligned sequences).

1.9.3 Association of subunits

The dimeric class Pi GST isoenzyme is globular with approximate dimensions of 45 Å x 55 Å x 60 Å (Dirr et al., 1994b; Wilce and Parker., 1994). The total buried surface area between monomers of class Pi isoenzyme is about 1300 Å² with approximately 14-15% of monomer's initial water-accessible surface area of solvent accessible area reduced upon dimerization of monomers (Reinemer et al., 1991; Reinemer et al., 1992; Dirr et al., 1994b). The buried surface area is within the range normally found for dimeric proteins of similar subunit molecular mass (Dirr et al., 1994b). The most striking feature of the structure of this dimeric class Pi GST is the distinctive V-shaped interface. This can be seen from the view perpendicular to the two fold axis of the dimeric structure of human class Pi isoenzyme in Fig.8. Two types of forces contribute towards the inter-subunit contact, namely the hydrophobic and polar interactions. Amino-acid pairs which participate in the

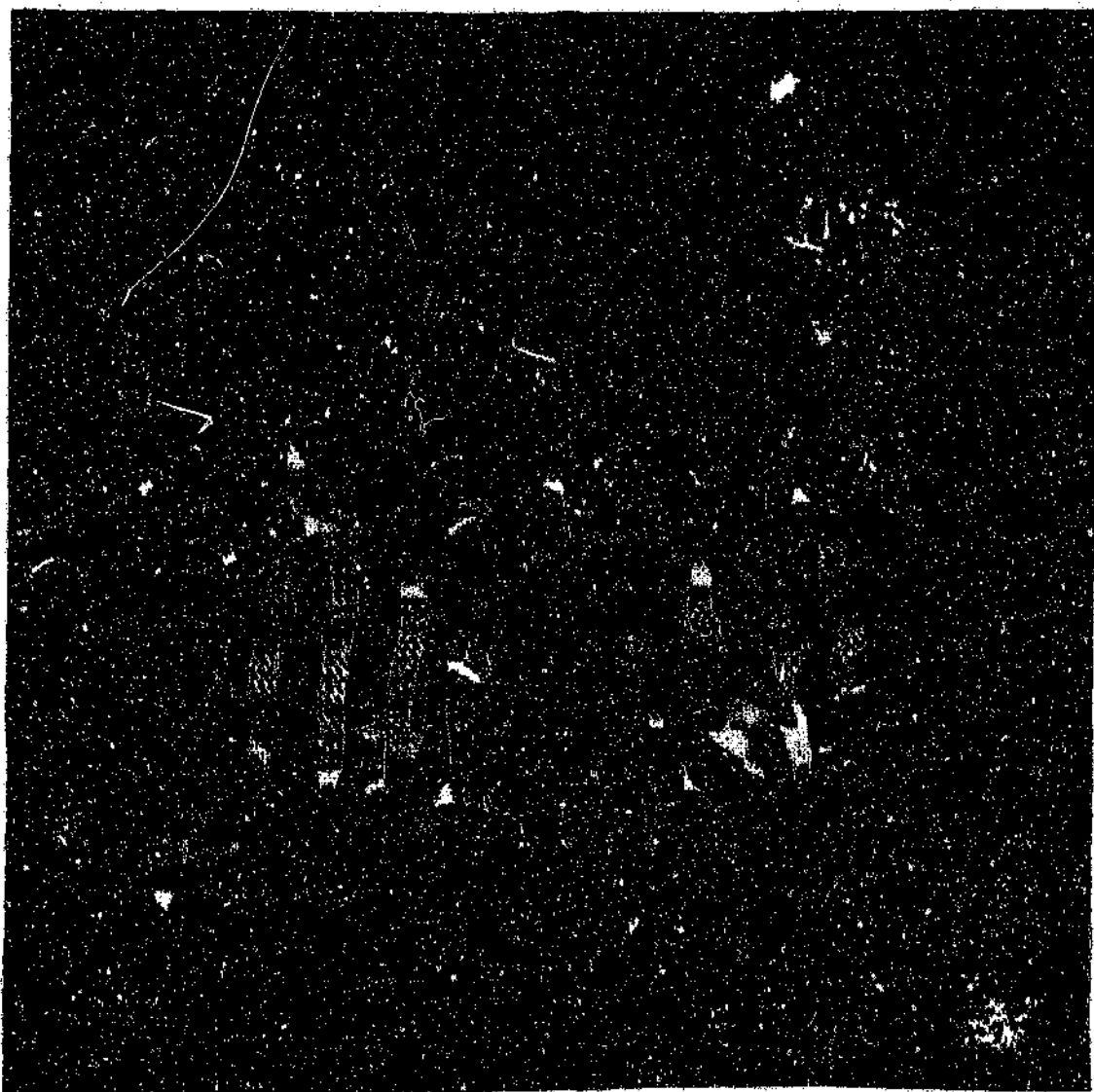


Fig.8 A ribbon representation of the backbone of hGSTP1-1 (Reinemer et al., 1992). The dimeric structure is viewed from perpendicular to the crystallographic 2-fold axis. Diagramme is generated using the graphic viewing programme RASMOL (Sayle and Miller-White., 1995).

inter-subunit polar interactions and which are related by local symmetry within 3.5 Å are as follows: Tyr 49 (subunit 1) - Met 91(subunit 2); Thr 67(1) - Asp94(2); Arg 74(1) - Thr 79(2); Arg 74(1) - Asp90(2); and Thr 75(1) - Gln 83(2). There are also amino acid pairs that were not found to have local symmetry relations between subunit 1 and 2 within 3.5 Å. Such amino acids pairs include: Gln64(1) - Asp94(2), Gln 64(1) - Gly95(2), Ala 87(1) - Arg74(2), and Met91(1) - Thr 67(2). Hydrophobic interactions are the dominant forces participating in the inter-subunit contact (Reinemer et al., 1992). Amino-acid pairs which involve hydrophobic interactions with local symmetry relationships and which occur within the 4 Å range, are as follows: between Leu48, Tyr49, helices α D (Met 91) and α E (Pro128 and Leu132); between strand β 4 (Leu60, Leu62 and Tyr63) and helix α D (Gln84, Ala87 and Met91); between helices α C (Thr67, His71 and Arg74) and helices α D (Ala86, Ala87, Asp90 and Met91). The only repulsive force involved in the association of the human class Pi isoenzyme subunits occurs between the symmetry related Arg70 residues of the individual monomers (Reinemer et al., 1992). The majority of the amino acids involved in the association of monomers are conserved throughout the class Pi isoenzyme (see Fig.5 for details of aligned sequences).

1.9.4 Active Site

Cytosolic glutathione transferases have two kinetically independent active sites per dimer, and each site has two distinctive functional regions: the G-site (G is short for glutathione) for binding of the physiological substrate (reduced glutathione), and the adjacent H-site (H is short for hydrophobic) for the binding of structurally diverse electrophilic substrates (Danielson and Mannervik., 1985). The "floor" of the active site consists of the top of strands β 1 and β 2 of domain 1, and the N-terminus of helices α A and α C. The "external wall" is formed by helices α B and

3₁₀B, while the "internal wall" is formed by the sub-structure of the large domain 2, the C-terminal loop and helix α D of two monomers (Garcia-Saez et al., 1994).

1.9.4.1 The Glutathione-binding site

The glutathione binding site can be identified when the enzyme is in complex with glutathione or glutathione analogues. A number of glutathione analogues have been co-crystallized with class Pi isoenzyme: S-hexylglutathione, glutathione sulphonate and S-(*p*-nitrobenzyl) glutathione (Reinemer et al., 1991; Reinemer et al., 1992; Dirr et al., 1994a; Garcia-Saez et al., 1994). The first competitive inhibitor used to complex with class Pi isoenzyme was glutathione sulphonate and the amino acids in contact with glutathione sulphonate were defined (Reinemer et al., 1991). This was further proved when the structure of human class Pi GST complexed with S-hexylglutathione was solved (Reinemer et al., 1992), and the refined crystal structure of porcine class Pi enzyme complexed with glutathione sulphonate at higher resolution (Dirr et al., 1994a). In the same year, Garcia-Saez et al. (Garcia-Saez et al., 1994) resolved the crystal structure of murine class Pi GST in complex with all three different glutathione analogues at an improved resolution of 1.8 Å, which further supports the assigned G-site. The extended conformation of glutathione analogues with class Pi GST was similar to those which complexed with other classes of GSTs. For example, the rat class Mu isoenzyme complexed with reduced glutathione (Ji et al., 1992), and human class Alpha isoenzyme complexed with S-benzylglutathione (Sinning et al., 1993). Plant class Theta isozyme complexed with S-hexylglutathione (Reinemer et al., 1996), and blowfly class Theta GST complexed with reduced glutathione (Wilce et al., 1995), while squid class Sigma GST complexed with 1-(S-glutathionyl)2,4-dinitrobenzene (Ji et al., 1995).

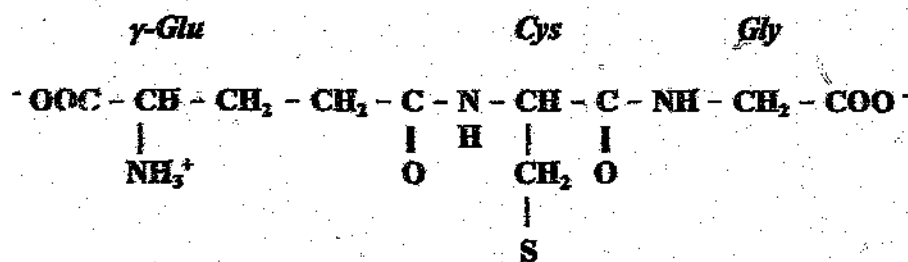
The G-site is formed mainly by helix α B, a loop connecting helix α B to strand β 3 and a loop connecting strand β 4 to helix α C. Recognition and binding of GSH at the G-site involves several side and main-chain polar interactions. Amino acids involved in the recognition and binding are identical in class Pi isozyme irrespective of the type of inhibitor co-crystallized with the enzyme. This is due to the > than 80 % amino acid sequence identity and conservation of amino acids involved in binding of glutathione analogues. Aligned amino acid sequences of several mammalian glutathione S-transferase displaying these residues are strictly conserved or conservatively replaced (Dirr et al., 1994b). Residues of different classes GSTs involved in recognition and binding of glutathione and its analogues are shown in Table.3.

Gln64 is hydrogen bonded to the nitrogen atom of the γ -Glu residue of glutathione, and this nitrogen atom is also hydrogen-bonded to Asp98 of the other subunit. The hydroxyl group of Ser65 interacts with one carboxylate oxygen of γ -Glu of glutathione, whereas the amide nitrogen of Ser65 is hydrogen bonded to the second carboxylate oxygen of the same γ -Glu residue. Arg13 is situated close to the terminal carboxylate group of the γ -Glu of glutathione and its guanidinium moiety is hydrogen bonded to the oxygen atom of γ -Glu in the porcine and human class Pi isozyme (Dirr et al., 1994a). Arg13 is also salt bridged with Glu97. In the case of murine class Pi isozyme, the orientation of the guanidinium moiety with the oxygen atom of carboxylate group did not form hydrogen bonding, although the distance between the two atoms fall into the allocated range needed for hydrogen bonding, 3.5Å (Garcia-Saez et al., 1994). Instead Arg13 is hydrogen-bonded and linked by salt bridge with Glu97. Stenberg et al (Stenberg et al., 1991) have shown that the replacement of the conserved Arg13 residue of human class Alpha isoenzyme with Alanine resulted in a dramatically reduced enzyme catalytic activity and altered

steady-state kinetic parameters. This can be interpreted as a reduced binding affinity toward glutathione. Widersten et al (Widersten et al., 1992) have shown the contribution of the forces between Arg13 and Glu97 residues towards the conformational stability in terms of thermostability. They replaced Arg13 with an Alanine residue in the human class Pi enzyme. This supports the concept of Arg13's participation in the binding of glutathione and its analogues at the active site, as well as the contribution of the salt bridge between Arg13 and Glu97 in stabilizing the protein conformation at the γ -Glu site of GSH. The N^ε of Gln51 of human class Pi enzyme is hydrogen bonded to the C-terminal carboxylate oxygen atom of the Cys residue of glutathione as well as to the carbonyl oxygen of γ -Glu. Leu52 interacts with its main chain by hydrogen bonding in an anti-parallel β -sheet manner with the atoms of the Cys residue of glutathione. This thus represents an important factor in the recognition and proper orientation of glutathione (Chen et al., 1988). However, there is a variation occurring in the class Mu isoenzyme when compared with Alpha and Pi classes. Class Mu isoenzymes have the distinctive character of special backbone conformation at the Cys-Gly peptide bond. The carbonyl oxygen of Cys is hydrogen bonded to the indole nitrogen of Trp7. This is in contrast with the Cys-Gly peptide backbone (in the case of Alpha and Pi classes), which have conserved Phe residue in the equivalent position (Dirr et al., 1994b).

The hydroxyl group of Tyr forms a bifurcated hydrogen bond to sulphonate oxygens O¹ and O² in the sulphonate complex. In the S - (p-nitrobenzyl) glutathione and S-hexylglutathione complexes, the hydroxyl oxygen of Tyr is at the correct hydrogen bonding range, except that it is hydrogen bonded to the sulphur atom (Garcia-Saez et al., 1994). A similar situation was observed in class Mu GST with glutathione (Ji et al., 1992). Gln51 is also hydrogen bonded to the C-terminal carboxylate

a. Structure of glutathione



b.

Glutathione moieties	hGSTP1-1	pGSTP1-1	mGSTP1-1	hGSTA1-1	rGSTM1-1	Arabidopsis thaliana	Schistosoma japonicum	Squid (Sigma class)	Lucilia cuprina	
$\gamma\text{-Glu}$	NH_3^+	Gln64	Gln62	Gln64	Gln66	Gln71	Gln66	Gln62	Gln64	
	COO^-	Asp98*	Asp96*	Asp96*	Asp100*	Asp105*	Asp100*	Asp96*	-	
	C=O	Arg13 Ser65 Gln51	Arg13 Ser63 Gln49	Ser65 Ser63 Gln51	Thr67	Ser72	Gln66 Ser67	Gln66 Ser67	Gln62 Ser63	Ser65 Arg66
Cys	NH	Leu52	Leu50	Leu52	Val55	Leu59	Val54	Leu54	Met50	Ile52
	C=O	Leu52	Leu50	Leu52	Val55	Trp7	Val54	Trp7	Met50	Ile52
	S	Tyr7	Tyr7	Tyr7 Arg14	Tyr8	Tyr6	Ser11	Tyr6	Tyr7	Ser9
Gly	NH	-	-	-	-	Asn58	-	Asn53	-	-
	COO^-	Trp38 Lys44 Gln51	Trp38 Lys42 Gln49	Trp38 Lys44 Gln51	Arg44 Arg130*	Arg42 Trp45 Lys49	His40 Lys41 Gln53	Lys44	Trp38 Lys42 Asn48	His38 His50

Table.3 (a) The structure of glutathione; (b) Amino acids involved in the specific polar interactions sequestering glutathione at the G-site of cytosolic glutathione S-transferases from different species. Asterisks indicate the interaction contributed from residues of neighbouring subunit (adopted and modified from Reinemer et al., 1996).

oxygen atoms of the Gly residue of glutathione. The other carboxylate oxygen atom of Gly is hydrogen bonded to both the N^ε of the indole ring of Trp38 and the amino nitrogen from the side chain of Lys44 (Garcia-Saez et al., 1994).

1.9.4.2 Binding site for hydrophobic substrates

The binding site for xenobiotic substrates of GST was initially identified when the human class Pi enzyme was complexed with S-hexylglutathione (Reinemer et al., 1992) and human class Alpha GST (hGST A1-1) complexed with S-benzyl GSH (Sinning et al., 1993). The benzyl or long hydrophobic hexyl group displayed the amino acids related to the H-site (Reinemer et al., 1992; Sinning et al., 1993). The H-site is made up of structural elements from both domains within the same subunit and includes the loop connecting $\beta 1$ to αA (Phe8, Pro9 and Val10); the beginning of αB (Val35 for human class Pi enzyme and Ile35 for murine class Pi isoenzyme); C-terminus of αD (Tyr108); and the C-terminus of the polypeptide chain (Gly205) (Dirr et al., 1994b; Garcia-Saez et al., 1994). The murine class Pi GST in complex with S-hexylglutathione and S-(p-benzyl) glutathione further verifies the location of the H-site in the human isoenzyme (Garcia-Saez et al., 1994). Comparison of aligned class Pi GST sequences have shown that Phe8, Pro9, Val10, Tyr108 and Gly205 are conserved, whereas amino acid at position 35 displayed the variation of hydrophobic amino acid isoleucine, valine and methionine (see details of multiple sequence alignment in Fig.5).

Comparisons of the H-site between the structures of class Pi enzyme complexes with S-hexylglutathione and class Alpha enzyme complexes with S-benzylglutathione show that the hexyl and benzyl groups of the analogues bind in approximately similar regions (Sinning et al., 1993).

As a consequence of sequence variation between different gene classes, there is a variation in the topologies of the H-site (Reinemer et al., 1992; Ji et al., 1992; Sinning et al., 1993; Garcia-Saez et al., 1994). This subsequently results in specific steric limitations within its gene class and further encourages the stereo-selectivity toward hydrophobic substrates at the H-site (Mannervik and Danielson., 1988). The GST supergene family generally exhibits higher affinities toward the more hydrophobic electrophiles because the recognition of the substrate at the H-site was mediated primarily by hydrophobic interactions. When a series of S-n-alkylglutathione derivatives were screened as inhibitors for the GST, it was observed that the inhibitory effect increased proportionally with the increase in the length of the hydrocarbon chain of the alkyl group (Askelof et al., 1975). Danielson et al (Danielson et al., 1987) pointed out that cytosolic GST exhibit increased binding affinity in response to increased hydrophobicity of 4-hydroxyalkenal substrates.

The C-terminus region of the class Pi and Mu polypeptide chain exhibit above-average temperature factors which demonstrate elevated conformational flexibility and is controlled by a hydrogen bond between the amide nitrogen of Gly203 (Pi) or the amide nitrogen and side chain of Ser209 (Mu) and the hydroxyl group of Tyr108 (Pi)/Tyr115(Mu) of the C-terminus end of α D (Dirr et al., 1994b). A highly flexible C-terminus will lower the barrier of product release and enhance the rate of product formation, since the rate limiting step in a nucleophilic aromatic substitution reaction is the product dissociation (Dirr et al., 1994b). The higher flexibility of the H-site will promote the accommodation of a broader range of structurally different hydrophobic electrophiles.

1.10 Site-directed mutagenesis of class Pi GSTs

Class Pi GSTs are frequently used in site-directed mutagenesis to study the contribution of amino acid residues towards catalytic activity, substrate binding and conformational stability (Tamai et al., 1991; Kong et al., 1991; Kolm et al., 1992; Nishihira et al., 1992; Manoharan et al., 1992a,b; Widersten et al., 1992; Kong et al., 1992c; Kong et al., 1993; Baker et al., 1994; Zimniak et al., 1994; Ricci et al., 1995). Results of mutations done on class Pi GSTs are summarised in Table.4.

1.11 Tryptophan residues

There are two tryptophan residues present in domain 1 of the subunit of the homodimeric class Pi isoenzyme and both tryptophan residues are evolutionary conserved amongst human, porcine, bovine, rat and murine class Pi isoenzymes (see aligned sequences in Fig.5). Trp28 is located at the N-terminus of the β 2 sheet and is non-specifically conserved within different classes of GSTs isoenzymes. The side-chain neighbours, which are within 5Å of Trp28 of human class Pi GST are: Leu17, Leu21, Arg18, Ala22, Met19, Phe8, Val5, Ser27, Glu197, Phe192 and Glu30 (Reinemer et al., 1992). It is thought that Trp28 residue may be involved in the binding of the non-substrate ligand (which may regulate enzyme activity of class Pi isoenzyme).

Tryptophan 38 is located at the N-terminus of helix α B at the active site of the human class Pi GST and is involved in the recognition of the Gly residue of glutathione. The side chain neighbours of Trp38 within 5 Å are Val5, Val6, Thr4, Pro53, Phe55, Glu31, Lys29 and Lys54 (Reinemer et al., 1992).

Residue mutated	Environment, possible function and effects of mutations	References
Tyr7	active site; catalytic; deprotonates glutathione and stabilizes the thiolate anion; replacement nearly abolishes all enzyme activity, but does not impair glutathione binding ability.	Manoharan et al., 1992a; Kolm et al., 1992; Kong et al., 1992a.
Arg11	play the structural role; interactions with domain 2 stabilizes the active-site loop; replacement diminishes catalytic function.	Manoharan et al., 1992b.
Arg13	binding and recognition of carboxyl group of γ -Glu moiety of GSH; diminished catalytic function and marked loss of GSH binding capacity.	Manoharan et al., 1992a,b; Widersten et al., 1992; Kong et al., 1992c.
Cys14	N-terminus of helix α A of domain 1; involved in the catalytic deprotonation of hydroxyl group of Tyr7; mutations resulted in loss of catalytic activity.	Kong et al., 1992; Tamei et al., 1991.
Arg18	in helix α A of domain 1; side-chain is buried and salt-linked to the conserved Glu30; mutations resulted decreased protein stability and S-conjugating activity ;	Manoharan et al., 1992b.
Trp38	active site; catalytic; mutation resulted marked reduction of GSH binding affinity and catalytic activity.	Nishihira et al., 1992a; Baker et al., 1994.
Lys44	part of helix α B; active site; involved in the interaction with the carboxylate group of Gly moiety of GSH; mutation resulted considerable loss of enzyme activity and GSH or GSH-analogues binding affinity.	Widersten et al., 1992; Kong et al., 1992c.

Table.4 A summary of site-directed mutagenesis on class Pi glutathione S-transferases.

Cys47	structural role; 3 ₁₀ -helix after helix αB; mutation resulted partial loss of enzyme activity; mutation induces a positive cooperativity in GST P1-1.	Kong et al., 1991; Tamai et al., 1991; Nishihira et al., 1992; Ricci et al., 1995.
Leu48	part of linker between 3 ₁₀ -helix and helix αC; mutation resulted considerable loss of enzyme activity.	Manoharan et al., 1992b.
Gln51	part of linker between 3 ₁₀ -helix and helix αC; mutation resulted substantially reduction of GSH binding ability and enzyme activity.	Widersten et al., 1992; Kong et al., 1992c.
Asp57	in β3; involved in correct packing of helix αC into β3 and β4 region; play a functional role which maintain the proper stable conformation of GST P1-1; mutation did not lower enzyme activity but reduced the thermostability of the enzyme.	Manoharan et al., 1992; Kong et al., 1993.
Gly58	end of β3; mutation caused partial loss of enzyme activity.	Manoharan et al., 1992b.
Gln64	active site; involved in binding of GSH; mutation caused dramatic reduction of GSH binding and enzyme activity.	Manoharan et al., 1992a,b; Widersten et al., 1992; Kong et al., 1992c.
Ile68	in helix αC; the side-chain formed part of the compact hydrophobic core structure; involved in the packing of αA onto β3 and β4; mutation resulted the unmeasurable enzyme activity.	Manoharan et al., 1992b.
Arg70	in helix αC; involved in polar interaction within its own subunit and with the other subunit at domain interface; mutation resulted instable protein.	Manoharan et al., 1992b.
His71	in helix αC; side-chain of His71 formed the compact hydrophobic core structure; mutation resulted partial loss of enzyme activity for H71R mutant and little reduction of enzyme activity for H71N mutant.	Kong et al., 1991; Manoharan et al., 1992b.

Ler72	in helix α C; formed part of hydrophobic core structure; mutation resulted partial enzyme activity.	Manoharan et al., 1992b.
Arg74	in helix α C; salt-linked to Asp90; mutation resulted instable protein.	Manoharan et al., 1992b.
Asp98	in helix α D at active site; involved in binding and recognition of GSH; in contact with neighbouring subunit; mutation did not alter the thermostability of the enzyme.	Manoharan et al., 1992a; Widersten et al., 1992; Kong et al., 1993.
Cys101	in helix α D; mutation did not alter the kinetic parameters.	Kong et al., 1991; Nishihira et al., 1992; Ricci et al., 1995.
Val104	in helix α D; helps to determine the geometry of H-site and may influence the enzyme activity by interacting with residues directly involved in substrate binding.	Zimniak et al., 1994.
Lys120	in helix α E; mutation resulted improved catalytic activity.	Manoharan et al., 1992b.
Asp152	in helix α F; mutation did not alter catalytic activity but introduced lower thermostability; contributed to the conformational stability of GST P1-1.	Kong et al., 1993.
His162	in helix α F; mutation did not alter the catalytic activity.	Kong et al., 1993.
Cys169	in 3_{10} -helix prior to helix α G; mutation did not alter the catalytic activity.	Kong et al., 1991.
Arg182	in helix α G; mutation resulted in partially impaired enzyme activity.	Manoharan et al., 1992b.

1.12 Conformational stability of class Pi GSTs

The conformational stability of class Pi GSTs has been examined under equilibrium conditions by monitoring a variety of structural and functional parameters (Dirr et al., 1991; Erhardt and Dirr., 1995). A highly co-operative two-state folding/unfolding mechanism of unfolding for the class Pi GSTs was suggested with only folded dimer and unfolded monomer present in equilibrium, with the folded monomer being suggested to be thermodynamically unstable. The conformation of class Pi GSTs is stable when compared with the conformational stability of other dimeric proteins (Neet and Timm., 1994).

1.13 Objective

The objective of this project is to study the contribution of the evolutionary conserved tryptophane residue at position 28 to the catalytic function and structural stabilization of class Pi GSTs. In this study, the *E. coli* JM109 containing plasmids encoding wild-type or the W28F mutant enzyme of hGSTP1-1 will be grown and the production of the enzyme will be over-expressed by the addition of IPTG. S-hexylglutathione affinity chromatography will be used to purify the enzyme, while homogeneity of the protein will be confirmed by SDS-PAGE, IEF, size-exclusion HPLC and western blotting. Steady-state enzyme kinetics, steady-state fluorescence spectroscopy, urea-induced unfolding experiments and urea-gradient gel electrophoresis will be used to investigate the importance of the evolutionary conserved Trp28 in maintaining a functional and stable class Pi GSTs structure. In addition, homology modelling of the W28F mutant enzyme will be used to aid this study.

Chapter 2

Material and Methods

2.1 Materials

pUC120 π expression plasmids encoding the wild-type and W28F mutant hGSTP1-1 were provided by Manoharan et al (Manoharan et al., 1992b). CDNB, reduced GSH, acrylamide, urea and isopropyl- β -D-thiogalactopyranoside were used from the highest grade of materials.

2.2 Over-expression and purification of recombinant protein

2.2.1 Culture growth and over-expression

The primary cultures of *E. coli* JM109, harbouring the pUC120 π plasmid encoding the wild-type human GSTP1-1 (Manoharan et al, 1992b), or the corresponding W28F mutants, were initiated by inoculating stock stab culture into LB broth (1 % (w/v) tryptone, 0.5 % (w/v) yeast extract and 0.5 % (w/v) NaCl, pH 7.0), supplemented with 100 μ g ampicillin / ml of LB broth. Primary cultures were grown to saturation on a rotary shaker at approximately 120 r.p.m. and 37°C. An overnight culture was diluted to 1 % (v/v) with freshly prepared sterile LB broth, supplemented with 100 μ g ampicillin / ml of LB broth. The secondary culture was grown to O.D₆₀₀ = 0.35 with continuous shaking at 120 r.p.m. and 37°C before the initiation of over-expression. Over-expression of the recombinant enzyme was initiated by the addition of 1 mM (final concentration) isopropyl- β -D-thiogalactopyranoside (IPTG), whereafter the culture was returned to the shaker and

grown overnight under the same conditions as mentioned above.

Bacteria were harvested by centrifugation for 20 min at 7 000g and 4°C, then resuspended in PBS, pH 7.4, containing 8 % NaCl (w/v), 0.2 % KCl (w/v), 1.44 % Na₂HPO₄ (w/v), 0.2 % KH₂PO₄ (w/v). The breakdown of bacterial cell walls was assisted by the addition of chicken egg lysozyme at 1 mg/ml bacterial suspension for 1 hour at room temperature. Cells were then disrupted by continuous sonication for 15 sec and cooled by using a dry ice and ethanol bath. Bacterial lysate was centrifuged for 20 minute at 10 000g and 4°C. Supernatant was collected and subjected to S-hexylglutathione affinity chromatography purification procedure. (see 2.2.2 for details).

2.2.2 S-hexylglutathione affinity chromatography

Purification of the wild-type hGSTP1-1 and W28F mutant enzymes was carried out according to the method described by Mannervik and Guthenberg (Mannervik and Guthenberg, 1981). S-hexylglutathione affinity column was regenerated with 100 ml of 8 M urea and then re-equilibrated with 0.1 M acetate buffer, pH 4, containing 0.5 M NaCl, 0.1 M Tris/HCl. The column was finally re-equilibrated with 20 mM Tris/HCl buffer, pH 7.8, containing 0.2 M NaCl and 0.02 % (w/v) sodium azide. The supernatant fraction was applied onto the affinity column at a constant flow rate of 25 ml/hr. The affinity column was washed with the same 20 mM Tris/HCl buffer, pH 7.8, until the absorbance of effluent at 280 nm was below 0.1 which indicated that the affinity column was free of unbound cytosolic proteins. Adsorbed enzymes were eluted from the column with 1 mM S-hexylglutathione in the 20 mM Tris-HCl buffer, pH 7.8, at a constant flow rate, while fractions containing high enzyme activity and protein concentration were pooled together.

The pooled fraction was concentrated by ultrafiltration using PM-10 membrane (Amicon). The enzyme was then subjected to buffer exchange by passing the enzyme through the sephadex G-25 column equilibrated with 20 mM sodium phosphate buffer, pH 6.5, containing 1 mM EDTA, 0.1 M NaCl and 0.2 % (w/v) sodium azide. The pooled fractions with high protein concentration and enzyme activity were pooled together and concentrated between 0.5 and 0.8 mg/ml.

2.3 Protein concentration determination

Protein concentration was determined by calculation of the extinction coefficient of human wild-type and W28F mutant enzyme from the known amino acid sequences from Manoharan et al (Manoharan et al., 1992b) according to the method devised by Perkins (Perkins., 1986).

$$\epsilon = 5550 \sum \text{Trp residues} + 1340 \sum \text{Tyr residues} + 150 \sum \text{Cys residues}$$

Where ϵ is the extinction coefficient, 5550 is the molar absorption coefficient of Trp residue, 1340 is the molar adsorption coefficient of Tyr residue, and 150 is the molar adsorption coefficient of Cys residue. The calculated extinction coefficient of dimeric wild-type and W28F mutant human GSTP1-1 were 49 600 $M^{-1}.cm^{-1}$ and 27 400 $M^{-1}.cm^{-1}$, respectively.

2.4 Homogeneity determinations

2.4.1 SDS-PAGE

SDS-polyacrylamide gel electrophoresis of the cell lysate and purified enzyme was performed according to the method of Laemmli (Laemmli, 1970). The discontinuous gel system was made up with 4 % (w/v) acrylamide stacking gel with 0.0625 M Tris/HCl buffer, pH 6.8, containing 0.1 % (w/v) SDS, 15 % (w/v) acrylamide separating gel with 0.375 M Tris/HCl buffer, pH 8.8, containing 0.1 % (w/v) SDS. The purified molecular mass marker proteins used were bovine serum albumin (bSA) (66 kDa), ovalbumin (45 kDa), glyceraldehyde-3-phosphate dehydrogenase (36 kDa), carbonic anhydrase (29 kDa), trypsinogen (24 kDa), trypsin inhibitor (20.1 kDa) and α -lactalbumin (14.2 kDa). Protein samples were prepared at 1:1 dilution with sample buffer (62.5 mM Tris/HCl buffer, pH 6.8, containing 2 % SDS (w/v)) 5 % (w/v) β -mercaptoethanol, 10 % (v/v) glycerol and 0.02 % (w/v) bromophenol blue. Samples were mixed and boiled for 3 minutes before application. Samples were applied to the wells of SDS-PAGE gel and electrophoresed at 120 V for 2-3 hours. 0.025 M Tris/HCl, 0.192 M glycine buffer, pH 8.3, containing 1 % (w/v) SDS was used as the electrolyte buffer. Gels were stained in Coomassie blue staining solution (2 % (w/v) Coomassie Brilliant blue R250, 13.5 % (v/v) glacial acetic acid and 18.75 % (v/v) ethanol) and destained with 40 % (v/v) ethanol and 10 % (v/v) glacial acetic acid until the background was clear.

2.4.2 Isoelectric focusing

Isoelectric focusing was performed using the BioRad Model 111 Mini-IEF gel kit. Monomer-ampholyte solution was prepared as follows: 2 ml monomer concentrate

(24.25 % (w/v) acrylamide and 0.75 % (w/v) bisacrylamide) mixed with 0.5 ml ampholyte solution with a pH range of 3.8 to 9.2 (BioRad) and 2 ml of 25 % (v/v) glycerol. The mixture was made up to 10 ml with deionized water and degassed for 5 minutes. The catalyst solution was prepared by mixing 15 μ l 10 % (w/v) ammonium persulphate with 50 μ l 0.1 % (w/v) riboflavin and 3 μ l TEMED. The monomer-ampholyte mixture was mixed with the catalyst solution and pipetted between the casting tray and a photosensitive plastic sheet then allowed the acrylamide gel mixture to polymerise for 45 minutes by exposing it to light. Once the plastic sheet with the gel was removed from the casting tray, the gel was irradiated for an additional 15 minutes. After which a template with wells for sample application was placed onto the gel. 2 μ l of isoelectric point calibration proteins (Sigma) and purified hGSTP1-1 enzyme (buffer exchanged with 20 mM sodium phosphate buffer, pH 6.5, containing 1 mM EDTA and 0.2 % (w/v) sodium azide) were applied onto the wells. Proteins were allowed time to diffuse into the gel with the template being removed just prior to the gel being placed onto the graphite electrodes of the electrophoresis cell. The gel was initially focused at 100 V for 15 minutes and subsequently focused at 200 V for 15 minutes, and finally at 450 V for 1 hour. The focused protein samples were fixed by immersing the gel in the fixing solution (4 % (v/v) sulphosalicylic acid, 12.5 % (v/v) trichloroacetic acid and 30 % (v/v) methanol) for 30 minutes. The IEF gel was stained with 27 % (v/v) isopropanol, 10 % (v/v) acetic acid and 0.04 % (w/v) Coomassie Brilliant Blue R-250 for 1 hour, and destained first in 12 % (v/v) isopropanol, 7 % (v/v) acetic acid and 0.5 % (w/v) CuSO_4 and then in 25 % (v/v) isopropanol and 7 % (v/v) acetic acid to remove the last trace of stain and copper sulphate in the first destaining solution. It is important not to over-destain the gel as the thin film of IEF gel can detach from the plastic sheet. The pI calibration proteins were purchased from Sigma and made up with the following proteins: amyloglucosidase (pI 3.6), trypsin inhibitor of soy bean (pI 4.6), β -lactoglobulin A from bovine milk (pI 5.1), carbonic anhydrase II from

bovine erythrocytes (pI 5.9), carbonic anhydrase I from human erythrocytes (pI 6.6), myoglobin from horse heart (pI 7.2) and trypsinogen from bovine pancreas (pI 9.3).

2.4.3 Size-exclusion HPLC

Size-exclusion HPLC is a useful method, and it can provide information about the homogeneity and hydrodynamic volume of biological macromolecules. Size exclusion HPLC was carried out using a Biosep-SEC-S3000 column with dimensions of 300 mm x 7.8 mm (Phenomenex), 20 mM sodium phosphate buffer, pH 7.5, containing 0.1 M NaCl, 0.02 % (w/v) sodium azide, which was degassed and filtered through a 0.45 μ m nylon membrane. The 20 mM sodium phosphate buffer was used as a solvent in the experiments. Blue dextran and tryptophan were used to establish the void and internal volumes of the HPLC column. Purified wild-type and W28F protein samples were loaded onto the column separately. Porcine class Pi isoenzyme was used as a reference protein. The molecular mass of both wild-type and W28F mutant enzymes was calibrated by the following proteins: bSA (66 kDa), ovalbumin (48 kDa), carbonic anhydrase (29 kDa), α -chymotrypsinogen (25 kDa) and myoglobin (17 kDa). The elution of protein samples was carried out at a flow rate of 0.5 ml/min. Elution profiles were detected at 280 nm by the UV-absorbance detector.

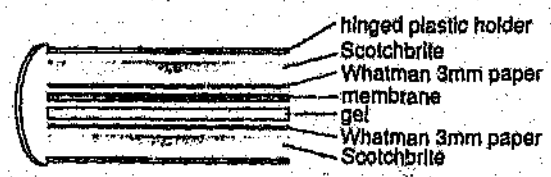
2.4.4 Western blot

Protein samples (2.3 and 4.6 μ g of homogeneous pGSTP1-1, 7 μ g of homogeneous wild-type hGSTP1-1 and 15 μ g bSA which was used as control sample) were separated according to molecular mass using the discontinuous SDS-PAGE gel system with 15 % (w/v) acrylamide in separation gel and electrophoresed (see details in section 2.4.1). One duplicate of the gel was stained with Coomassie

Brilliant Blue R250, while the other duplicate was used for the electro-transfer of protein from the acrylamide gel to the nitrocellulose membrane. The nitrocellulose membrane and Whatman 3MM paper were trimmed to the size of the gel and pre-soaked in a transfer buffer (25 mM Tris/HCl and 192 mM glycine buffer, pH 8.3, containing 20 % (w/v) methanol). The blotting sandwich was assembled according to the figure shown in Fig.9a, and was tightly secured with elastic bands, then placed in the transferring apparatus (Trans-Blot Cell, BioRad) in the correct orientation (see Fig.9b). The membrane was closed to the anode and the gel was facing the cathode to ensure that the protein would migrate into the nitrocellulose membrane). A constant current of 200 mA was applied overnight at 4 °C. The nitrocellulose membrane was removed from the transferring apparatus.

The non-specific binding sites on the membrane were blocked by incubating the membrane with 1 % (w/v) fat free powdered milk, 20 mM Tris/HCl buffer, pH 7.5, containing 0.5 M NaCl for 30 minutes with continuous shaking, at room temperature. The membrane was washed twice with the 20 mM Tris/HCl buffer, pH 7.5, containing 0.5 M NaCl and 0.05 % (v/v) Tween-20, for 10 minutes. This was followed by incubating the membrane with 500-fold diluted rabbit polyclonal anti-hGSTP1-1 antiserum (Gulick et al., 1992) in 1 % (w/v) fat free powdered milk in the 20 mM Tris/HCl buffer, pH 7.5, containing 0.5 M NaCl, for 60 minutes with continuous shaking. The nitrocellulose membrane was washed twice with 20 mM Tris/HCl buffer, pH 7.5, containing 0.5 M NaCl and 0.05 % (v/v) Tween-20 prior to incubation with the secondary antibody (5000-fold diluted goat anti-rabbit IgG

a



b

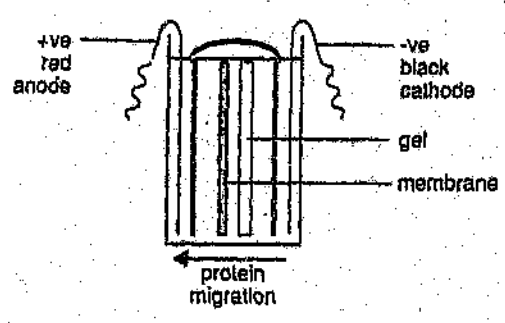


Fig.9 Western blotting apparatus. (a) Assembly of the blotting "sandwich"; (b) Orientation of the "sandwich" in the blotting tank (adopted from Soutar and Wade., 1990).

conjugated with alkaline phosphatase in the 20 mM Tris/HCl buffer, pH 7.5, containing 0.5 M NaCl, with 1 % (w/v) fat-free milk powder), for 60 minutes with continuous shaking. The nitrocellulose membrane was washed with 0.05 % Tween-20 in the 20 mM Tris/HCl buffer, pH 7.5, containing 0.5 M NaCl. The colour of the blot was developed by immersing the membrane in the colour developing solution (3 mg 5-bromo-4-chloro-3-indoyl phosphate and 6 mg Nitro blue tetrazolium in 10 ml of 10 mM Tris/HCl buffer, pH 9.5 containing 100 mM NaCl and 5 mM $MgCl_2$) until the colour changed to a visible purple one. The reaction was stopped by immersing the membrane in deionized water for 10 minutes and the deionized water was changed once or twice, depending on the degree of colour development, until the residual-colour of the developing solution was removed. The membrane was air-dried before being photographed.

2.5 Steady-state kinetic studies

2.5.1 Routine enzyme assay

GST catalytic activity was monitored by the spectrophotometric assay developed by Habig and Jakoby (Habig and Jakoby.,1981). The standard enzyme assay was measured at 340 nm with final concentration of 1 mM 1-chloro-2,4-dinitrobenzene (CDNB) and 1 mM reduced glutathione (GSH) in 0.1 M potassium phosphate buffer, pH 6.5, containing 1 mM EDTA, 0.2 % (w/v) sodium azide. Specific enzyme activity was determined over a range of different concentrations of enzyme under the standard assay condition. Non-enzymatic rate was substrated from assay containing enzymes.

2.5.2 V_{max} and K_m

The Michaelis-Menten constant (K_m) of wild-type and W28F mutant hGSTP1-1 toward reduced GSH, was determined by assaying the enzyme with reduced glutathione (0 and 6 mM), and maintaining the CDNB concentration at 2 mM, which is the upper limit of CDNB solubility in aqueous solutions. The K_m of the enzyme toward CDNB was determined by assaying the enzyme with reduced glutathione fixed at 6 mM and CDNB up to 2 mM.

2.5.3 Catalytic efficiency (k_{cat}/K_m)

At a sufficiently low concentration of substrate, the catalytic activity of GST with substrate becomes a first-order reaction and the Michaelis-Menten equation can be reduced to a first-order equation. This implies that the initial velocity of the enzyme catalysed reaction is proportional to the substrate concentration (Marnervik and Danielson., 1988).

Michaelis-Menten equation:

$$V_o = V_{max} [S] / (K_m + [S]) \quad (\text{Eq.1})$$

If [S] is negligible when compared with K_m , then

$$V_o = V_{max} [S] / K_m \quad (\text{Eq.2})$$

since
$$V_{\max} = k_{\text{cat}} [E]_t \quad (\text{Eq.3})$$

then equation 3 becomes

$$V_o = k_{\text{cat}} [E]_t [S] / K_m \quad (\text{Eq.4})$$

Where V_o is the initial velocity, $[E]_t$ represents the total active site (subunit) concentration, k_{cat} is the apparent turnover number, K_m is the Michaelis-Menten constant, and $[S]$ represents the substrate concentration. Provided the protein concentration is known, one can then calculate the k_{cat}/K_m value from the slope of a V_o vs $[S]$ plot. The catalytic efficiency value was confirmed by repeating the experiment with different amounts of enzyme.

2.5.4 Inhibition by glutathione analogues

GSH analogues (S-hexylglutathione and glutathione sulphonate) were used to determine the effect of replacement of Trp28 by Phe on the enzyme activity of human GSTP1-1. Experiments were performed according to the method of Kolm et al (Kolm et al., 1992). 2.88 μg of enzyme was diluted in 0.1 M potassium phosphate buffer, pH 6.5, containing 1 mM EDTA, 0.2 % (w/v) sodium azide. Glutathione sulphonate or S-hexylglutathione was added to the enzyme solution to form a final concentration of 0 to 160 μM . The activity of the enzyme in the presence of glutathione analogues was measured by the addition of 1 mM reduced glutathione and 1 mM CDNB. The activity was monitored spectrophotometrically at 340 nm and the concentration of glutathione analogues, which gave 50 % inhibition (I_{50}), was determined by plotting % residual activity vs log glutathione analogue concentration.

2.6 Thermal-inactivation studies

Thermal-inactivation studies of GST enzymes were performed according to the method of Kong et al (Kong et al., 1993b). Briefly, 1 μ M of Wild-type and W28F mutant enzyme were prepared with 20 mM sodium phosphate buffer, pH 6.5, containing 100 mM NaCl, 1 mM EDTA and 0.2 % (w/v) sodium azide, with the addition of 2 mM DTT (final concentration to prevent oxidative inactivation). Enzyme samples were then incubated for 10 minutes at a temperature between 30 to 60 ° and then assayed with 1 mM reduced GSH and 1 mM CDNB at room temperature for residual activity (see section 2.5.1 for details of the routine assay). Thermal inactivation experiments were also performed by incubating the enzyme samples for different time periods at 55 °C. Residual activity was also assayed at 1 mM reduced GSH and 1 mM CDNB at room temperature, as above.

2.7 Steady-state fluorescence spectroscopy

Fluorescence spectroscopy is a useful technique for studying proteins and their interactions with other molecules, as it is very sensitive and can be done quickly. The period for the emission to occur is short, since the fluorescence emission occurs within an average of 10^{-8} sec after light absorption (Lakowicz., 1983). The classical energy level diagram proposed by A. Jablonski briefly explains the physics behind the phenomenon of fluorescence emission (Lakowicz., 1983) (see Fig.10). According to this "explanation," fluorophores can exist at three different electronic energy levels. These levels are S_0 , S_1 and S_2 , respectively. In addition to this, three vibrational energy levels occur within each electronic energy level and they are designated 0, 1 and 2. The fluorophore at the ground state (S_0) can absorb incoming light and then become excited to a higher vibrational energy state (which can either be at S_1 or S_2). In most cases, the fluorophore relaxes to the lowest

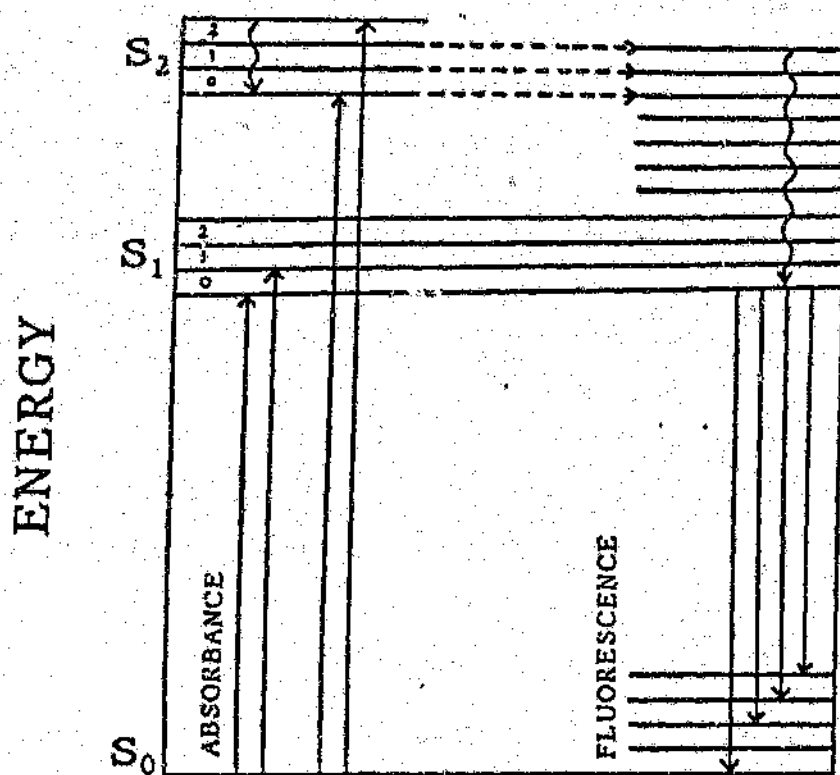


Fig.10 Photophysical events of the emission of fluorescence of fluorophores (Lackowicz., 1983).

vibrational energy level of S_1 rapidly at an averaged rate of 10^{12} sec^{-1} . This process is called the "internal conversion", and is usually completed prior to emission. Emission occurs at a fast rate (10^8 sec^{-1}) when the lowest excited vibrational state of S_1 rapidly reaches thermal equilibrium (duration is about 10^{-12} sec). High emissive rates imply that the fluorescence lifetime (the average period of time in which a fluorophore remains in the excited state) is very short (10 nsec). Upon emission of fluorescence, the excited fluorophore returns to the ground state (S_0). Excited fluorophores possess higher energy than the emitted fluorescence and, thus, the fluorescence at the longer wavelength can be detected by recording the emission of the fluorophore at wavelengths longer than the excitation wavelength.

Substances that display significant fluorescence generally possess delocalized electrons present in conjugated double bonds. Trp, Tyr and Phe are the amino acids which contribute to the ultraviolet fluorescence properties of proteins in general. Proteins are usually excited at wavelengths equal to or higher than 280 nm. This excludes Phe's contribution to the overall emission because Phe is excited at approximate 255 nm and with the low quantum yield of Phe, the contribution of Phe residue to emission spectra of protein becomes minimal. When a protein is excited at 280 nm, Trp and Tyr residues are excited, whereas when excitation occurs at $\geq 295 \text{ nm}$, Trp is primarily excited. Tyr fluorescence is generally weak and insensitive to solvent. The contribution of protein fluorescence by Tyr residues can be overcome by excitation of the protein at 295 nm. Trp is the dominant fluorophore and the maximum emission of Trp and indole derivatives are sensitive to solvent polarity and specific interactions between the indole ring and solvent. The emission maximum is, therefore, closely related to the averaged location of Trp within the protein matrix.

2.7.1. Steady-state fluorescence emission

Steady-state fluorescence spectroscopies were performed at room temperature using the Hitachi model 850 fluorescence spectrophotometer. The excitation and emission bandwidths were both set at 5 nm. 1 μM of enzyme (final concentration) was prepared in 20 mM EDTA, 0.2 % (w/v) sodium azide. Samples were excited at 295 nm and emission spectra were recorded from 300 nm to 400 nm. All spectra/data were corrected for buffer blanks.

2.7.2 Quantum yields

The quantum yield of a protein can reflect the degree of exposure of Trp residue and its immediate environment. The quantum yield is the ratio of the number of photons emitted to the number absorbed (Lakowicz., 1983). Quantum yields of the wild-type and W28F mutant enzymes were calculated by comparing the area under the corrected fluorescence spectra of the wild-type or W28F mutant enzyme with a solution of N-acetyl-tryptophanamide (NATA). NATA is the standard reference of free tryptophan and it was corrected to the same absorption at excitation wavelength by using the known quantum yield of NATA. Equal concentration of enzyme (4 μM of wild-type hGSTP1-1 or 6.45 μM W28F mutant enzyme) or NATA were excited at 295 nm and their fluorescence spectra were recorded and buffer baselines were corrected, see 2.7.1. Quantum yields were then calculated from the following equation (Parker and Rees., 1960):

$$\phi_m = (I_U / I_Q) \times (A_Q / A_U) \times \phi_Q \quad (\text{Eq.5})$$

where ϕ_m = quantum yield of wild-type or W28F hGSTP1-1.

ϕ_Q = quantum yield of NATA which is 0.13 (Lehrer., 1971).

I_U = area under the corrected fluorescence spectrum of unknown compound or protein (wild-type or W28F hGSTP1-1).

I_Q = area under the corrected fluorescence spectrum of reference compound (NATA)

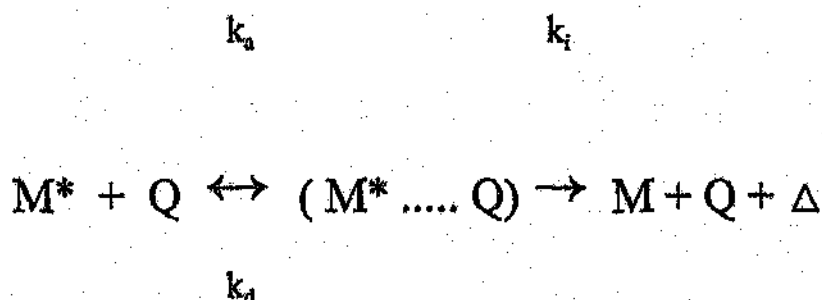
A_Q = Absorbance of reference compound (NATA) at 295 nm.

A_U = Absorbance of protein (wild-type or W28F mutant GST P1-1) at 295 nm.

2.7.3 Acrylamide quenching

An excellent way to experimentally determine the degree of exposure of tryptophan residues in solution is by fluorescence quenching (Lehrer., 1971). The theory behind quenching of fluorescence is by using low molecular mass quenchers which decrease the fluorescence intensity of the indole ring of the tryptophan residue via physical contact with the excited indole ring. A variety of substances have been found to act as quenchers of indole fluorescence; these include iodide, molecular oxygen and acrylamide. The iodide ion is an ionic quencher and is heavily hydrated and able to quench only surface localized Trp residues. The disadvantages of using an ionic quencher is that electrostatic effects between the quencher and the polyelectrolytic protein can influence the quencher's quenching action leading to an over or underestimation of the exposure of fluorophore. Small oxygen molecules can diffuse to the protein interior rapidly, but the molecular oxygen is regarded as relatively hydrophobic and will accumulate in the apolar region of proteins facilitating the quenching of buried Trp residues (Eftink and Ghiron., 1976). Acrylamide is a polar uncharged quenching probe, and is very sensitive to the exposure of Trp residues in proteins. It has also been shown to quench the fluorescence of indole derivative predominately by collisional processes (Eftink and

Ghiron., 1976). Trp fluorescence serves as an index for measuring environmental, local and overall conformational changes. The following scheme describes the bimolecular quenching reaction between the excited state of an indole ring (M^*) and acrylamide (Q) (Eftink and Ghiron., 1976).



where $M^* \dots Q$ = complex formed by diffusional encounter between M^* and Q
 Q = acrylamide.

k_a = diffusion limited rate constant for collision between acrylamide and the indole ring.

k_d = dissociation rate constant of $M^* \dots Q$ complexes.

k_i = rate constant for dissipation of energy.

Δ = dissipated energy as heat

Aliquots of a stock acrylamide solution were added directly to the protein sample (2 μ M) to a quencher (acrylamide) concentration of 0.5 M. Proteins were excited at 295 nm, emission measured at 340 nm and at room temperature. Fluorescence intensity values were corrected for dilution effects and the quenching data analyzed according to the classical Stern-Volmer equation (Lehrer., 1971).

$$F_0 / F = 1 + K_{sv} [Q] \quad (\text{Eq.6})$$

where F_0 is the fluorescence intensity of Trp in the absence of quencher (Q). F is the fluorescence intensity of Trp in the presence of quencher and K_{sv} is the collisional quenching constant.

2.8 Solvent-induced equilibrium unfolding

Solvent-induced equilibrium unfolding is a common method used to estimate the conformational stability of a protein of interest (Ahmad and Bigelow., 1982; Pace., 1986). Denaturation curves are especially useful for measuring the difference in conformational stability among proteins differing slightly in chemical structure. An example of this is the difference in amino acid sequence by selective single amino acid site-directed mutagenesis or slight alteration as result of chemical modifications. It is also possible to use this method to elucidate the overall mechanism of a protein folding process.

Several biophysical techniques can be used to monitor the protein unfolding process: ultraviolet difference spectroscopy, circular dichroism, optical rotation, fluorescence, NMR, etc. One has to choose a technique and optimal experimental conditions for monitoring unfolding. Optical rotation is less sensitive and requires a considerable amount of protein, whereas circular dichroism and difference spectroscopy generally require considerably more, but comparable amounts of, protein. NMR requires larger amounts of protein but can produce more detailed results especially when used to monitor multi-state folding/unfolding mechanisms. Fluorescence is one of the most commonly used techniques to monitor the

equilibrium unfolding process and is based on the differences of intrinsic tryptophan fluorescence intensities at different denaturation concentrations as a result of the protein being unfolded to different degrees. The other advantage is that only small amounts of protein are required to give a measurable signal.

2.8.1 Urea-induced unfolding equilibrium

The wild-type (1 μ M or 10 μ M) and W28F mutant (1 μ M) enzymes were prepared in 20 mM sodium phosphate buffer, pH 6.5, containing 1 mM EDTA, 0.1 M NaCl and 0.2 % (w/v) sodium azide. Urea stock solutions were prepared at 10 M and adjusted to pH 6.5, and then added to protein samples to form a final urea concentration of 8 M. Two hours were allowed for the unfolding of protein by urea to reach a state of equilibrium. Tryptophan residues were excited at 295 nm and their emission monitored at 340 nm for folded protein, and 355 nm for unfolded protein (see section 2.7.1 for details of fluorescence spectroscopy method).

All readings were corrected for the buffer baseline. Urea blanks were also monitored at the same wavelength as above and were subtracted. The enzyme solutions were assayed for activity after the fluorescence intensity was recorded (see section 2.5.1 for details of routine enzyme assay).

2.8.2 Graphical analysis of denaturation curves

Linear extrapolation analysis of denaturation data was performed as described by Pace (Pace, 1986). Relative fluorescence intensity ($F_{355\text{nm}}/F_{340\text{nm}}$) was plotted as a function of denaturant concentration. The linear portions of the plots preceding and following the denaturation transition, which represent the values observed for the folded (Y_f) and unfolded protein (Y_u), were defined by linear regression. The values

were extrapolated into the non-linear portion of the transition curve and the fraction of unfolded protein (f_d) at each denaturant concentration was calculated, as described by Pace (Pace., 1986).

$$f_d = (Y - Y_n) / (Y_d - Y_n) \quad (\text{Eq.7})$$

where f_d is the fraction of unfolded protein, Y is the measured value, Y_n is the observed value for the folded protein and Y_d is the observed value for unfolded protein.

Equilibrium constants (K_D) and the corresponding Gibb's free energies of unfolding (ΔG_D) were then calculated according to the following equations (8 and 9, below) at each denaturant concentration in the transition region:

$$K_D = 2 Pt [f_d / (1 - f_d)] \quad (\text{Eq.8})$$

The following equation is for the calculation of the Gibb's free energy (ΔG_D):

$$\Delta G_D = - RT \ln[K_D] \quad (\text{Eq.9})$$

Where R is the gas constant and T is the temperature.

The linear dependence of ΔG_D on denaturant concentration observed in the transition was assumed to continue to zero denaturant concentration (Schellman., 1978).

Extrapolation to zero denaturant concentration was used to calculate the conformational stability of the protein in the absence of denaturant (ΔG^{H_2O}) by the following relationship (Pace., 1986):

$$\Delta G_D = \Delta G^{H_2O} - m [\text{urea}] \quad (\text{Eq.10})$$

where m is a measure of the responsiveness of the protein to solvent-induced unfolding.

2.9 Urea-gradient gel electrophoresis

This is a useful technique to study the urea-induced unfolding of a protein (Creighton., 1986). This technique involves electrophoresis of a protein through a polyacrylamide gel slab with a continuous linear gradient of urea between 0 to 8 M, perpendicular to the direction of protein migration (Creighton., 1986). The shape of the protein molecule changes upon encountering different concentrations of urea in the polyacrylamide gel and this will result in changed mobility when passing through the pores of the polyacrylamide gel. Protein in its compact, closely-folded state always migrates faster than the more extended and expanded unfolded state. Advantages of this technique are: (1) It is easy, simple and gives a continuous visual picture of different mobilities of protein molecules across the urea gradient. (2) It reveals the electrophoretic distribution of molecules, thereby resolving populations which are slowly interconverted. (3) Conformational stability of native conformation in the absence of urea can be extrapolated, provided the interconversion between conformations is rapid. On the other hand, if the transition is relatively slow, one can also estimate an approximate value of rate constant and identify possible unfolding/refolding kinetic intermediates. (4) This technique is

also one of the most sensitive methods to detect the homogeneity of a protein. For example, it can detect variants with similar mobility in both folded and unfolded states but which differ slightly in sensitivity to urea-induced unfolding.

However, there are certain limitations to this technique. The main limitation is that it is not sensitive enough to detect small changes in conformation. For example, changes in net charges upon unfolding can be compensated for by the change in conformation and given a constant electrophoretic mobility (Hollecker and Creighton., 1982). But limitations such as this one are more than compensated by the advantages.

The gradient gels were casted in specially designed casting apparatus (see Goldenberg and Creighton., 1984; Creighton., 1986); the glass plates (830 mm x 830 mm) were held apart by three plastic spacers (1.5 mm) (a long spacer on the right, which when removed formed a trough on what would be the top of the gel (for sample to be layered into); the second smaller spacer on the left, and the third spacer at the bottom). The plates and spacers were held together and sealed with tape. The gradient was prepared from two stock solutions: a 15 % acrylamide solution [15 % (w/v) acrylamide, 0.004 % (w/v) riboflavin, 0.05 M Tris-acetate pH 8 and 0.12 % (v/v) TEMED] and a 11 % acrylamide solution [11 % (w/v) acrylamide and 8 M urea, buffer and catalytic agents were as the same as first solution].

The setup of the apparatus for casting of the urea-gradient gel can be seen in Fig. 11. Briefly, the assembled glass plate plates were placed in a casting tank and butanol with bromophenol blue as indicator pumped into the casting tank until it reached a height of 2-3 cm from the bottom of the tank. This was followed by pumping in approximately 3 ml of the 15 % (w/v) acrylamide solution into the apparatus. 11 ml of each 15 % (w/v) acrylamide solution without urea and 11 % (w/v) acrylamide

solution with 8 M urea was placed in separate beakers (see Fig.11). The urea-gradient was generated by pumping the low concentration solution into the casting tank, using two channels of a peristaltic pump, while simultaneously mixing the high concentration solution (11 % (w/v) acrylamide with 8 M urea) which pumped through the other single channel of the pump with the low concentration solution (see Fig.11). After the gradient was formed, 10 ml of 11% (w/v) acrylamide solution, containing 8 M urea, was pumped into the tank, so that the gel was finally composed of a 1 cm length of the solution with 8 M urea. Urea-gradient gels were then allowed to photopolymerized by the exposure to light. Once the gels were polymerized and removed from the casting tank, the three spacers were removed and two small spacers added to the side of the trough created for sample application. After this, the vertical edges of the glass were sealed with tape (so that the urea gradient was perpendicular to the direction of electrophoresis). Unfolded enzyme was prepared in 8 M urea, 10 % (v/v) glycerol and 0.002 % (w/v) bromophenol blue, with 2-3 hours allowed for the protein to unfold. Folded protein was prepared with glycerol and 0.002 % (w/v) bromophenol blue as a dye. Urea-gradient gels were pre-electrophoresed in order to remove excessive reacted urea before sample application (The urea solution can produce cyanate which reacts with amino groups of protein and then introduces electrophoretic charge heterogeneity.). Electrophoresis was carried out at a constant current of 15 mA per gel for 3 hours in 0.05 M Tris-acetate buffer, pH 8 (The buffer system was a continuous buffer system). Gels were stained and destained as in the SDS-PAGE procedure (see section 2.4.1).

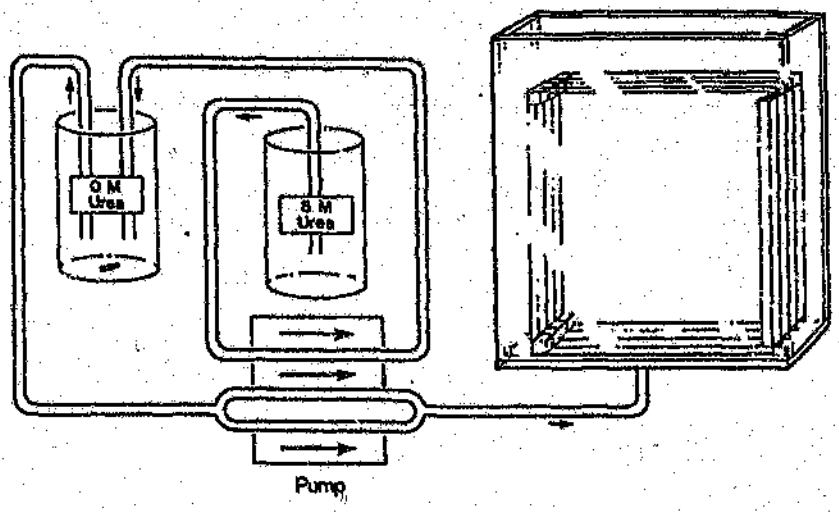


Fig.11 Apparatus for preparing urea-gradient gels (adopted from Creighton., 1986).

2.10 Homology modelling

Homology modelling is a widely used knowledge-based technique for protein structure modelling. One can use it to predict how amino acid substitutions could alter a protein's structure when the three-dimensional structure of a mutant protein is not available. The modelling procedure uses experimentally determined protein structures as templates to predict the conformation of another protein with similar amino acid sequences (Sali and Blundell., 1994; Sali., 1995). Application of the programme PROMOD is made possible from Swiss-Model (Peitsch., 1995; Peitsch., 1996), and it is an automated protein modelling server at the Geneva Biochemical Research Institute, Glaxo Wellcome research and development, S.A. Switzerland. The modelling server can be accessed from the following URL address : <http://expasy.hcuge.ch/swissmod/SWISS-MODEL.html>.

Modelling starts with the superposition of 3D structures based on the diagonals of sequence similarity called SIM (Huang and Miller., 1991). Regions with sequence similarity are selected automatically and the corresponding residues matched in 3D space. The primary match can be further refined by using expanding context spheres from 0.1 to 3Å. The second step is to generate multiple sequence alignment with the sequence of interest to be modelled using FASTA (Pearson and Lipman., 1988) and BLAST (Altschul et al., 1990). A three-dimensional framework for the new protein sequence is generated based on the sequence alignment and consideration of atoms topologically identical to the new structure and identical to at least one supplied known three-dimensional structure. Atoms which occupy a similar portion of space and are expected to have a structural-counter part in the new structure were used to compute the co-ordinates of the new structure. Side chains with incorrect (deviant) geometries were then removed.

The supplied template of three-dimensional structures may not contain all the necessary loop residues required to build the model. However, it is possible to search a database of structural fragments derived from Brookhaven Protein Data Bank (Abola et al., 1987) and the best fitted fragment or framework used to construct a new loop. Conformational space is searched for space allocation for the loop and for each α -carbon in the loops from 7 of the allowed Φ - Ψ angle combinations. This would exclude loops which are in steric conflict with the surrounding context. Alternatively, it can compute a small framework from the five best fitted data. Incomplete and incorrect backbone is rebuild based on the position of α -carbons and the best fitted backbone fragment is searched from a data base of crystallographic structures of 7 allowed Φ - Ψ angle combinations.

Once the building of the backbone is completed, lacking or incomplete side chains must be added on. The distorted, but complete, side-chains are corrected and the incomplete or lacking side-chains are rebuild with a search from a library of allowed side-chain rotamers sorted by increasing frequency of occurrence in known three-dimensional structures.

The additional van der Waal's exclusion test for each residue in its spacial context is applied and the most frequently acceptable rotamer replaced in the model. Residues which cannot be rebuild are withheld, allowing for other rotamers to be tested. Six such passes are performed with an incremental tolerance of 0.15 Å. In the seventh pass, the still absent side chains are added in their most probable rotamer, regardless of any exclusion test. Dihedral angle (i.e. the psi, phi, omega and chi angles) constraints can also be added to select rotamers.

The packing density of the completed model was checked by using an algorithm from PROMOD which detects both internal and external surfaces and computes the centre and size of each individual cavity. A comparison of the size and distribution of intramolecular cavities between model and crystal structure may help to uncover any mis-folds in the model structure. Mis-folded areas can also be identified by the method described by Luthy (Luthy et al., 1992). Lastly, the mutant model was refined by CHARMM (Brook et al., 1983).

The W28F mutant model was built based on the known three-dimensional structure of human placental glutathione S-transferase (Reinemer et al., 1992) with the Trp28 replaced by Phe28. The PDB identify code of human placental GST is 1GSS.

Chapter 3

Results and Discussion

3.1 Purification and Yield

The purification of wild-type and W28F mutant human GSTP1-1 yielded 2 and 0.5-1 mg/litres of culture medium, respectively. Yields of pure class Pi recombinant GST were in good agreement with those reported in the literature (Manoharan et al., 1992b; Kong et al., 1993b; Zimniak et al., 1994). Similar purification was reported for recombinant rat class Pi GST (Tamai et al., 1991). Studies on the inhibition character of glutathione analogues showed that wild-type and W28F mutant hGSTP1-1 shared similar affinities toward S-hexylglutathione and glutathione sulphonate as the I_{50} values were very close for both wild-type and mutant enzymes (see Fig.16 and Fig.17). This excluded the lower yield of W28F mutant enzyme resulted from weaker binding of W28F mutant enzyme to the affinity matrix.

Class Pi GST is highly susceptible to oxidation and covalent modification, which can result in reduced catalytic ability and conformational stability (Sluis-Cremer and Dirr., 1995). The enzymes were purified using the S-hexylglutathione immobilized Sepharose affinity chromatography at pH 7-7.8, rather than the widely used immobilized-GSH affinity chromatography at pH 9.6 (Simons and Van der Jagt., 1977), in order to prevent pH-induced oxidation. Low yields of purified mutant enzyme can possibly be attributed to an inefficient protein synthesis system, but the final folded conformation was sensitive to proteolysis. It is possible that the enzyme has lower intrinsic stability in a final folded state. Baker et al (Baker et al., 1994)

produced recombinant hGSTP1-1 as N-terminal ubiquitin fusion, with the *Saccharomyces cerevisiae* ubiquitin-specific protease co-expressed; this allows the co-translational cleavage of engineered ubiquitin - GST fusion proteins expressed in *E. coli*. In their research, they observed a marked improvement on the yield of enzyme after the ubiquitin was cleaved by the ubiquitin-specific protease in the *E. coli* cytoplasm.

3.2 Homogeneity

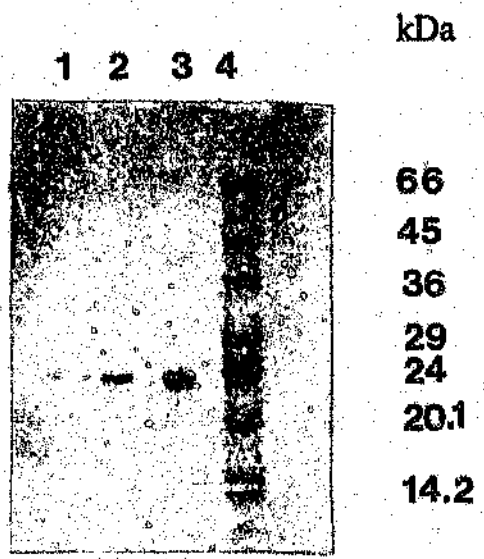
3.2.1 SDS-PAGE

The homogeneity of the purified enzyme was evaluated by SDS-polyacrylamide gel. Wild-type and W28F mutant enzyme appeared to be pure and homogeneous as represented in Fig.12a. The relative molecular mass of the wild-type and W28F mutant subunit of hGSTP1-1 was estimated at close to 23.5 kDa from the SDS-polyacrylamide gel electrophoresis gel (see Fig.12b), similar to the values published by others such as Kolm et al (Kolm et al., 1992; Kong et al., 1993b; Zimniak et al., 1994).

3.2.2 Isoelectric focusing

Wild-type and W28F mutant enzymes were shown to share similar pI values (pI = 4.8) (see Fig.13a,b), which were in close agreement with the published literature value of 4.6 (Widersten et al., 1992). Multiple bands of wild-type and W28F hGSTP1-1 between pI 4.6 and 5.1 were observed.

a



b

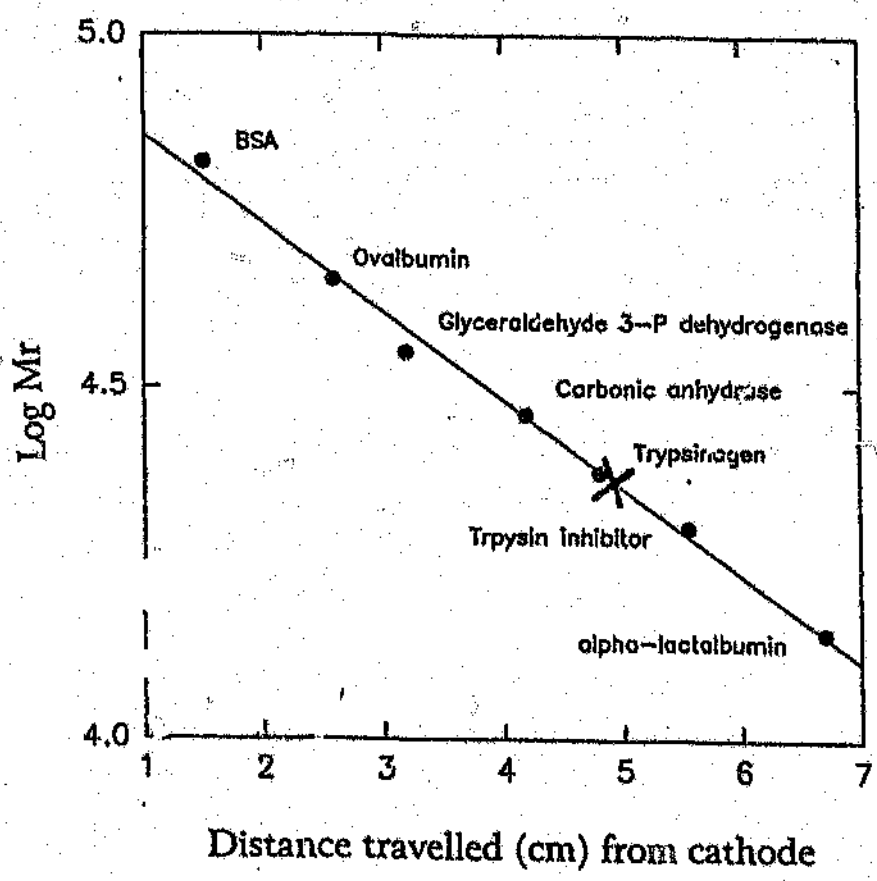
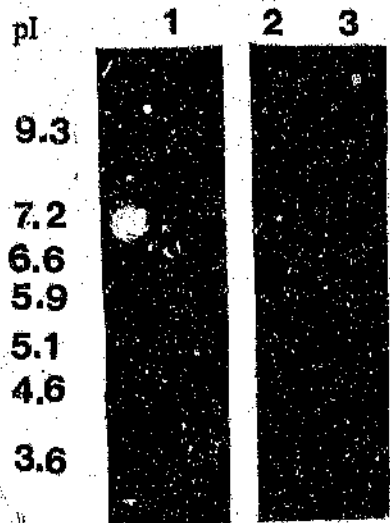


Fig.12 hGST P1-1 by SDS-PAGE. (a) 15 % SDS PAGE gel showing the migration of homogeneous subunit of wild-type and W28F hGST P1-1, Lane 1: wild-type hGSTP1-1; lane 2: W28F mutant hGSTP1-1; lane 3: pGSTP1-1; lane 4: molecular mass marker protein. (b) Calibration curve of the molecular mass marker proteins. The estimated molecular mass for the subunit of both wild-type and W28F hGST P1-1 is about 23.5 kDa (marked with X). Details of conditions and molecular mass markers can be found in section 2.4.1.

a

80

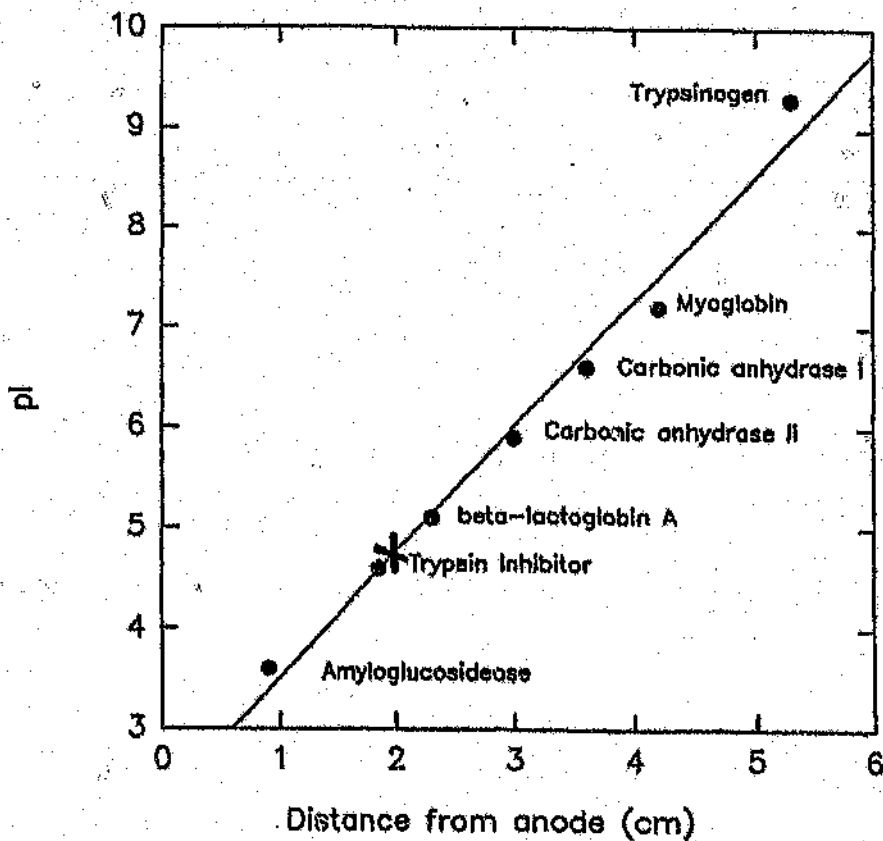
b

Fig.13 Determination of the isoelectric point of wild-type and W28F mutant hGST P1-1. (a) IEF gel showing the focused proteins. Lane 1: pI marker proteins; lane 2: wild-type hGST P1-1; lane 3: W28F mutant hGST P1-1. (b) Calibration curve for the isoelectric point marker proteins. The pI of both wild-type and W28F hGST P1-1 was 4.8 (marked with an X), both enzymes appear as multiple bands between pI 4.6 and 5.1. Details of conditions and pI marker proteins can be found in section 2.4.2.

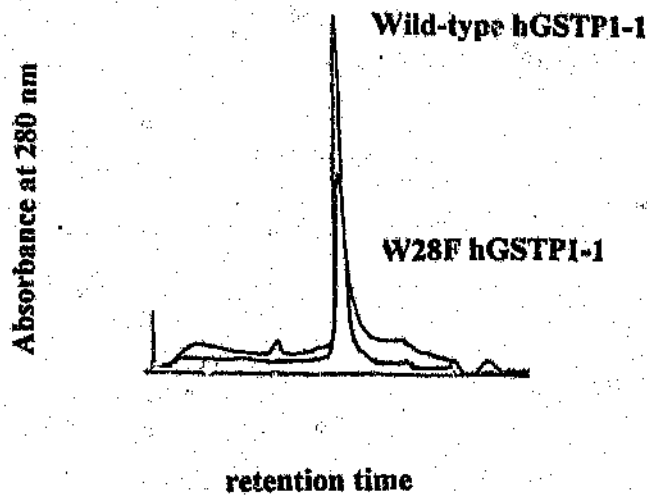
3.2.3 Size-exclusion HPLC

The molecular mass of the native wild-type and W28F mutant enzymes estimated from size-exclusion HPLC experiments were close to 47kDa, (see Fig.13a) as in accordance with other reported values (Kolm et al., 1992; Kong et al., 1993b; Zimniak et al., 1994). Single elution peaks were observed for wild-type and W28F mutant enzyme, indicating the purified enzymes were homogenous (see Fig.14b). The size-exclusion profiles showed that the two enzymes did not differ in terms of their hydrodynamic volume, thus indicating that the W → F replacement did not cause a change in hydrodynamic volume and quaternary structure of the dimeric hGSTP1-1.

3.2.4 Western blot

The western blot analysis is shown in Fig.15. Wild-type hGSTP1-1 and pGSTP1-1 is shown to react with the primary antibodies (rabbit polyclonal anti-hGSTP1-1 antibodies), whereas BSA did not as expected. The homogeneity of the enzyme was again confirmed and the specific antibody and class Pi GST interaction observed; the results of the western blot experiment were close to those of Manoharan et al (Manoharan et al., 1992b). Human and porcine GST P1-1 were shown to share a very high degree of structural similarity and primary sequence identity (83%) which was the reason for the rabbit polyclonal anti-hGSTP1-1 antiserum reacting with porcine GSTP1-1.

a



b

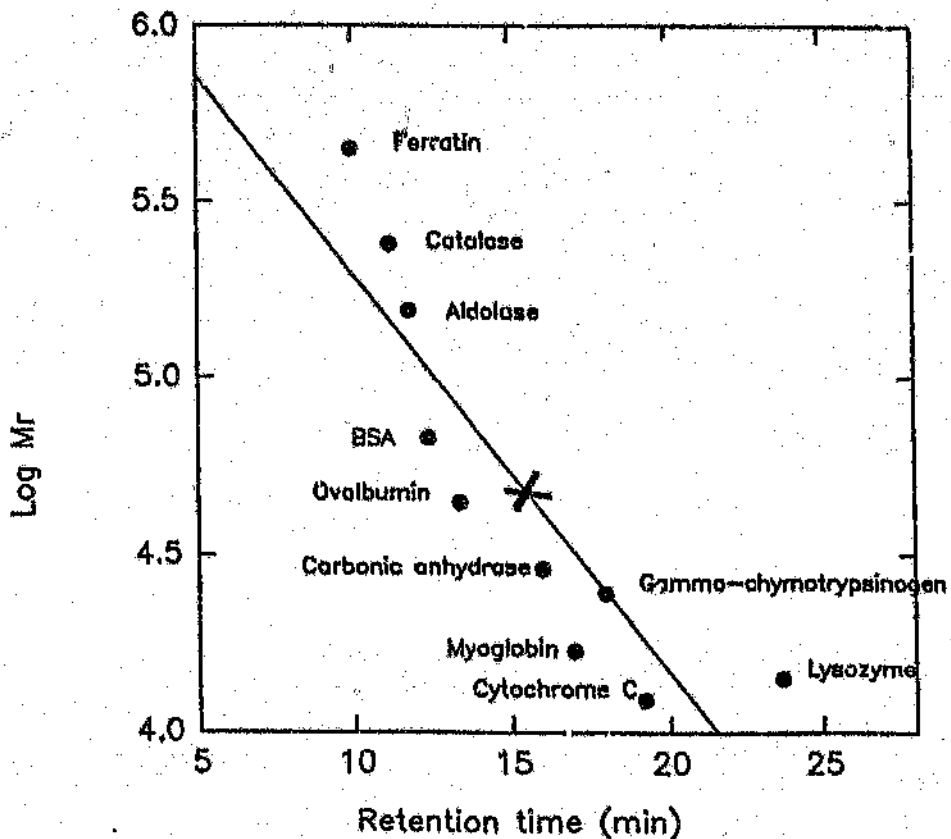


Fig.14 (a) Retention profile of wild-type and W28F mutant hGST P1-1 from the size-exclusion HPLC column. (b) Determination of the molecular mass of the native and W28F mutant hGST P1-1 by size-exclusion HPLC. The molecular mass both wild-type and W28F mutant proteins estimated from the calibration curve is 47 kDa (marked with an X). Details of the conditions and molecular mass marker proteins can be found in section 2.4.3.

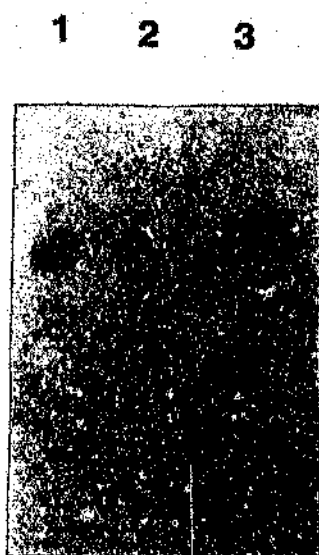


Fig.15 Western blot of the wild-type hGST P1-1. (1) and (2) are porcine GST P1-1 and (3) is the wild-type hGST P1-1. Enzymes were electrophoresed in 15 % (w/v) acrylamide gel and then transferred to a nitrocellulose membrane, blots were incubated with a polyclonal antiserum raised against human glutathione S-transferase class Pi, then with a secondary alkaline phosphatase-conjugated antibody. Nitro blue tetrazolium/5-bromo-4-chloro-3-indolyl phosphate was used for colour development of the glutathione S-transferase bands. Details of methods and conditions for the western blot can be found in section 2.4.4.

3.3 Steady-state enzyme kinetics

Details of the steady-state enzyme kinetic data are shown in Table.5. The steady-state enzyme kinetic parameters of wild-type enzyme for reduced glutathione and CDNB were in agreement with published values for wild-type recombinant human GSTP1-1 (Manoharan et al., 1992b; Kolm et al., 1992; Kong et al., 1993b; Zimniak et al., 1994; Ricci et al., 1995). The sterically-conserved substitution of W → F (Bordo and Agros., 1991) in hGSTP1-1 halved the specific activity of the enzyme when compared with the wild-type enzyme. The catalytic efficiency value (k_{cat}/K_m) of W28F mutant towards reduced glutathione and CDNB were both reduced (see Table.5). K_m for reduced glutathione remained unchanged and a large increase in K_m towards CDNB was observed. Mutant enzyme also exhibited much lower maximum velocity in catalysing the conjugation of reduced GSH and CDNB.

The I_{50} (S-hexylglutathione) of wild-type enzyme resembled the values reported by others such as Kolm et al (Kolm et al., 1992; Kong et al., 1992c; Kong et al., 1993). I_{50} value for wild-type and W28F mutant enzymes were 14 and 12.6 μ M when S-hexylglutathione was used. I_{50} value for wild-type and W28F mutant enzyme was 16.6 μ M when glutathione sulphonate was used (See Fig.15 and Fig.17 for the inhibition results).

The replacement of Trp28 by Phe did not cause changes in the inhibition characteristics (the I_{50} values) and S-hexylglutathione was confirmed to be a more effective competitive inhibitor for both wild-type and mutant enzymes when compared with glutathione sulphonate. The hydroxyl group of Tyr7 formed a hydrogen bonds with the sulphonate oxygens of glutathione sulphonate at the G site, thus resulting in tight binding ($K_d = 4 \mu$ M; Dirr et al., 1991a).

According to Askelof et al (Askelof et al., 1975), the inhibitory effects of glutathione analogues increase by increasing the length of the hydrocarbon chain of alkyl moieties in S-substituted glutathione analogues. When the hydrophobic hexyl moiety of S-hexylglutathione fitted into the H-site, it prevented the electrophilic substrate's binding to the H-site, and subsequently lowered the enzyme activity.

A major effect of the Trp28 → Phe mutation was a decrease in the turnover number and apparent affinity for the electrophilic substrate (CDNB). The interaction between glutathione and the G-site did not seem to be affected significantly by the mutation as the K_m for reduced glutathione and the I_{50} values for the competitive inhibitors (S-hexylglutathione and glutathione sulphonate) remained unchanged. Although the Trp28 → Phe substitution did not cause a change in the global conformation as seen in the size-exclusion HPLC profile (see Fig. 14b), the kinetic data suggested a local distortion in the topography at the hydrophobic (electrophilic substrate) binding site (H-site) of the enzyme.

Kinetic parameters of wild-type and W28F mutant of human GSTP1-1

Parameters (unit)	Wild-type	W28F mutant
Specific enzyme activity ($\mu\text{mol}/\text{min}/\text{mg}$)	3.54	2.66
Varied [GSH]		
V_{max} ($\mu\text{mol}/\text{min}$)	36	11.7
K_{M} (mM)	0.26	0.28
$k_{\text{cat}}/K_{\text{M}}$ ($\text{mM}^{-1}.\text{sec}^{-1}$)	324	184
Varied [CDNB]		
V_{max} ($\mu\text{mol}/\text{min}$)	9.6	2.2
K_{M} (mM)	0.75	2
$k_{\text{cat}}/K_{\text{M}}$ ($\text{mM}^{-1}.\text{sec}^{-1}$)	116.2	50.9

Table.5 Kinetic parameters of wild-type and W28F mutant GST P1-1. Measurements were made in 0.1 M potassium phosphate buffer, pH 6.5, containing 1 mM EDTA, 0.2 %(w/v) sodium azide, at 25°C. Kinetic activity was monitored spectrophotometrically at 340 nm. Details of conditions and methods under section 2.5.1 to 2.5.3.

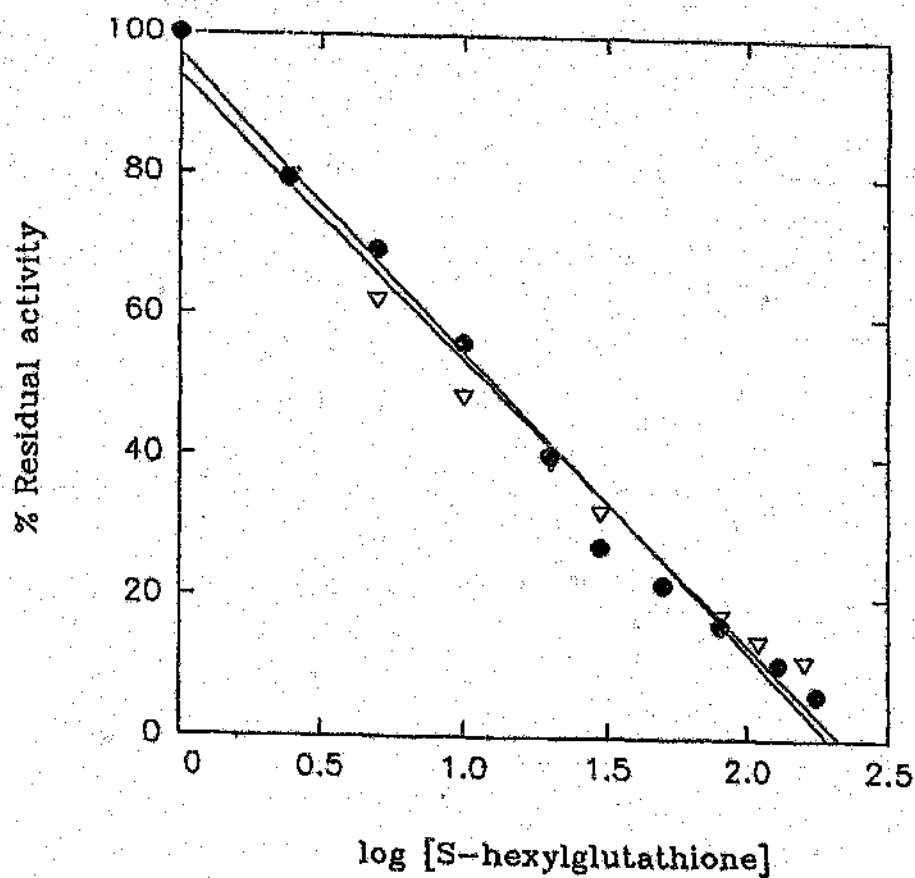


Fig.16 Inhibition of enzyme activity by S-hexylglutathione. (●) wild-type hGST P1-1, (▽) the W28F mutant enzyme. The I_{50} (Wt) = 14 μ M and I_{50} (W28F) = 12.5 μ M. Correlation coefficients of wild-type and W28F mutant enzyme are 0.98 and 0.97, respectively. Details of the experimental conditions can be found in section 2.5.4.

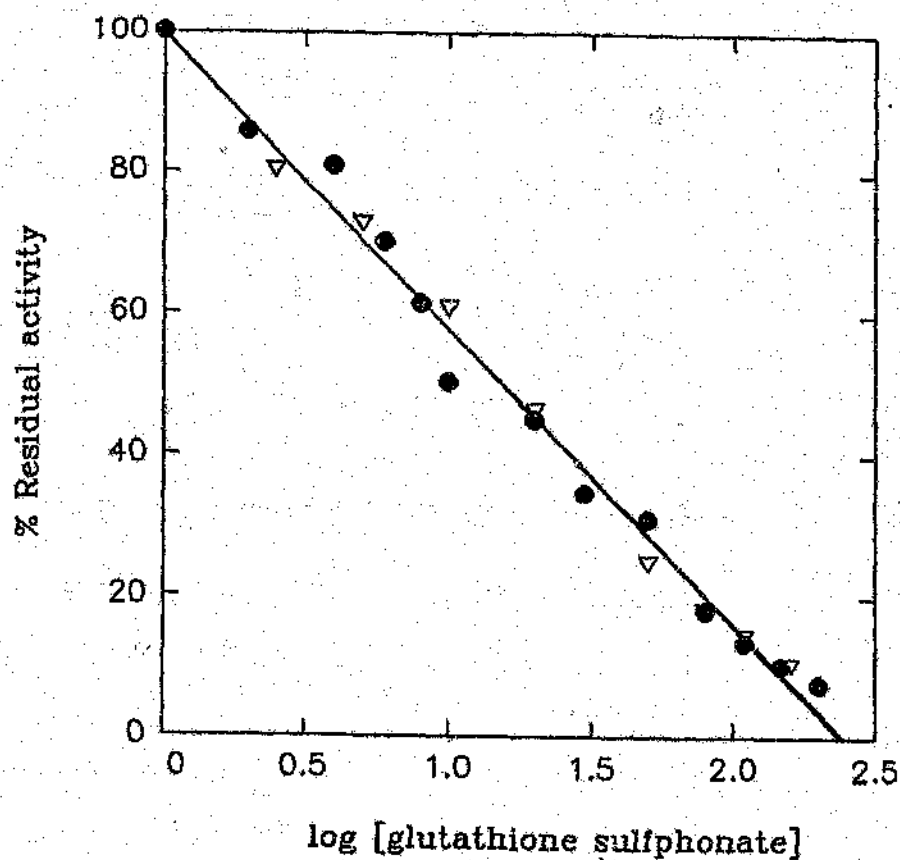


Fig.17 Inhibition of enzyme activity by glutathione sulfonate. (●) wild-type hGST P1-1, (▽) the W28F mutant enzyme. The I_{50} (Wt and W28Fmutant) = 15 μ M. The correlation coefficients of wild-type and W28F mutant enzyme are calculated to be 0.99 and 0.96, respectively. Details of the experimental conditions can be found in section 2.5.4.

3.4 Heat-inactivation studies

Thermostability of wild-type and W28F mutant enzymes was determined by investigating the enzymes' catalytic activity at elevated temperatures. Replacement of Trp with Phe residues resulted in an observable decrease in enzyme thermostability, as seen in Fig.18. W28F mutant was less thermostable than wild-type enzyme. T_m values (temperature at which 50% enzyme maintained activity) for wild-type enzyme are 52 °C and 45 °C for W28F mutant. At 60 °C, the W28F mutant enzyme was totally inactivated, whereas the wild-type enzyme maintained a 10% activity. The heat inactivation profile of wild-type recombinant enzyme was in agreement with that obtained by others such as Kong et al (Kong et al., 1993b), where the T_m of this enzyme was 55 °C.

The time-dependence data at 55°C also indicated the wild-type protein to be more thermostable when compared with the W28F mutant. The $t_{1/2}$ (wild-type) = 8 min and $t_{1/2}$ (W28F) = 2 min (see Fig.19). Therefore, the data indicates Trp28 to be important for maintaining a proper stable conformation of class Pi GST.

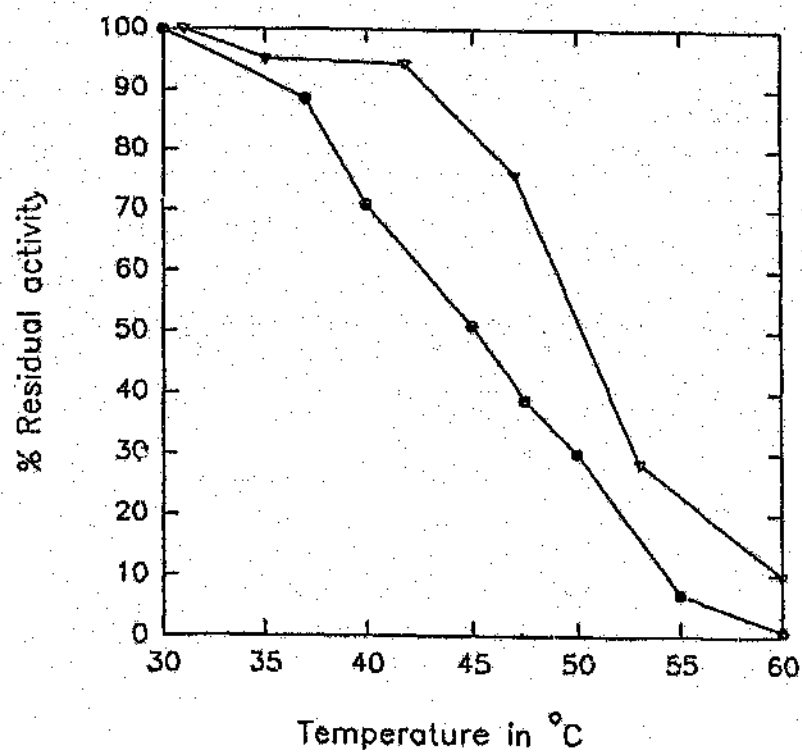


Fig.18 Thermal inactivation of wild-type (∇) and W28F mutant (\bullet) hGST P1-1 with temperature. Details of experimental methods and conditions can be found in section 2.6.

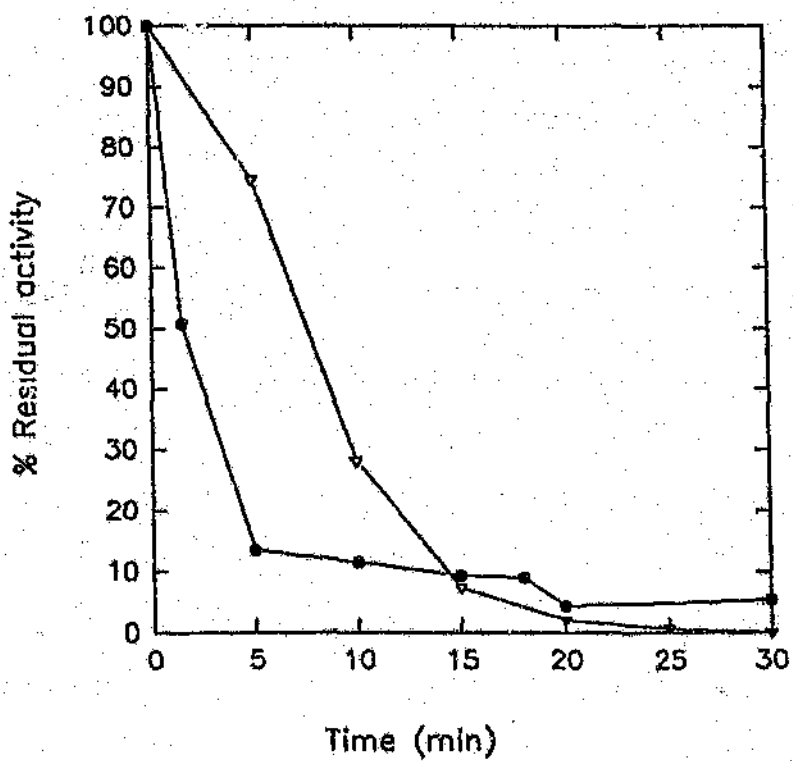


Fig.19 Time-dependence of thermal inactivation of wild-type (∇) and W28F mutant (\bullet) hGST P1-1. Experiments were performed at 55 °C. Details of experimental methods and conditions can be found in section 2.6.

3.5 Fluorescence spectroscopy

3.5.1 Fluorescence emission spectra

Fluorescence emission spectra of wild-type and W28F mutant enzymes are shown in Fig.20 and represent typical profiles of partially solvent-exposed tryptophan residues (Burstein et al., 1973). The maximum emission wavelength of both wild-type and mutant enzymes was 340 nm. W28F mutant enzyme exhibited 56% emission intensity of wild-type enzyme. The spectral data suggest that the two Trp residues differ only slightly in exposure to the exterior environment.

3.5.2 Quantum yield

The quantum yield of wild-type and W28F mutant enzymes was estimated to be 0.026 and 0.02, respectively. This low quantum yield of these two enzymes is thus indicative of tryptophan residues in a hydrophobic microenvironment (Burstein et al., 1973). A similar quantum yield was obtained for porcine class Pi isoenzyme by Dirr and Reinemer (Dirr and Reinemer., 1991), which is an indication of tryptophan residue being partially buried in the protein matrix. The emission data and the quantum yields imply that the fluorescence intensity observed for wild-type hGSTP1-1 is slightly dominated by the emission of Trp38. The calculated accessible surface area of pGSTP1-1 shows that Trp28 has a larger accessible surface area when compared with Trp38 (Reinemer et al., 1991). It should be noted that Trp38 is involved in binding the glutathione sulphonate at the active site and that this would cause a change in the accessibility of Trp38.

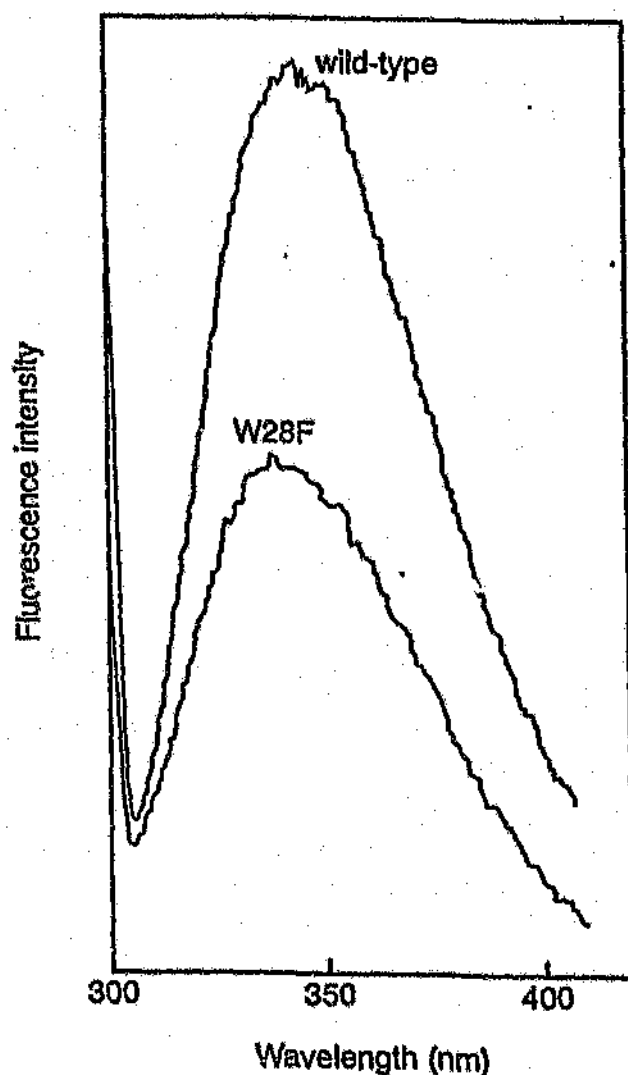


Fig.20 Corrected fluorescence emission spectra of $2 \mu\text{M}$ native wild-type and W28F mutant hGST P1-1. The steady-state fluorescence spectroscopy were performed at room temperature using the Hitachi model 850 fluorescence spectrophotometer. The excitation and emission bandwidth were both set at 5 nm. 20 mM sodium phosphate buffer, pH 6.5, containing 100 mM NaCl, 1mM EDTA, 0.2 %(w/v) sodium azide. Samples were excited at 295 nm and recorded from 300 to 400 nm. Spectra were corrected for the buffer blanks.

3.5.3 Acrylamide quenching studies

Acrylamide is a neutral polar quencher which can gain access to deeply buried tryptophan residues, and the quenching of excited tryptophan fluorescence can provide information with regard to the tryptophan residue's accessibility to the exterior environment of proteins (Eftink and Ghiron., 1976). In the acrylamide quenching studies, the Stern-Volmer plot was used to calculate the acrylamide quenching parameters (Lehrer., 1971). The acrylamide quenching result of wild-type and W28F mutant hGSTP1-1 can be seen in Fig.21. The linear relationship suggests that a dynamic quenching mechanism is the major quenching mechanism, and that static quenching by acrylamide was negligible. If static quenching is not negligible, then an upward curving Stern-Volmer plot would be observed (Eftink and Ghiron., 1981). An upward curving plot indicated that all Trp residues were nearly equally accessible, or that the fluorescence was dominated by a single Trp residue. The linear Stern-Volmer plot of wild-type enzyme also implies that the two tryptophan residues differ only slightly in their accessibility to quencher (Eftink and Ghiron., 1976).

Effective Stern-Volmer quenching constant (K_{sv}) determined from the plots, were 4.3 and 1.34 M^{-1} for wild-type and W28F mutant enzyme, respectively. The K_{sv} for N-acetyl-tryptophanamide (NATA) was estimated to be 17 M^{-1} , which was very close to the value reported by Eftink and Ghiron (Eftink and Ghiron., 1977). The values of K_{sv} generally range from 0.1 M^{-1} to 10 M^{-1} for deeply buried to highly exposed tryptophan residues of proteins (Eftink and Ghiron., 1981). The difference in K_{sv} values implies that the Trp28 residue is slightly more accessible to quencher than Trp38. Surface area calculations from the crystal structure of human placental class Pi GST (Reinemer et al., 1992) indicated that both tryptophan residues are partially

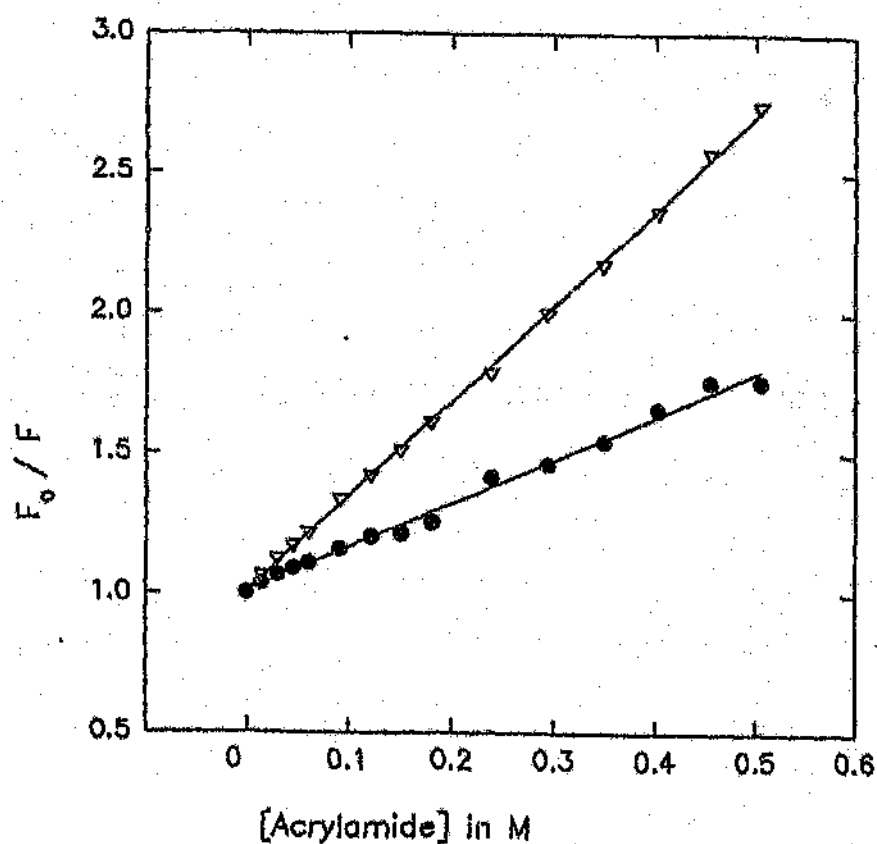


Fig.21 Stern-Volmer plot for acrylamide quenching of wild-type (∇) and W28F mutant (\bullet) hGST P1-1. F_0 and F are the fluorescence intensities in the absence and presence of acrylamide, respectively. Coefficients of correlation are 0.93 for wild-type and 0.88 for W28F mutant. Details of conditions used in the experiment can be found in section 2.7.3.

exposed to solvent with slight differences in their surface accessibility (approximately 16% exposure to solvent).

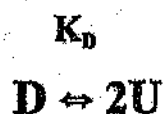
3.6 Urea-induced equilibrium unfolding studies

Two types of probes were used here: those sensitive to different structural phenomenon, and those differing in levels of sensitivity. It is sometimes referred to as the multiple variable test (Brandts., 1969) and any presence of stable intermediates will be detected by using different physical techniques. Tryptophan fluorescence (structural probe) was used to monitor the immediate environment of the Trp residues which represent the localized environment of the Trp residues. Denaturation by urea causes a red shift in the emission spectrum of wild-type and W28F mutant hGSTP1-1 from 340 nm to 355 nm as the fluorophore becomes exposed upon unfolding. Enzyme activity (functional probe) will give a more indirect, global assessment of the unfolding/refolding process. The dimeric structure is required for GST to be catalytically functional and dissociation of the dimer into its subunits will result in a loss of functionality.

The urea-induced equilibrium unfolding curves of wild-type enzyme showed that the unfolding transition was monophasic and sigmoidal, both of which are characteristic of a highly co-operative unfolding transition (Creighton., 1990; Jackson and Fersht., 1991) (see Fig.22 a, b). The good correlation which occurred between the structural and functional probes was observed. The result corresponded well with those obtained for the porcine class GSTP1-1 (Dirr and Reineiner, 1991; Erhardt and Dirr, 1995; Shuis-Cremer and Dirr., 1995) which unfolded in a two-state manner. Linear slopes for the pre- and post- transition regions are common features of a denaturant-

induced curve and are presumably due to solvent perturbation effects; i.e., the interaction of solvent molecules with the native and unfolded proteins (Pace., 1986).

The two-state model for the denaturation of dimeric proteins, where only the native dimer (D) and unfolded monomer (U) are the two significant populations present at equilibrium, is described by the following scheme:



In the two-state model, only the folded dimers and unfolded monomers are populated, whereas folded monomers are unpopulated because they are thermodynamically unstable relative to the native dimer and unfolded monomer (Creighton et al., 1990).

A protein concentration-dependence study indicated a shift to a higher urea concentration from 4 M (1 μ M wild-type hGSTP1-1) to 4.47 M urea (10 μ M wild-type hGSTP1-1) which was consistent with the two-state model of denaturation (Bowie and Sauer, 1989) (see Fig.23). Concentration dependency was also observed in porcine class isoenzyme (Erhardt and Dirr., 1995).

The following equations explain the dependence of equilibrium unfolding on protein concentration provided that the folded monomer state was essentially unpopulated.

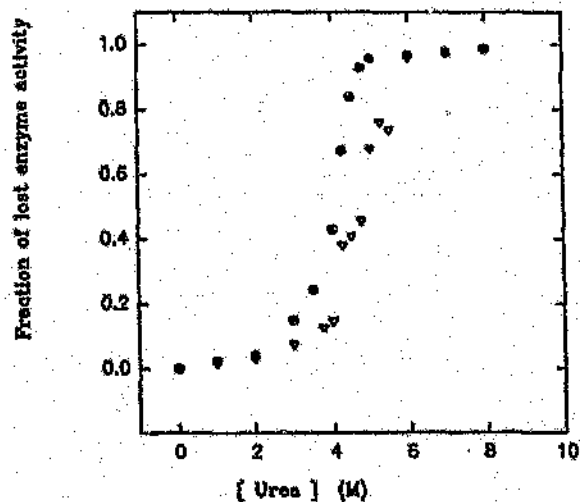
$$K_D = [U]^2/[D] \quad (\text{Eq.11})$$

$$K_D = 2 Pt [f_u^2 / (1-f_u)] \quad (\text{Eq.12})$$

where D is the native dimer and U is the unfolded monomer, respectively. Pt is the total protein concentration. f_u is the fraction of unfolded protein and K_D is the equilibrium constant of the two-state unfolding process (Bowie and Saucer., 1989). Protein concentration (in terms of monomer concentration) is determined by both folded dimer and unfolded monomer concentrations, $Pt = 2[U] + [D]$. According to the law of mass action, by increasing the concentration of protein, the proportion of native dimer at each denaturant concentration will increase and the mid-point of transition will shift to a higher denaturant concentration as protein concentration increases (Timm and Neet., 1992).

The dependence on protein concentration is an unique characteristic of the coupled denaturation and dissociation of oligomeric protein system, and is a typical feature of two-state unfolding models of dimeric proteins as has been observed for various dimeric proteins (Bowie and Saucer., 1989; Gittleman and Matthews., 1990; Timm and Neet., 1992; Mann et al., 1993; Timm et al., 1994).

a



b

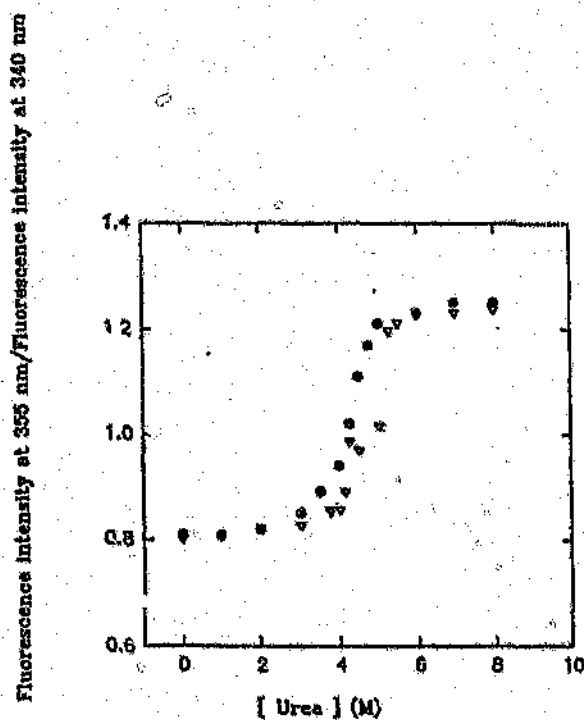


Fig.22 Raw data of the concentration-dependence experiment of wild-type hGST P1-1. (a) Relative loss of enzyme activity vs [urea]. (b) relative fluorescence intensity vs [urea]; (∇) 10 μM enzyme and (\bullet) 1 μM enzyme. Details of conditions of experiment can be found in section 2.8.1.

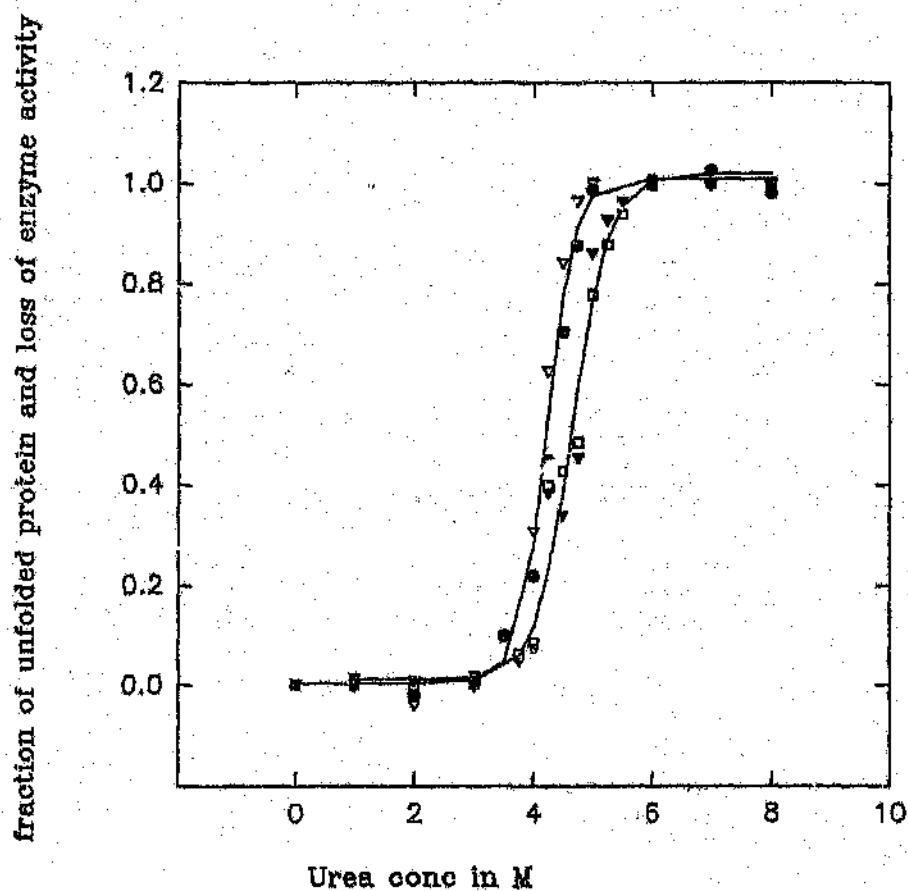


Fig.23 Concentration-dependence of wild-type hGST P1-1. (●) the relative loss of enzyme activity of 1 μ M enzyme; (▽) the fraction of unfolded protein of 1 μ M enzyme; (▼) the fraction of unfolded protein of 10 μ M enzyme; (□) the relative loss of enzyme activity of 10 μ M enzyme. The data is converted from Fig.22 according to section 2.8.2.

Conformational stability of wild-type and W28F mutant enzyme

ΔG^{H_2O} represents the difference in Gibb's free energy between the native and unfolded protein in the absence of denaturant and provides an estimation of protein conformational stability. Fig.24 was transformed and iterated according to the method described in section 2.8.3. The linear dependence of ΔG^{H_2O} on urea concentration was observed in the transition region. The ΔG^{H_2O} values for wild-type and W28F mutant GSTP1-1 were extrapolated from the transition region to zero denaturant in Fig.24 are 18.8 and 14.5 kcal/mol, respectively. The value of wild-type enzyme was very close to the reported value of porcine class Pi GST (Dirr and Reinemer., 1991; Erhardt and Dirr., 1995). ΔG^{H_2O} of wild-type class Pi GST was very closed to the range of conformational stability of dimeric proteins (amino acid residues per subunits ranged between 118 and 209) for which chemical-induced denaturation was two-state; and ΔG^{H_2O} ranged between 19.2 and 27.8 kcal/mol (Neet and Timm., 1994).

The unfolding process of W28F mutant was monitored using only the enzyme activity as the probe because of the small amount of enzyme available and the sensitivity of the probe. It was assumed that the structural and functional probes were highly correlated as observed for wild-type hGSTP1-1 (see Fig.25) and pGST P1-1 (Erhardt and Dirr., 1995). Unfolding of W28F mutant protein also followed a two-state process with a monophasic transition, see Fig.24. The mid-point of the transition was estimated to be 3.7 M urea (wild-type hGSTP1-1) and 4.2 M urea (W28F mutant of hGSTP1-1). W28F mutant protein unfolded at a lower urea concentration, indicating a lower intrinsic stability of the W28F mutant enzyme. A *m*-value can be expressed as the gradient of the transition region and is determined by the number and types of groups which become exposed to solvent as the protein unfolds (Greene and Pace.,

type and W28F mutant enzymes obtained from Fig.25 were 2635 and 1955 cal/mol.M urea, respectively. In Fig.25, the linear dependence of ΔG on urea concentration was also observed. Myers et al (Myers et al., 1995) pointed out that both the m -values and heat capacity changes were correlated and depended on the accessible surface area of the protein.

The change in solvent-accessible area (ΔASA) can be calculated according to the following equation (Myers et al., 1995):

$$\Delta ASA = - 907 + 93 (\text{number of amino acid residues}) \quad (\text{Eq.13})$$

The m -value for urea denaturation can then be calculated from the following equation (Myers et al., 1995):

$$m = 374 + 0.11 (\Delta ASA) \quad (\text{Eq.14})$$

The heat capacity change (ΔCp) upon unfolding on ΔASA can be calculated from the following equation (Myers et al., 1995):

$$\Delta Cp = - 251 + 0.19 (\Delta ASA) \quad (\text{Eq.15})$$

The calculated m value for urea denaturation from Eq.14 for wild-type hGST P1-1 is 2412.3 cal/mol/M urea and the ΔCp calculated from Eq.15 for wild-type enzyme is 3269.7 cal/mol/K. The calculated m -value is close to the experimentally determined m -value

W28F mutant enzyme was thermodynamically less stable when compared with the wild-type protein. Despite the m -value being dependent on the composition and amount of polypeptide chain that is exposed to solvent upon unfolding, the composition of the polypeptide chain of W28F mutant did not differ significantly from the wild-type enzyme except for the replacement of Trp with Phe. W28F mutant protein has a smaller m -value (gentler transition slope) when compared with the wild-type. The difference between the slopes of the two enzymes simply reflect the difference in the cooperativity of the unfolding/refolding transition (Gittleman and Matthews., 1990; Myers et al., 1995). Thomson et al (Thomson et al., 1989) pointed out that differences in m -values (transition slopes) may result from differences in the pathway of unfolding but this is excluded from the possibility because the unfolding/folding of wild-type and W28F mutant enzyme both proved it approached the two-state unfolding/folding mechanism. The larger m -value (or steeper transition slope) reflects the folded conformation of wild-type protein was less accessible to solvent and more resistant to solvent-induced denaturation. The W28F mutant was more accessible to solvent and less resistant to solvent-induced denaturation when it started to unfold at lower urea concentration. Because the two proteins did not differ in terms of hydrodynamic volume, it can be concluded that the slight loss of cooperativity at transition region came from alteration of forces which contributed to the folded protein stability as a result of Trp28 \rightarrow Phe mutation.

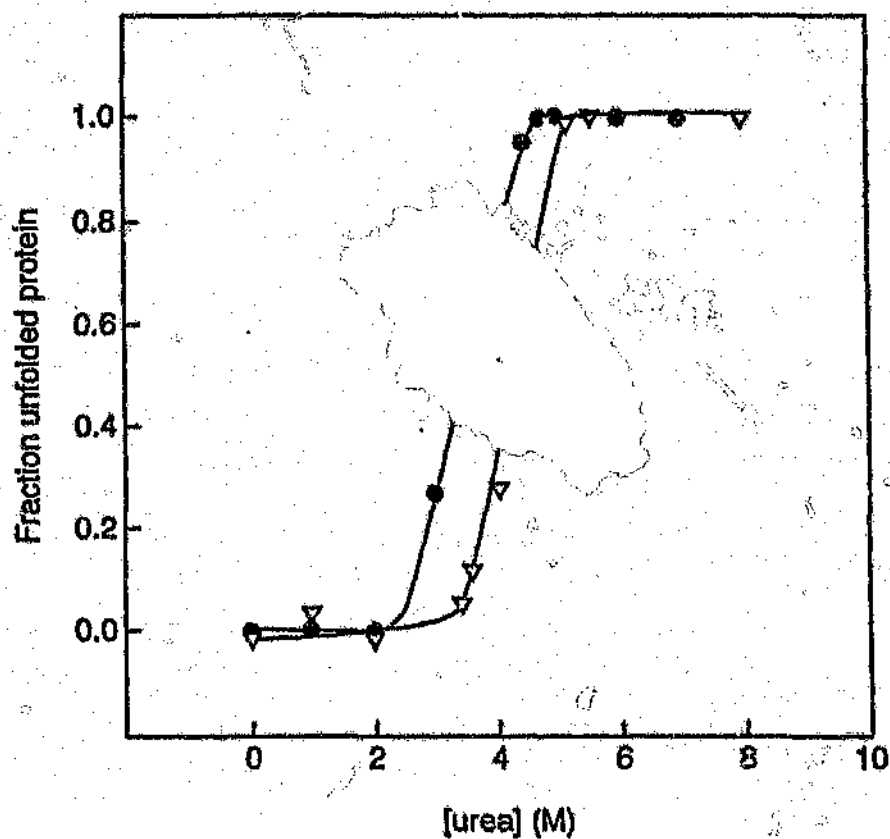


Fig.24 Urea unfolding of the wild-type (▽) and W28F mutant hGSTP1-1(●). The fraction of unfolded protein is determined from the enzyme activity data. Details of experimental methods and conditions can be found in section 2.8.1. The data is converted according to section 2.8.2.

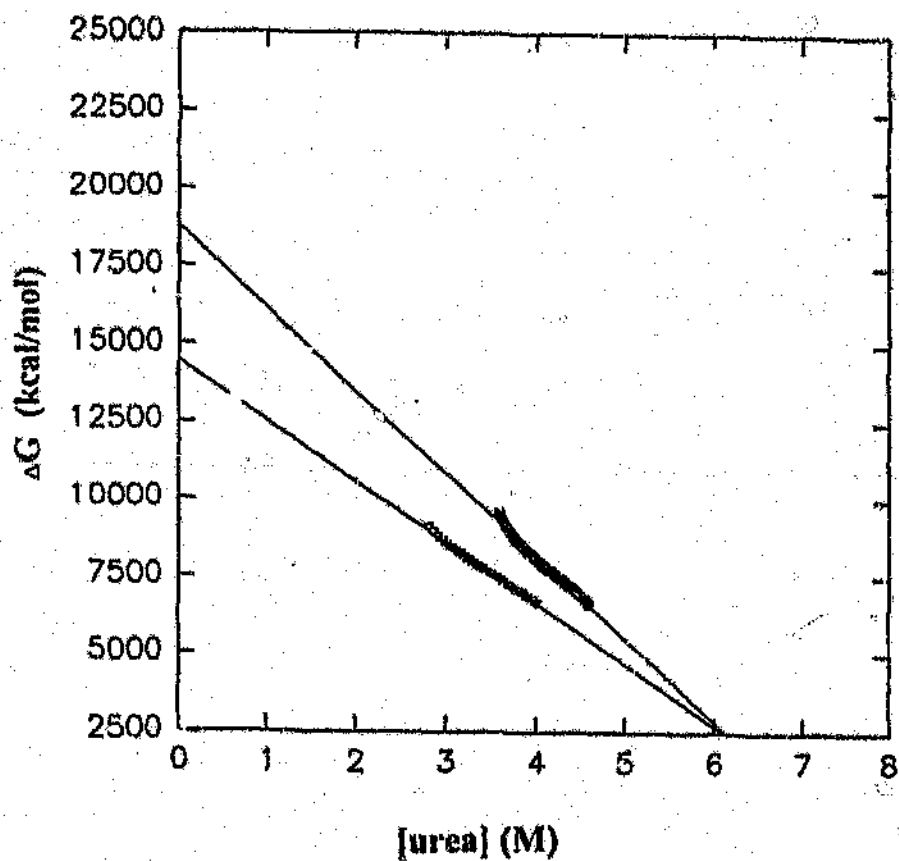
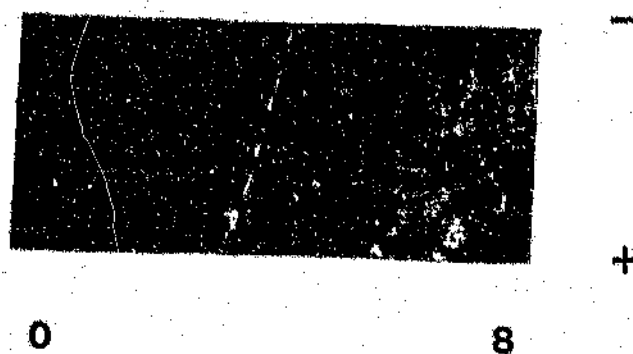


Fig.25 ΔG as a function of urea concentration, where (●) is the wild-type hGST P1-1; (▽) is the W28F mutant enzyme. Data points were calculated from transitional region in Fig.24 using equation in section 2.8.2. ΔG^{H_2O} (Wt) = 18.8 kcal/mol and ΔG^{H_2O} (W28F) = 14.5 kcal/mol.

3.7 Urea-gradient gel electrophoresis

Fig.20 a and b show the electrophoretic mobility of hGSTP1-1 across a 0 to 8 M gradient of urea. The smooth sigmoidal protein band between native and unfolded enzyme with a single transition was observed, indicating a rapid and reversible equilibrium transition between unfolded and native conformational states (Creighton., 1979), see Fig.26. It also indicates the unfolding mechanism to be a co-operative two-state mechanism. The mid-point of the transition is approximately at 4.2 M urea, which is consistent with the mid-point data for the unfolding of wild-type enzyme monitored by structural and functional probes. The refolding of unfolded protein also resembled the two state folding/unfolding mechanism with a smooth linear unfolded and folded region, the transition region being broken with diffusion occurred at both ends, see Fig.26b. The unfolding and refolding patterns of the wild-type enzyme were similar, which implied a rapid two-state mechanism with rapid conformational transitions. The broken curve of refolding of the enzyme was due to the interconversion between different conformations at the transitional region being slower than the time scale of the electrophoresis and thus only the native and unfolded forms were accumulated in and trapped by the acrylamide gel. One possible refolding kinetic barrier was the *cis-trans* isomerization of peptide bonds preceding Pro53 of hGST P1-1 (Reinemer et al., 1992). It is interesting to note that the rate of *cis-trans* isomerization is inherently very temperature dependent. *Cis-trans* isomerization is intrinsically slow, with the half-time for isomerization of an individual bond being of the order of 20 min at 0°C (Creighton., 1986; Creighton., 1990).

a**b**

Urea (M)

Fig.26 Urea-gradient gel electrophoretograms of (a) native wild-type hGST P1-1 and (b) unfolded wild-type hGST P1-1. The proteins were electrophoresed in 0.05 M Tris/Acetate buffer, pH 8, at room temperature. The mid-point of transition for both (a) and (b) is 4.2 M urea. Details of the experimental method can be found in section 2.9.

3.8 Structural basis for destabilization

The Trp28 → Phe mutation of hGST P1-1 as a result of the W28F mutant has (a) lower catalytic ability, (b) greater susceptibility to heat inactivation, and (c) a decrease in conformational stability. Folded proteins are only marginally stable, and even the smallest interaction can contribute significantly to its stability. Forces which have positive contributions to the stability of folded protein are: hydrogen bonding, ion pairing, and van der Waal's interactions and hydrophobic interactions. The opposition forces are due mainly to the entropic effect (Matthews., 1987; Dill., 1990).

In the crystal structure of hGST P1-1 (Reinemer et al., 1992), a putative intrachain hydrogen bond was observed between the partially buried indole ring of Trp28 and the buried side chain Glu30 (see Fig.29a). The donor-acceptor (NE1 of Trp28 and OE2 of Glu30) distance is 3.2 Å. This particular hydrogen bond pair is also observed in porcine (Reinemer et al., 1991; Dirr et al., 1994b) and murine class Pi crystal structures (Garcia-Saez et al., 1994). Shirley et al (Shirley et al., 1992) pointed out that there were three possible fates for a hydrogen bonding pair upon mutation: (1) it could form a new intramolecular hydrogen bond, (2) it could form a hydrogen bond with polar solvent, or (3) it could fail to form a hydrogen bond all together. In order to distinguish between the three possibilities, we have to look at the crystal structure of the protein. A replacement of Trp with Phe excluded the first possibility of formation of a new hydrogen bond with the pair. Secondly, the position at which amino acid 28 is situated is buried (considering that the Trp28 only has 16% surface accessibility to solvent).

One cannot only account the loss of hydrogen bonding between the Glu30 and Trp28 being due to the loss of conformational stability, and one must also include all

possible factors which reflect the loss of conformational stability. The reported average free energy involved in hydrogen bonding was approximately 1.3 ± 0.6 kcal/mol in stabilizing structures such as globular proteins and double-helical nucleic acid in aqueous solution (Shirley et al., 1992).

Ion pairing for protein stability in terms of ion pairs buried in the protein core can be seen in the studies by Barlow and Thornton (Barlow and Thornton., 1983). In the crystal structure of human GSTP1-1, an ion pair is identified between the partially buried side chain of Glu30 and the buried side chain of Arg18 (intratomic distance is 3.2 Å). This Arg-Glu ion pair is conserved in the hydrophobic core of domain 1 in the Alpha/Mu/Pi/*Schistosoma japonicum* isoenzymes, which strongly suggests its contribution to the maintenance of thermodynamically stable GSTs. A conservative ion pair of Arg-Asp in the octopus class Sigma isoenzyme (Ji et al., 1995) further supports the contribution of this evolutionary significant ion pair. Furthermore, the guanidinium moiety of Arg18 is hydrogen bonded to the carbonyl oxygen in the active-site peptide backbone at a non-polar residue (Val10/Pi; Ala11/Alpha; Trp7/Mu; Leu10/Sigma; Ile9/*S.japonicum*) in the active site. This Trp28-Glu30-Arg18 triad is situated below the active site loop (Phe8 to Gly12) of domain 1 in the class Pi isoenzyme which constitutes the H-site (Reinemer et al., 1992; Dirr et al., 1994b).

Class Pi isoenzyme has 8 Arg residues per monomer, half of which have very low solvent accessible surface areas (Reinemer et al., 1992) (see Fig.5 for amino acid sequence alignment of class Pi GSTs). It is unusual for a charged amino acid to exist in a buried hydrophobic environment as it would prefer to be situated at the surface of a protein, as the burial of unpaired charged residues in the non-polar interior would be energetically costly (Dao-pin et al., 1991). The Arg-Glu ion pair most likely plays a role as a stabilizing force within the hydrophobic environment of Trp28. The Trp28-Glu30-Arg18 cluster forms a hydrogen-bonded network and any disruption

of this could affect the stabilizing effect of the network in this part of the structure. The absence of hydrogen bonding between Phe28 and Glu30, as in W28F mutant, could cause a partial destabilization of polar interactions between the Arg-Glu ion pair and, as a consequence, in the destabilization of the Trp28-Glu30-Arg18 cluster. This would subsequently affect both the topology at the H-site, which is situated above the triad, and the thermodynamic stability of the protein.

The contribution of the Arg-Glu ion pair to protein stability was also confirmed by the low yields of expressed R18D mutant hGSTP1-1 (Manoharan et al., 1992b). Furthermore, replacement of Arg20 in hGST A1-1 with Ala (topological equivalent to Arg18 of hGST P1-1) resulted in a 85% loss of specific enzyme activity, which further supports the important structural role of the conservative Arg-Glu ion pair (Stenberg et al., 1991).

Research suggests that the hydrophobic effect is especially important in stabilizing the folded structures of protein (Kauzmann., 1959). In the crystal structure of hGST P1-1, Trp28 is situated in a hydrophobic region and interacts with the hydrophobic amino acid side chains of Val5, Ala15, Met19, Leu21 and Phe192. One would expect a slight loss of hydrophobicity in this region as a result of the replacement of Trp28 with Phe since Phe is less hydrophobic than Trp, when compared with the hydrophobicity scales in terms of Gibb's free energy contributed from amino acid side chains (Pickett and Sternberg., 1993; Eriksson et al., 1993). Amino acid substitutions can also result in a possible loss or gain in potential van der Waal contacts and can thus create strain and disorder which could affect packing and conformational stability (Kellis et al., 1988; Sandberg and Terwilliger., 1989). Phe residue has smaller van der Waal's volume (about 83% of Trp) when compared with Trp residue. Phe has smaller side chain when compared with Trp (a volume constraints). This difference in the sizes of the side chain would also affect the side

chain packing within the immediate surrounding of amino acid 28. A loss of van der Waal's contact between the side chain of Trp28 and Phe192 may result from replacing Trp28 with Phe, as seen in the structure constructed by homology modelling; (Fig.29 a and b). One must also consider the contribution from the side-chain conformational entropy (steric constraints) in order to accommodate the change of Trp to Phe.

The possibility of a cavity being created would remove this favourable van der Waal's interaction from the folded protein and result in a lower Gibb's free energy for the folded protein. The replacement can create a small cavity within the vicinity of the aromatic side chain of Phe, with the protein being able to respond to the difference by slight shift of backbone position in order to avoid the creation of cavity change (structural adjustment). Eriksson et al (Eriksson et al., 1993) observed structural adjustment in the crystal structure of bacteriophage T4 lysozyme mutants. However, the possibility of structural adjustment will remain unanswered until a W28F mutant crystal structure becomes available.

When Trp28 is hydrogen bonded to Glu30, there is much less rotational freedom and the motion of the indole ring is restricted and settled to the highest possible conformational free energy state where the aromatic ring of Phe would be able to have more rotational freedom although the rotation of aromatic ring of Phe is by 180° (π^2) and will produce an indistinguishable state. The flipping motion of the aromatic ring will not lead to a distinct conformational state because the change in energy as a result of the motion of the aromatic ring is best described as the change in vibrational entropy (S_{vib}) (Pickett and Sternberg., 1993).

Entropic effects dominate free energy changes during the folding of a protein, and a major unfavourable entropic effect arises from the main chain conformational entropy

major unfavourable entropic effect arises from the main chain conformational entropy (Pickett and Sternberg, 1993). Inspection of the mutant model indicated that the Trp28 → Phe mutation did not result in main chain conformational change as the amino acid back bone did not change much.

3.9 Homology modelling

When the 3-D structure of a mutant protein is not available, homology modelling is useful for structural predictions for mutated regions. There has been much interest in using homology modelling to predict the structural effect of amino acid substitutions (Zimniak et al., 1994; Sali., 1995; Lee., 1996). Construction of a refined model of hGSTP1-1 W28F mutant was based on the known 3-D structures of human, porcine and murine GST P1-1 (Reinemer et al., 1992; Dirr et al., 1994; Garcia-Saez et al., 1994). When the modelled 3-D structure of the mutant protein was aligned with porcine and murine GSTP1-1, the average root-mean-square (RMS) error for 1562 atoms is about 0.78 Å and for 206 C^α- atoms is 0.46 Å, an indication of a good quality refined model was expected because of the high sequence identity between the wild-type (template structure) and W28F (target structure) mutant enzyme. At least 40 % sequence identity between target and template structures is required to build a model with a main-chain error of as low as 1 Å for 90 % of the main-chain residues (Srinivasan and Blundell., 1993). For the W28F mutant model, the Phe28 residue was build with a tolerance of 0.75 Å. The subunit structure of W28F mutant hGST P1-1 model can be seen in Fig.27.

The final model was verified by the programme called 3-D profiles, developed by Luthy et al (Luthy et al., 1992). This programme compares the mutant amino acid sequence with the statistical preference of an amino acid for its environment. This is defined by: (1) the area of the residue that is buried; (2) the fraction of side-chain

area that is covered by polar atoms (O and N); and (3) the local secondary structure. The total scores of mutant model calculated by 3-D profiles is 122.27, which fall into a reasonably good correct folded structure for 209 amino acids. The profile scores for a model depends on the length of the protein; the larger the protein the better the score. The analysis of secondary structural content of the W28F mutant model shows that the helical structure is about 58.37 %, β -sheet structure is about 6.69 %, and the non-helical/sheet conformation is about 34.92 %. An average 3-D-1D score (a score which indicates the presence or absence of mis-folded region) of 0.61 per residue also suggests a good model with no mis-folded region in the W28F mutant model of hGSTP1-1.

The 3-D model of W28F mutant protein displayed good stereochemistry and overall structural identity when compared with the crystal structure of the wild-type enzyme (Reinemer et al., 1992). See Fig.28 for the stereoview of the local environment of Trp28 and Phe28. While limited, the model can provide insights regarding the effects of amino acid substitution. Upon inspection of the W28F mutant model, it was observed that the distance between the Phe28 and Phe192 residues increased from 3.89 Å to 5 Å. Trp28 and Phe192 are the two residues involved in hydrophobic interactions between β 2 and α 7. A widening of space between Phe28 (β 2) and Phe 192 (α 7) was also observed. The effective distance for hydrophobic interaction is within 4 Å. The G site did not differ between wild-type structure and the mutant model, but a slight distorted H site was observed in the W28F mutant model. This was supported by kinetic data with the Trp28 \rightarrow Phe mutation resulting in a decrease in the turnover number and apparent affinity for the electrophilic substrate (CDNB). This mutation also did not affect the interaction between the reduced glutathione and the G-site, which was confirmed by the enzyme steady-state kinetic results.

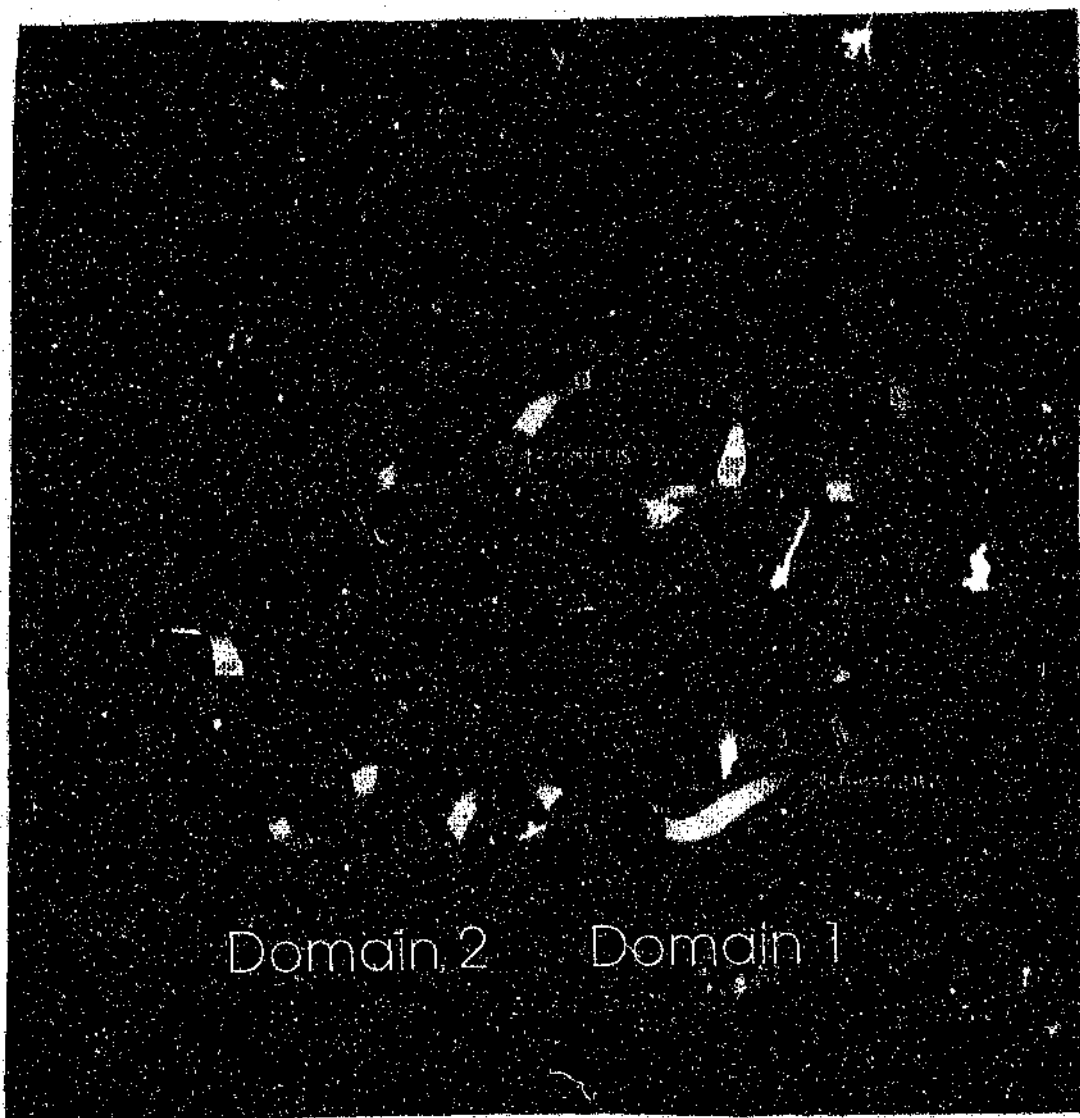


Fig.27 Ribbon representation of subunit backbone structure of W28F mutant hGST P1-1. Model is constructed according to method described in section 2.10. The structure is represented at perpendicular to the crystallographic two-fold axis. The structure is generated by using RASMOL (Sayle and Miller-White., 1995).

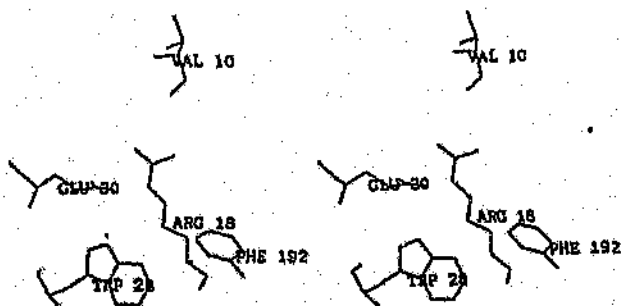
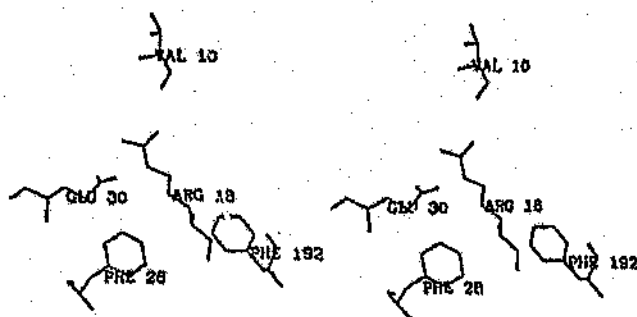
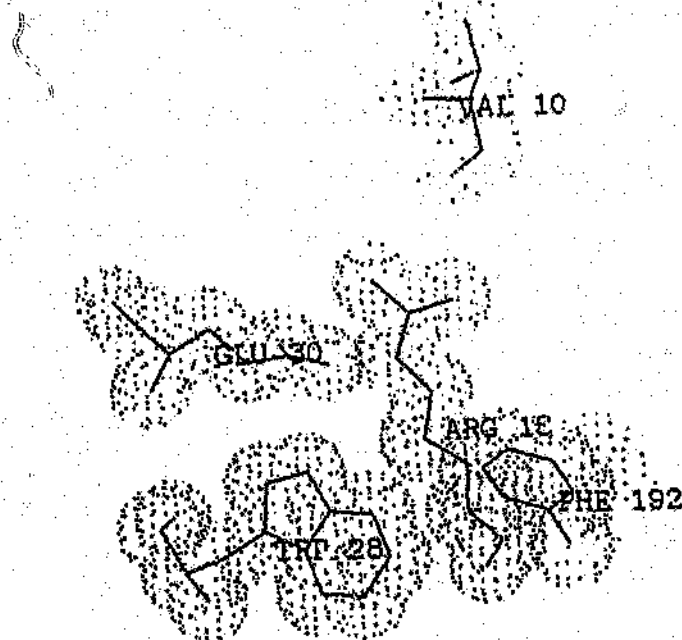
a**b**

Fig.28 Stereoview of the local environment of (a) Trp28 residue of hGST P1-1 (Reinemer et al., 1992) (wild-type) and (b) Phe28 residue of W28F mutant hGST P1-1. Where Val10, Arg18, Phe28(or Trp28) and Phe192 residues are selected because of their involvement in the electrostatic interaction and hydrophobic interaction with Phe 28 or Trp28. Diagrammes are generated by using HYPERCHEM.

a



b

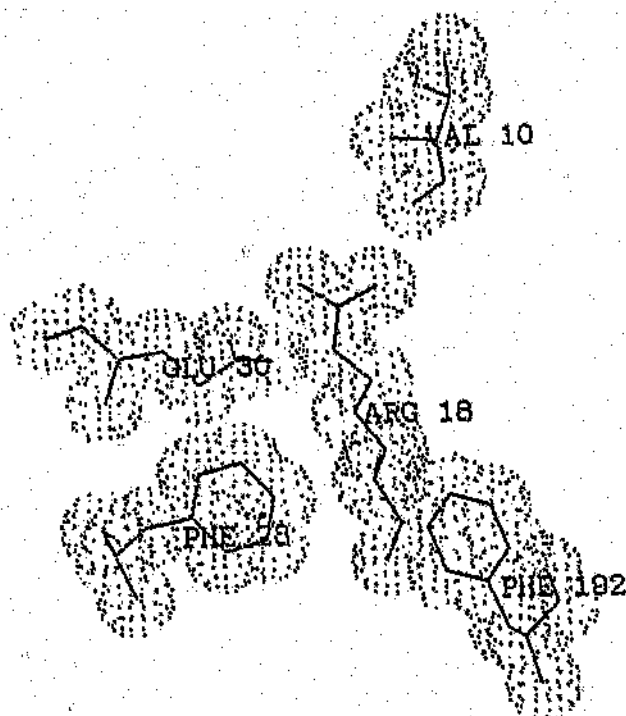


Fig.29 Local environment of (a) wild-type and (b) W28F mutant hGST P1-1 with Val10, Arg18, Trp28, Glu30 and Phe192 selected (Reinemer et al., 1992). Dotted spheres represent the van der Waals surface. Structure is generated using

3.10 Conclusion

The findings of this study show that the evolutionary conserved Trp28 plays an important structural role in maintaining the correct conformation at the H-site and in the stability of hGSTP1-1 structure. The exact structural basis for the destabilization by the Trp28 → Phe is not yet known until the crystal structure of W28F mutant becomes available. In terms of the overall structure and function of the G-site, the mutant protein appears to be correctly folded but with some local distortion at the H-site. Upon inspection of the crystal structure of hGSTP1-1, a Trp28-Glu30-Arg18 triad, which is located in domain 1 below the active site loop (Phe8 to Gly12), was discovered and this was seen to play a role in stabilizing the network of polar interaction in that region. Furthermore, the guanidinium moiety of Arg18 is hydrogen bonded to the carbonyl oxygen in the active-site peptide backbone at a non-polar residue (Val10) in the H-site. Truncation of the Trp28-Glu30 hydrogen bond possibly impacted on the interaction between Glu30-Arg18, thus affecting both the topology at the H-site and the stability of the protein.

Chapter 4

References

- Abbott, W.A., Griffith, O.W. and Meister, A. (1986) γ -glutamyl-glutathione natural occurrence and enzymology, *J.Biol.Chem.* 261, 13657-13661.
- Abola, E., Bernstein, F.C., Bryant, S.H., Koetzle, T.F. and Weng, J. (1987) Protein data bank. In Crystallographic databases-information content, software systems, scientific applications. (Allen, F.H., Bergerhoff, G. and Sievers, R., eds), pp107-132, Commission of the international union of crystallography, Bonn, Cambridge, Chester.
- Adang, A.E.P., Brussee, J., Meyer, D.J., Coles, B., Ketterer, B., Van Der Gen, A. and Mulder, G.J. (1988) Substrate specificity of rat liver glutathione S-transferase isoenzymes for a series of glutathione analogues, modified at the γ -glutamyl moiety, *Biochem.J.* 255, 721-724.
- Adang, A.E.P., Meyer, D.J., Brussee, J., VanDerGen, A., Ketterer, B. and Mulder, G.J. (1989) Interaction of rat glutathione S-transferase 7-7 and 8-8 with γ -glutamyl- or glycyl-modified glutathione analogues, *Biochem.J.* 264, 759-764.
- Adang, A.E.P., Brussee, J., Van Der Gen, A. and Mulder, G.J. (1990) The glutathione - binding site in glutathione S-transferase. Investigation of the cysteinyl glycyl, and γ -glutamyl domains, *Biochem.J.* 269, 47-54.
- Adams, P.A., Goold, R.D. and Mikakana, C.N.T. (1989) Active site solvation contributes significantly to inactivation of the glutathione S-transferase (GST), *Biochem.Pharmacol* 38, 3124-3126.
- Ahmand, F. and Bigelow, C.C. (1982) Estimation of the free energy of stabilization of ribonuclease A, lysozyme, α -lactalbumin and myoglobin, *J.Biol.Chem.* 257, 12935-12940.
- Akerboom, T.P.M., Bilzer, M. and Sies, H. (1982) Competition between transport of glutathione disulfide (GSSG) and glutathione S-conjugate from perfused rat liver into bile, *FEBS Lett.* 140, 73-76.
- Altschul, S.F., Gish, W., Miller, W., Myers, E.W. and Lipman, D.J. (1990) Basic local alignment search tool, *J.Mol.Biol.* 215, 430-410.

- Anders, M.W., and Pohl, L.R. (1985) Bioactivation of foreign compounds, Halogenated alkanes. (Anders, M.W.ed.), pp283-315, Academic Press, New York.
- Armstrong, R.N. (1991) Glutathione S-transferase: reaction mechanism, structure and function, *Chem Toxicol.* 4, 131-140.
- Askelof, P., Guthenberg, C., Jakobson, I. and Marnervik, B. (1975) Purification and characterization of two glutathione S-aryltransferase activities from rat liver, *Biochem. J.* 147, 513-522.
- Baker, R.H., Smith, S.A., Marano, R., McKee, J. and Board, P.G. (1994) Protein expression using cotranslational fusion and cleavage of ubiquitin, *J.Biol.Chem.* 269, 25381-25386.
- Barlow, D.J. and Thornton, J.M. (1983) Ion-pairs in proteins, *J.Mol.Biol.* 168, 867-885.
- Beckett, G.B. and Hayes, J.D. (1993) Glutathione S-transferase: Biomedical applications, *Adv.Clin.Chem.* 30, 281-381.
- Bico, P., Chen, C.Y., Jones, M., Erhardt, J. and Dirr, H.W. (1994) Class Pi glutathione S-transferase : Meisenheimer complex formation, *Biochem.Mol. Biol.Int.* 33, 887-892.
- Blocki, F.A., Logan, M.S.P., Baoli, C. and Wackett, L.P. (1994) Reaction of rat liver glutathione S-transferase and bacterial dichloromethane dehalogenase with dihalomethanes, *J.Biol.Chem.* 269, 8826-8830.
- Board, P.G. (1981a) Transport of glutathione S-conjugate from human erythrocytes, *FEBS Lett.* 124, 163-165
- Board, P.G.(1981b) Biochemical genetics of glutathione S-transferase in man, *Am.J.Hum.Genet.* 33, 36-43.
- Booth, J., Boyland, E. and Sims, P. (1961) An enzyme from rat liver catalysing conjugations with glutathione, *Biochem.J.* 79, 516-524.
- Bordo, D. and Argos, P. (1991) Suggestions for safe residue substitutions in site-directed mutagenesis, *J.Mol.Biol.* 217, 721-729.

- Bowie, J.U. and Saucer, R.T. (1989) Equilibrium dissociation and unfolding of the arc repressor dimer, *Biochemistry*. 28, 7139-7143.
- Boyer, T.D., Vessey, D.A., Holcomb, C. and Saley, N. (1984) Studies of the relationship between the catalytic activity and binding of non-substrate ligands by the glutathione S-transferase, *Biochem.J.* 217, 179-185.
- Boyer, T.D. (1986) Covalent labelling of the nonsubstrate ligand-binding site of glutathione S-transferase with bilirubin-Woodward's reagent K, *J.Biol.Chem.* 261, 5363-5367.
- Boyer, T.D. and Vessey, D.A. (1987) Inhibition of human cationic glutathione S-transferase by non-substrate ligands, *Hepatology*. 7, 843-848.
- Boyer, T.D. (1989) The glutathione S-transferase: An update, *Hepatology*. 9, 486-496.
- Boyland, E. and Chasseaud, L.F. (1969) The role of glutathione and glutathione S-transferase in mercapturic acid biosynthesis, *Adv.Enzymol.Rel.Areas.Mol.Biol.* 32, 173-219.
- Brandits, J.F. (1969) Structure and stability of biological macromolecules. (Timasheff, S. N. and Fasman, G.D., eds), pp213-290, Marcel Dekker, New York.
- Brooks, B.R., Bruccoleri, R.E., Olafson, B.D., States, D.J., Swaminathan, S. and Karplus, M. (1983) A programme for macromolecular energy, minimization and dynamics calculation, *J.Comp.Chem.* 4, 187-217.
- Buetler, T.M. and Eaton, D.L. (1992) Glutathione S-transferase: a amino acid sequence comparison, classification and physiogenetic relationship, *Environ.Carcino.Ecotox.Rev.* C10, 181-203.
- Burstein, E.A., Vedenkina, N.S. and Ivkova, M.N. (1973) Fluorescence and the location of tryptophan residues in protein molecules, *Photochem.photobio.* 18, 263-279.
- Chang, M., Rao, M.K., Rieddeanna, P., Li, C.H., Tu, C.P.D., Lorey, E.J. and Reddy, C.C. (1987a) Specificity of the glutathione S-transferase in the conversion of Leukotriene A4 to C4, *Arch.Biochem.Biophys.* 259, 536-547.

- Chang, M., Hong, Y., Burgess, J.R., Tu, C.P.D. and Reddy, C.C. (1987b) Isozyme specificity of the glutathione S-transferase in the formation of PGF₂ and PGE₂, *Arch.Biochem.Biophys.* 259, 548-557.
- Chang, C., Saltzman, A.G. and Sorensen, N.S. (1987) Identification of glutathione S-transferase Yb₁ mRNA as the androgen-repressed mRNA by cDNA cloning and sequence analysis, *J.Biol.Chem.* 262, 11901-11903.
- Charmichael, J., Forrester, L.M., Lewis, A.D., Hayes, P.C. and Wolf, C.R. (1988) Glutathione S-transferase isozymes and glutathione peroxidase activity in normal and tumour samples from human lung, *Carcinogenesis.* 9, 1617-1621.
- Chen, W.J., Graminski, G.F. and Armstrong, R.N. (1988) Dissection of the catalytic mechanism of isoenzyme 4-4 of glutathione S-transferase with alternative substrates, *Biochemistry.* 27, 647-654.
- Cho, S.I., Zalneraitis, B., Ohmi, N. and Arias, I.M. (1981) Prediction of cadaver kidney function by ligandin analysis, *J.Surg.Res.* 30, 361-364.
- Coles, B. and Ketterer, B. (1990) The role of glutathione and glutathione transferase in chemical carcinogenesis, *CRC.Crit.Rev.Biochem.Mol.Biol.* 25, 47-70.
- Coombs, B. and Stakelum, G.S. (1961) A liver enzyme that conjugate sulphobromophthalein sodium with glutathione, *J.Clin.Invest.* 40, 981-988.
- Creighton, T.E. (1979) Electrophoretic analysis of the unfolding of proteins, *J.Mol.Biol.* 129, 235-264.
- Creighton, T.E. (1986) Detection of folding intermediates using urea-gradient gel electrophoresis, *Methods Enzymol.* 131, 156-172.
- Creighton, T.E. (1990) Protein folding, *Biochem.J.* 270, 1-16.
- Danielson, U.H. and Mannervik, B. (1985) Kinetic independence of the subunits of cytosolic glutathione transferase from the rat, *Biochem.J.* 231, 263-267.
- Danielson, U.H., Esterbauer, H. and Mannervik, B. (1987) Structure-activity relationships of 4-hydroxyalkenals in the conjugation catalysed by mammalian glutathione transferases, *Biochem.J.* 247, 707-713.

- Dao-pin, S., Anderson, D.E., Basse, W.A., Dahlquist, F.W., and Matthews, B.W., (1991) Structural and thermodynamic consequences of burying a charged residue within the hydrophobic core of T4 lysozyme, *Biochemistry*. 30, 11521-11529.
- Deisseroth, A.B. (1993) Current trends and future direction in the genetic therapy of human neoplastic disease, *Cancer*. 72, 2069-2074.
- Di Ilio, C., Del Boccio, G., Aceto, A., Casaccia, R., Mucilli, F. and Federici, G. (1987) Elevation of glutathione transferase activity in human lung tumour, *Carcinogenesis*. 9, 335-340.
- Di Ilio, C., Del Boccio, G., Aceto, A. and Federici, G. (1988) Alteration of glutathione transferase isozyme concentrations in human renal carcinoma, *Carcinogenesis*. 8, 861-864.
- Dill, K.A. (1990) Dominant forces in protein folding, *Biochemistry*. 29, 7133-7155.
- Dirr, H.W., Mann, K., Huber, R., Ladenstein, R. and Reinemer, P. (1991) Class π glutathione S-transferase from pig lung. Purification, biochemical characterization, primary structure and crystallization, *Eur.J.Biochem.* 196, 693-698.
- Dirr, H.W. and Reinemer, P. (1991) Equilibrium unfolding of class π glutathione S-transferase, *Biochem.Biophys.Res.Commun.* 180, 294-300.
- Dirr, H.W., Reinemer, P and Huber, R. (1994a) Refined crystal structure of porcine class Pi glutathione S-transferase (pGSTP1-1) at 2.1 Å resolution, *J.Mol.Biol.* 243, 72-92.
- Dirr, H.W., Reinemer, P. and Huber, R. (1994b) X-ray crystal structures of cytosolic glutathione S-transferase: implications for protein architecture, substrate recognition and catalytic function, *Eur.J.Biochem.* 220, 645-661.
- Dolan, M.E., Pegg, A.E., Dumenco, L.L., Moschel, R.C. and Gerson, S.L. (1991) Comparison of the inactivation of mammalian and bacterial O⁶-alkylguanine-DNA alkyltransferase by O⁶-benzylguanine and O⁶-methylguanine, *Carcinogenesis*. 12, 2305-2309.
- Eftink, M.R. and Ghiron, C.A. (1976) Exposure of tryptophanyl residues in proteins: Quantitative determination by fluorescence quenching studies, *Biochemistry*. 15, 672-680.

- Effink, M.R. and Ghiron, C.A. (1981) Fluorescence quenching studies with proteins, *Anal. Biochem.* 114, 199-227.
- Endicott, J.A. and Ling, V. (1989) The biochemistry of P-glycoprotein-mediated multidrug resistance, *Annu. Rev. Biochem.* 58, 137-171.
- Erhardt, J. and Dirr, H. (1995) Native dimer stabilizes the subunit tertiary structure of porcine class Pi glutathione S-transferase, *Eur. J. Biochem.* 230, 614-620.
- Eriksson, A.E., Baase, W.A. and Matthews, B.W. (1993) Similar hydrophobic replacement of Leu99 and Phe153 within the core of T4 lysozyme have different structural and thermodynamic consequences, *J. Mol. Biol.* 229, 747-769.
- Garcia-Saez, I., Parraga, A., Phillips, M.F., Mantle, T.J. and Col, M (1994) Molecular structure at 1.8 Å of mouse liver class pi glutathione S-transferase complexed with S-(p-Nitrobenzyl)glutathione and other inhibitors, *J. Mol. Biol.* 237, 298-314.
- Gittleman, M.S. and Matthews, C.R. (1990) Folding and stability of trp Aporepressor for *Escherichia coli*, *Biochemistry.* 29, 7011-7020.
- Goldenberg, D.P. and Creighton, T.E. (1984) Review: Gel electrophoresis in studies of protein conformation and folding, *Anal. Biochem.* 138, 1-18.
- Graminski, G.F., Kubo, Y. and Armstrong, R.N. (1989a) Spectroscopic and kinetic evidence for the thiolate anion of glutathione at the active site of glutathione S-transferases, *Biochemistry.* 28, 3562-3568.
- Graminski, G.F., Zhang, P., Sesay, M.A., Ammon, H.L. and Armstrong, R.N. (1989b) Formation of the 1-(S-glutathionyl)-2,4,6-trinitrocycloheadienate anion at the active site of glutathione S-transferase: Evidence for enzymatic stabilization of σ -complex intermediates in nucleophilic aromatic substitution reaction, *Biochemistry.* 28, 6252-6258.
- Greene, R.F. and Pace, C.N. (1974) Urea and guanidine hydrochloride denaturation of ribonuclease, lysozyme, α -chymotrypsin and β -lactoglobulin, *J. Biol. Chem.* 249, 5388-5393.
- Guengerich, F.P. (1991) Reactions and significance of cytochrome P-450 enzymes, *J. Biol. Chem.* 266, 10019-10022.

Gulick, A.M., Goihl, A.L. and Fahl, W.E. (1992) Structural studies on human glutathione S-transferase π : Family of native-specific monoclonal antibodies used to block catalysis, *J. Biol. Chem.* 267, 18946-18952.

Gulick, A.M. and Fahl, W.E. (1995) Mammalian glutathione S-transferase; Regulation of an enzyme system to achieve chemotherapeutic efficiency, *Pharmac. Ther.* 66, 237-257.

Guthenberg, C., Akerfeldt, K. and Mannervik, B. (1979) Purification of glutathione S-transferase from human placenta, *Acta. Chem. Scand. Ser. B* 33, 595-596.

Habig, W.H., Pabst, M.J. and Jacoby, W.B. (1974) Glutathione S-transferase - the first enzymatic step in mercapturic acid formation, *J. Biol. Chem.* 249, 7130-7139.

Habig, W.H. and Jacoby, W.B. (1981) Assays for differentiation of glutathione S-transferase, *Method Enzymol.* 77, 398-405

Harada, S.A., Abei, M., Tanaka, N., Agarwari, D.P. and Goedde, H.W. (1987) Liver glutathione S-transferase polymorphism in Japanese and its pharmacogenetic importance, *Hum. Genet.* 75, 322-325

Hayes, J.D. and Mantle, T.J. (1986) Anomalous electrophoretic behaviour of the glutathione S-transferase Ya and Yk subunits isolated from man and rodents. A potential pitfall for nomenclature, *Biochem. J.* 237, 731-740.

Hayes, J.D. and Wolf, C.R. (1988) Role of glutathione transferase in drug resistance. In glutathione conjugation: mechanisms and biological significance. (Sies, H and Ketterer, B., eds), pp316-356, Academic Press, London.

Hayes, J.D. (1989) Purification and characterization of a polymorphic Yb-containing glutathione S-transferase, GST ψ , from human liver, *Clin. Chem. Enzyme. Commun.* 1, 245-264.

Hayes, J.D. and Wolf, C.R. (1990) Molecular mechanisms of drug resistance, *Biochem. J.* 272, 281-295.

Hayes, P.C., Bouchier, I.A.D. and Beckett, G.J. (1991) Glutathione S-transferase in humans in health and disease, *Gut.* 32, 813-818.

Hebert, H., Schmidt-Krey, I., and Morgenstern, R. (1995) The projection structure of microsomal glutathione transferase, *EMBO. J.* 14, 3864-3869.

- Hiratsuka, A., Sebata, N., Kawashima, K., Okuda, H., Ogura, K., Watabe, T., Satoh, K., Hatayama, I., Tsuchida, S., Ishikawa, T. and Sato, K. (1990) A new class of rat glutathione S-transferase Yrs-Yrs inactivating reactive sulphate ester as metabolites of carcinogenic arylmethanols, *J.Biol.Chem.* 265, 1973-1981.
- Hollecker, M. and Creighton, T.E. (1982) Effect on protein stability of reversing the charge on amino groups, *Biochem.Biophys.Acta.* 701, 395-404.
- Howie, A.F., Forrester, L.M., Glancey, M.J., Schlager, J.J., Powis, G., Beckett, G.J., Hayes, J.D. and Wolf, C.R. (1990) Glutathione S-transferase and glutathione peroxidase expression in normal and tumour human tissues, *Carcinogenesis.* 11, 451-458.
- Huang, X. and Miller, M. (1991) A time-efficient, linear-space local similarity algorithm, *Adv.Appl.Math.* 12, 337-367.
- Huskey, S.E.W., Huskey, W.P and Lu, A.Y.H. (1991) Contribution of thiolate "desolvation" to catalysis by glutathione S-transferase isoenzymes 1-1 and 2-2: evidence from kinetic solvent isotope effects, *J.Am.Chem.Soc.* 113, 2283-2290.
- Hussy, A.J., Hayes, J.D. and Beckett, G.J. (1987) The polymorphic expression of neutral glutathione S-transferase in human mononuclear leucocytes as measured by specific radioimmunoassay, *Biochem.Pharmacol.* 36, 4013-4015.
- Ishigaki, S., Abramovitz, M. and Listowsky, I. (1989) Glutathione S-transferase are major cytosolic thyroid hormone binding proteins, *Arch.Biochem.Biophys.* 273, 265-272.
- Ishikawa, T., Esterbauer, H. and Sies, H. (1986) Role of cardiac glutathione S-transferase and of the glutathione S-conjugate export system in biotransformation of hydroxy-nonenal in the heart, *J.Biol.Chem.* 261, 1576-1581.
- Ishikawa, T. (1989a) Leukotriene C4 inhibits ATP-dependent transport of glutathione S-conjugate across rat heart sarcolemma: Implication for leukotriene C4 translocation mediated by glutathione S-conjugate carrier, *FEBS Lett.* 246, 177-180.
- Ishikawa, T. (1989b) ATP/Mg²⁺-dependent cardiac transport system for glutathione S-conjugates: A study using rat heart sarcolemma vesicles, *J.Biol.Chem.* 264, 17343-17348.

- Ishikawa, T. (1992) The ATP dependent glutathione S-conjugate export pump, *TIBS*. 17, 463-468.
- Ishikawa, T. (1993) Glutathione S-conjugate export pump in Structure and function of glutathione transferase. (Tew, K.D., Pickett, C.B., Mantle, T.K., Mannervik, B., Hayes, J.D., eds), pp211-221, CRC Press, Boca Raton.
- Jackson, S.E. and Fersht, A.R. (1991) Folding of chymotrypsin inhibitor. Evidence for a two-state transition, *Biochemistry*. 30, 10428-10435.
- Ji, X., Zhang, P., Armstrong, R.N. and Gilliland, G.L. (1992) A three-dimensional structure of a glutathione S-transferase from the mu gene class. Structural analysis of the binary complex of isoenzyme 3-3 and glutathione at 2.2 Å resolution, *Biochemistry*. 31, 10169-10184.
- Ji, X., von Rosenvinge, E.C., Johnson, W.W., Tomarev, S.I., Piatigorsky, J., Armstrong, R. and Gilliland, G.L. (1995) Three-dimensional structure, catalytic properties and evolution of a sigma class glutathione S-transferase from squid, a progenitor of the lens S-crystallins of Cephalopods, *Biochemistry*. 34, 5317-5258.
- Kamisaka, K., Habig, W.H., Ketley, J.N., Arias, I.M. and Jakoby, W.B. (1975) Multiple forms of human glutathione S-transferase and their affinity for bilirubin, *Eur.J.Biochem.* 60, 153-161.
- Kando, T., Murao, M. and Taniguchi, N. (1982) Glutathione S-conjugate transport using inside-out vesicle from human erythrocytes, *Eur.J.Biochem.* 125, 551-554.
- Kano, T., Sakai, M., Muramatsu, M. (1987) Structure and expression of a human class glutathione S-transferase messenger RNA, *Cancer Res.* 47, 5726-5730.
- Kaplowitz, N., Percy-Robb, I.W. and Javitt, N.B. (1973) Role of hepatic anion-binding protein in bromosulphthalein conjugation, *J.Exp Med.* 138, 483-487.
- Karshikoff, A., Reinemer, P., Huber, R. and Ladenstein, R. (1993) Electrostatic evidence for the activation of the glutathione thiol by Tyr7 in π class glutathione transferase, *Eur.J.Biochem.* 215, 663-670.
- Kauzmann, W. (1959) Some factors in the interpretation of protein denaturation, *Advan.Protein.Chem.* 14, 1-63.

Kellis, J.T., Nyberg, K., Sali, D. and Fersht, A.R. (1988) Contribution of hydrophobic interactions to protein stability, *Nature*. 333, 784-786.

Kiratsuka, A., Sebata, N., Kawashima, K., Okuda, H., Ogura, K., Watabe, T., Satoh, K., Hatayama, I., Tsuchida, S., Ishikawa, T. and Sato, K. (1990) A new class of rat glutathione S-transferase Yrs-Yrs inactivating reactive sulfate esters as metabolites of carcinogenic arylmethanols, *J.Biol.Chem.* 265, 11973-11981.

Kitamura, T., Jansen, P., Hadenbrook, C., Kamimoto, Y., Gathmaitan, Z. and Arias, I.M. (1990) ATP-dependent bile canalicular transport of organic anions in mutant (TR-) rats with conjugated hyperbilirubinemia, *Proc.Natl.Acad.Sci.U.S.A.* 87, 3557-3561.

Kobayashi, K., Sogame, Y., Hsara, H. and Hayashi, K. (1990) Mechanism of glutathione S-conjugate transport in canalicular and basolateral rat liver membranes, *J.Biol.Chem.* 265, 7737-7739.

Kodate, C., Fukushi, A., Narita, T., Kudo, H., Soma, Y. and Sato, K. (1986) Human placental form of glutathione S-transferase (GST- π) as a new immunohistochemical marker for human colonic carcinoma, *Jpn.J.Cancer.Res.* 77, 226-229.

Kolm, R.H., Sroga, G.E. and Mannervik, B. (1992) Participation of phenolic hydroxyl group of Tyr-8 in the catalytic mechanism of human glutathione transferase P1-1, *Biochem.J.* 285, 537-540.

Kong, K.H., Inoue, H. and Takahashi, K. (1991) Non-essentiality of cysteine and histidine residues for the activity of human class pi glutathione S-transferase, *Biochem.Biophys.Res.Comm.* 18, 748-755.

Kong, K.H., Nishida, M., Inoue, H. and Takahashi, K. (1992a) Tyrosine-7 is an essential residue for the catalytic activity of human class Pi glutathione S-transferase: chemical modification and site-directed mutagenesis studies, *Biochem.Biophys.Res.Comm.* 182, 1122-1129.

Kong, K.H., Takasu, K., Inoue, H. and Takahashi, K. (1992b) Tyrosine 7 in human class Pi glutathione S-transferase is important for lowering the pKa of the thiol group of glutathione in the enzyme-glutathione complex, *Biochem.Biophys.Res.Comm.* 184, 194-197.

- Kong, K.H., Inoue, H. and Takahashi, K. (1992c) Site-directed mutagenesis of amino acid residues involved in the glutathione binding of human glutathione S-transferase P1-1, *J.Biochem.* 112, 725-728.
- Kong, K.H., Inoue, H. and Takahashi, K. (1993) Site-directed mutagenesis study on the roles of evolutionary conserved aspartic acid residues in human glutathione S-transferase P1-1, *Protein Eng.* 6, 93-99.
- Laemmli, U.K. (1970) Cleavage of structural proteins during the assembly of the head of bacteriophage T4, *Nature.* 227, 680-685.
- Lakowicz, J.R. (1983) Principle of fluorescence spectroscopy. Plenum Press, New York.
- Lee, C. (1996) Testing homology modelling on mutant proteins: predicting structural and thermodynamic effects in the Ala98-Val mutants of T4 lysozyme, *Folding and Design.* 1, 1-12.
- Lehrer, S. (1971) Solute perturbation of protein fluorescence. The quenching of the tryptophyl fluorescence of model compounds and lysozyme by Iodide ion, *Biochemistry.* 10, 3254-3263.
- Lewis, A.D., Forrester, L.M., Hayes, J.D., Warding, C.J., Carmichael, J., Harris, A.L., Mooghen, M. and Wolf, C.R. (1989) Glutathione S-transferase isozymes in human tumours and tumour derived cell lines, *Br.J.Cancer.* 60, 327-312.
- Listowsky, I., Abramovitz, M., Homma, H. and Niitsu, Y. (1988) Intracellular binding and transport of hormones and xenobiotics by glutathione S-transferases, *Drug Metabolism Rev.* 19 (3&4), 305-318.
- Listowsky, I. (1993) Glutathione S-transferase. Intracellular binding, dextoxification and adaptive responses. Hepatic transport and bile secretion: physiology and pathophysiology. (Tavolon, N. and Berk, P., eds), vol.26, pp397-405, Raven Press, New York.
- Liu, S., Zhang, P., Ji, X., Johnson, W.W., Gilliland, G.L. and Armstrong, R.N. (1992) Contribution of tyrosine 6 to the catalytic mechanism of isoenzyme 3-3 of glutathione S-transferase, *J.Biol.Chem.* 267, 4296-4299.
- Luthy, R., Bowie, J.U. and Eisenberg, D. (1992) Assessment of protein models with three-dimensional profiles, *Nature.* 356, 83-85.

Mann, C.J., Royer, C.A. and Matthews, C.R. (1993) Tryptophan replacements in the trp aporepressor from *E. coli*. Probing the equilibrium and kinetic folding models, *Protein Sci.* 2, 1853-1861.

Mannervik, B. and Guthenberg, C. (1981) Glutathione transferase (human placenta). *Methods Enzymol.* 77, 231-235.

Mannervik, B., Alin, P., Guthenberg, C., Jansson, H., Tahir, M.K., Warholm, M. and Jornvall, H. (1985) Identification of three classes of cytosolic glutathione transferase common to several mammalian species: correlation between structural data and enzymatic properties, *Proc. Nat. Acad. Sci. U.S.A.* 82, 7202-7206.

Mannervik, B. (1985) The isoenzymes of glutathione transferase, *Adv. Enzymol.* 57, 357-417.

Mannervik, B. and Danielson, U.H. (1986) Glutathione transferase: structure and catalytic activity, *CRC Crit. Rev. Biochem. Mol. Biol.* 23, 283-337.

Mannervik, B., Awasthi, Y.C., Board, P.G., Hayes, J.D., Di Ilio, C., Ketterer, B., Listowsky, I., Morgenstern, R., Muramatsu, M., Pearson, W.R., Pickett, C.B., Sato, K., Widersten, W. and Wolf, C.R. (1992) Nomenclature for human glutathione transferase, *Biochem. J.* 282, 305-308.

Manoharan, T.H., Gluick, A.M., Reinemer, P., Dirr, H.W., Huber, R. and Fahl, W.E. (1992a) Mutational substitution of residues implicated by crystal structure in binding the substrate glutathione to human glutathione S-transferase π , *J. Mol. Biol.* 226, 319-322.

Manoharan, T.H., Gluick, A.M., Puchalski, R.B., Servais, A.L., Fahl, W.E. (1992b) Structural studies on human glutathione S-transferase π : Substitution mutations to determine amino acids necessary for binding glutathione, *J. Biol. Chem.* 267, 18940-18945.

Matthews, B.W. (1987) Genetic and structural analysis of the protein stability problem, *Biochemistry.* 26, 6888-6891.

McLellan, L.I. and Hayes, J.D. (1987) Sex-specific constitutive expression of the pre-neoplastic marker glutathione S-transferase, YfYf, in mouse liver, *Biochem. J.* 245, 339-406.

McTigue, M.A., Williams, D.R. and Tainer, J.A. (1995) Crystal structure of a schistosomal drug and vaccine target: Glutathione S-transferase from *Schistosoma japonica* and its complex with the leading antischistosomal drug praziquantel, *J.Mol.Biol.* 246, 21-27.

Meyer, D.J., Coles, B., Pemble, S.E., Gilmore, K.S., Graser, G.M. and Ketterer B. (1991) Theta, a new class of glutathione transferase purified from rat and human, *Biochem.J.* 274, 409-414.

Moorghen, M., Cairns, J., Forrester, L.M., Hayes, J.D., Hall, A., Cattan, A.R., Wolf, C.R. and Harris, A.L. (1991) Enhanced expression of glutathione S-transferase in colorectal carcinoma compared to non-neoplastic mucosa, *Carcinogenesis*. 12, 13-17.

Morgenstern, R. and DePierre, J.W. (1988) Membrane bound glutathione transferase. In: Glutathione conjugations. Mechanisms and biological significance. (Sies, H. and Ketterer, B., eds), pp157-174, Academic Press, London.

Myers, J.K., Pace, C.N. and Scholtz, J.M. (1995) Denaturant m values and heat capacity changes: Relation to changes in accessible surface areas of protein unfolding, *Protein.Sci.* 4, 2138-2148.

Neet, K.E. and Timm, D.E. (1994) Conformational stability of dimeric proteins: Quantitative studies by equilibrium denaturation, *Protein.Sci.* 3, 2167-2174.

Nishihira, J., Ishibashi, T., Sakai, M., Nishi, S., Kondo, H. and Makita, A. (1992) Identification of the fatty acid binding site on glutathione S-transferase P, *Biochem. Biophys.Res.Commun.* 189, 197-215.

Pabst, M.J., Habig, W.H. and Jakoby, W.B. (1973) Mercapturic acid formation: The several glutathione transferase of rat liver, *Biochem.Biophys.Res.Commun.* 52, 1123-1128.

Pace, C.N. (1986) Determination and analysis of urea and guanidine hydrochloride denaturation curves, *Methods Enzymol.* 131, 266-280.

Parker, C.A. and Rees, W.T. (1960) Correction of fluorescence spectra and measurement of fluorescence quantum efficiency, *Analyst.* 85, 587-600.

Pearson, W.R. and Lipman, D.J. (1988) Improved tools for biological sequence comparison, *Proc.Natl.Acad.Sci.U.S.A.* 85, 2444-2448.

- Peitsch, M.C. (1995) Protein modelling by E-mail, *Bio/Technology*. 13, 658-660.
- Peitsch, M.C. (1996) ProMod and Swiss-Mode: Internet-based tools for automated comparative protein modelling, *Biochem Soc Trans.* 24, 274-279.
- Penington, C.J. and Rule, J.S. (1992) Mapping the substrate-binding site of a human class Mu glutathione transferase using nuclear magnetic resonance spectroscopy, *Biochemistry*. 31, 2912-2920.
- Pemble, S.E., Taylor, J.B. and Ketterer, B. (1986) Tissue distribution of rat glutathione transferase subunit 7, a hepatoma marker, *Biochem.J.* 240, 885-889.
- Pemble, S.E. and Taylor, J.B. (1992) An evolutionary perspective on glutathione transferase inferred from class-Theta glutathione transferase cDNA sequences, *Biochem.J.* 287, 957-963.
- Perkin, S.J. (1986) Protein volumes and hydration effects: The calculation of partial specific volumes, neutron scattering match point and 280-nm absorption coefficients for proteins and glycoproteins from amino acid sequences, *Eur.J.Biochem.* 157, 169-180.
- Pickett, C.B. and Lu, A.Y.H. (1989) Glutathione S-transferase: gene structure, regulation and biological function, *Annu.Rev.Biochem.* 58, 743-764.
- Pickett, S.D. and Sternberg, M.J.E. (1993) Empirical scale of side-chain conformational entropy in protein folding, *J.Mol.Biol.* 231, 825-839.
- Porter, T.D. and Coon, M.J. (1991) Cytochrome P-450. Multiplicity of isoforms, substrates, and catalytic and regulatory mechanisms, *J.Biol.Chem.* 266, 13469-13472.
- Raghunathan, S., Chandross, R.J., Kretsinger, R.H., Allison, T.J., Penington, C.J. and Rules, G.S. (1994) Crystal structure of human class mu glutathione transferase GSTM2-2. Effects of lattice packing on conformational heterogeneity, *J.Mol.Biol.* 238, 815-832.
- Reinemer, P., Dirr, H.W., Ladenstein, R., Schaffer, J., Gallay, O. and Huber, R. (1991) The three-dimensional structure of class π glutathione S-transferase in complex with glutathione sulphonate at 2.3 Å resolution, *EMBO.J.* 10, 1997-2005.

Reinerner, P., Dirr, H.W., Ladenstein, R., Huber, R., Lo Bello, M., Federici, G. and Parker, M.W. (1992) Three-dimensional structure of class π glutathione S-transferase from human placenta in complex with S-hexylglutathione at 2.8 Å resolution, *J.Mol.Biol.* 227, 214-226.

Reinerner, P., Prade, L., Hof, P., Neufeind, T., Huber, R., Zettl, R., Palme, K., Schell, J., Koelln, I., Bartunik, H.D. and Bieseler, B. (1996) Three-dimensional structure of glutathione S-transferase from *Arabidopsis thaliana* at 2.2 Å resolution: Structural characterization of herbicide-conjugating plant glutathione S-transferase and a novel active site architecture, *J.Mol.Biol.* 255, 289-309.

Ricci, G., Bello, M.L., Caccuri, A.M., Pastore, A., Nuccetelli, M., Parker, M., and Federici, G. (1995) Site-directed mutagenesis of human glutathione transferase P1-1, *J.Biol.Chem.* 270, 1243-1248.

Roberts, D.D., Lewis, S.D., Ballou, D.P., Olson, S.T. and Shafer, J.A. (1986) Reactivity of small thiolate anion and cysteine-25 in papain toward methylmethanethiosulphonate, *Biochemistry.* 25, 5595-5601.

Sali, A. and Blundell, T.L. (1994) Comparative protein modelling by satisfaction of spatial restraints. In Protein Structure by Distance analysis. (Bohr, H. and Brunak, S., eds), pp64-86, IOS Press, Amsterdam.

Sali, A. (1995) Modelling mutations and homologous proteins, *Curr.Op.in Biotech.* 6, 437-451.

Samuelsson, B., Dahlen, S.E., Lindgren, J.A., Rouzer, C.A. and Serhan, C.N. (1987) Leukotrienes and lipoxins: Structure, biosynthesis and biological effects, *Science.* 237, 1171-1175

Sandberg, W.S., and Terwilliger, T.C. (1989) Influence of interior packing and hydrophobicity on the stability of a protein, *Science.* 245, 54-57.

Sayle, R. and Miller-White, J. (1995) Rasmol: " Biomolecular graphics for all", *TIBS.* 20, 333-379.

Schaffer, J., Gallay, O. and Ladenstein, R. (1988) Glutathione transferase from bovine placenta. Preparation, biochemical characterization, crystallization and preliminary crystallographic analysis of a neutral class π enzymes, *J.Biol.Chem.* 263, 17405-17411.

- Schellman, J.A. (1978) Solvent denaturation, *Biopolymers*. 17, 1305 - 1322.
- Scholtz, R., Wackett, L.P., Egli, C., Cook, A.M. and Leisinger, T. (1988) Dichloromethane dehalogenase with improved catalytic activity isolated from a fast-flowing dichloromethane-utilizing bacterium, *J.Bacteriol.* 170, 5698-5704.
- Seidegard, J., Pero, R.W., Miller, D.G and Beattie, E.J. (1986) A glutathione transferase in human leukocytes as a marker for the susceptibility to lung cancer, *Carcinogenesis*. 7, 751-753.
- Seidegard, J., Vorachek, W.R., Pero, R.W. and Pearson, W.R. (1988) Hereditary differences in the expression of the human glutathione transferase active on trans-stilbene oxide are due to a gene deletion, *Pro.Natl.Acad.Sci.U.S.A.* 85, 7293-7297.
- Seidegard, J., Pero, R.W., Markowitz, M.M., Roush, G., Miller, D.G. and Beattie, E.J. (1990) Isoenzymes(s) of glutathione transferase (class Mu) as a marker for the susceptibility to lung cancer: A follow up study, *Carcinogenesis*. 11, 33-36.
- Shea, T.C., Kelley, S.L. and Jenner, W.D. (1988) Identification of an anionic form of glutathione transferase present in many human tumours and human tumour cell lines, *Cancer Res.* 48, 527-533.
- Shiratori, Y., Soma, Y., Maruyama, H., Sato, S., Takano, A. and Sato, K. (1987) Immunohistochemical detection of the placental form of glutathione S-transferase in dysplastic and neoplastic human uterine cervix lesions, *Cancer.Res.* 47, 6806-6809.
- Shirley, B.A., Stanssens, P., Hahn, U. and Pace, C.N. (1992) Contribution of hydrogen bonding to the conformational stability of ribonuclease T1, *Biochemistry*. 31, 725-732.
- Simons, P.C. and Van der Jagt, D.L. (1977) Purification of glutathione S-transferase from human liver by glutathione-affinity chromatography, *Anal.Biochem.* 82, 334-341.
- Singh, S. V., Kurosky, A. and Awasthi, Y.C. (1987) Human liver glutathione S-transferase ψ . Chemical characterisation and secondary structure comparison with other mammalian glutathione S-transferase, *Biochem. J.* 243, 61-67.
- Sinning, I., Kleywegt, G.J., Cowan, S.W., Reizemer, P., Dirr, H.W., Huber, R., Gilliland, G.L., Armstrong, R.N., Ji, X., Board, P.G., Olin, B., Mannervik B. and Jones, T.A. (1993) Structure determination and refinement of human alpha class

glutathione S-transferase A1-1, and a comparison with the mu and pi class enzymes, *J.Mol.Biol.* 232, 192-212.

Sluis-Cremer, N. and Dirr, H. (1995) Conformational stability of Cys⁴⁵-alkylated and hydrogen peroxide-oxidised glutathione S-transferase, *FEBS Lett.* 371, 94-98.

Soma, Y., Satoh, K. and Sato, K. (1986) Purification and subunit-structural and immunological characterization of five glutathione S-transferase in human liver and the acid form as a hepatic tumour marker, *J.Biol.Chem.* 258, 11321-11325.

Sorrentino, B.P., Brandt, S.J., Bodine, D., Gottesman, M., Pastan, I., Cline, A., and Nienhuis, A.W. (1992) Selection of drug-resistant bone marrow cells in vivo after retroviral transfer of human MDR1, *Science.* 257, 99-103.

Soutar, A.K. and Wade, D.P. (1990) Ligand binding. Protein function: a practical approach. (Creighton, T.E.ed), pp66-69, IRL Press, Oxford, England.

Srinivasan, N. and Blundell, T.L. (1993) An evaluation of the performance of an automated procedure for comparative modelling of protein tertiary structure, *Protein.Eng.* 6, 501-512.

Stenberg, G., Board, P.G. and Mannervik, B. (1991) Mutation of an evolutionary conserved tyrosine residue in the active site of a human class alpha glutathione transferase, *FEBS Lett.* 293, 153-155.

Stockman, P.K., Beckett, G.J. and Hayes, J.D. (1985) Identification of a basic hybrid glutathione S-transferase from human liver. Glutathione S-transferase δ is composed of two distinct subunits (B₁ and B₂), *Biochem.J.* 227, 457-465.

Stockman, P.K., McLellan, L.I. and Hayes, J.D. (1987) Characterization of the basic glutathione S-transferase B₁ and B₂ subunits from human liver, *Biochem.J.* 244, 55-61.

Strange, R.C., Faulder, C.G., Davis, B.A., Hume, R., Brown, J.A.H., Cotton, W. and Hopkinson, D.A. (1984) The human glutathione S-transferase: Studies on the tissue distribution and genetic variation of the GST1, GST2 and GST3 isozymes, *Ann.Hum.Genet.* 48, 11-20.

Strange, R.C., Matharoo, B., Faulder, G.C., Jones, P., Cotton, W., Elder, J.B. and Deakin, M. (1991) The human glutathione S-transferase: A case-control study of the incidence of the GST 1-0 phenotype in patients with adenocarcinoma,

Carcinogenesis. 12, 25-28.

Suguoka, Y., Kano, T., Okuda, A., Sakai, M., Kitagawa, T. and Muramatsu, M. (1985) Cloning and the nucleotide sequence of rat glutathione S-transferase P cDNA, *Nucleic Acids Res.* 13, 6049-6057.

Tamai, K., Shen, H., Tsuchida, S., Hatayama, I., Satoh, K., Yasui, A., Oikawa, A., Sato, K. (1991) Role of cysteine residues in the activity of rat glutathione transferase P(7-7): elucidation by oligonucleotide site-directed mutagenesis, *Biochem. Biophys. Res. Commun.* 179, 790-797.

Thomson, J.A., Shirley, B.A., Grimsley, G.R. and Pace, C.N. (1989) Conformational stability and mechanism of folding of ribonuclease T1, *J. Biol. Chem.* 264, 11614-11620.

Timm, D.E. and Neet, K.E. (1992) Equilibrium denaturation studies of mouse β -nerve growth factor, *Protein. Sci.* 1, 236-244.

Timm, D.E., De Haseth, P.L. and Neet, K.E. (1994) Comparative equilibrium denaturation studies of the neurotrophins: Nerve growth factor, brain-derived neurotrophic factor, neurotrophin 3 and neurotrophin 4/5, *Biochemistry*. 33, 4667-4676.

Tipping, E. and Ketterer, B. (1981) The influence of soluble binding proteins on lipophile transport and metabolism in hepatocytes, *Biochem. J.* 195, 441-452.

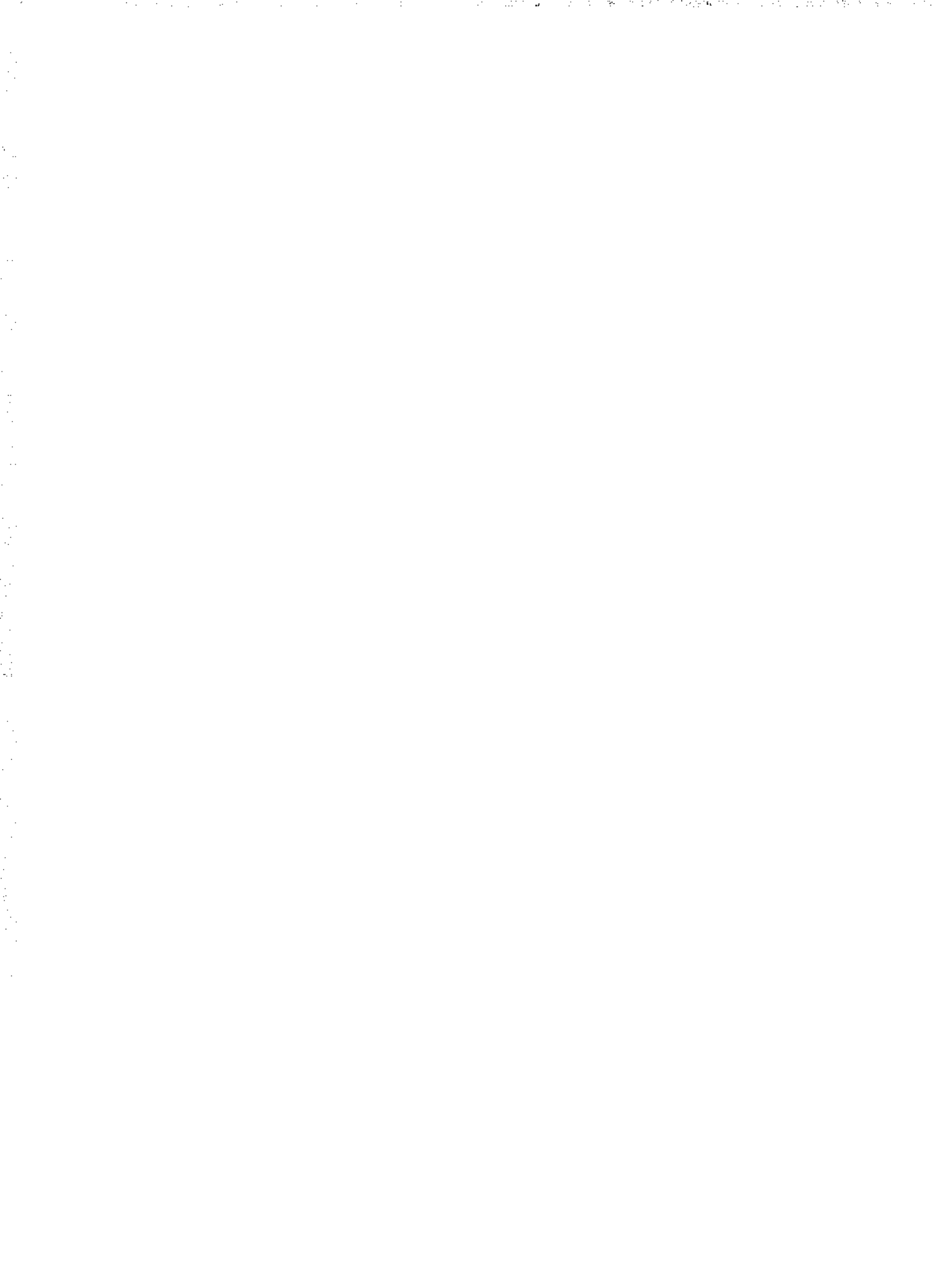
Tsuchida, S. and Sato, K. (1992) Glutathione transferase and cancer, *CRC Review in Biochem. Mol. Biol.* 27(4,5), 337-384.

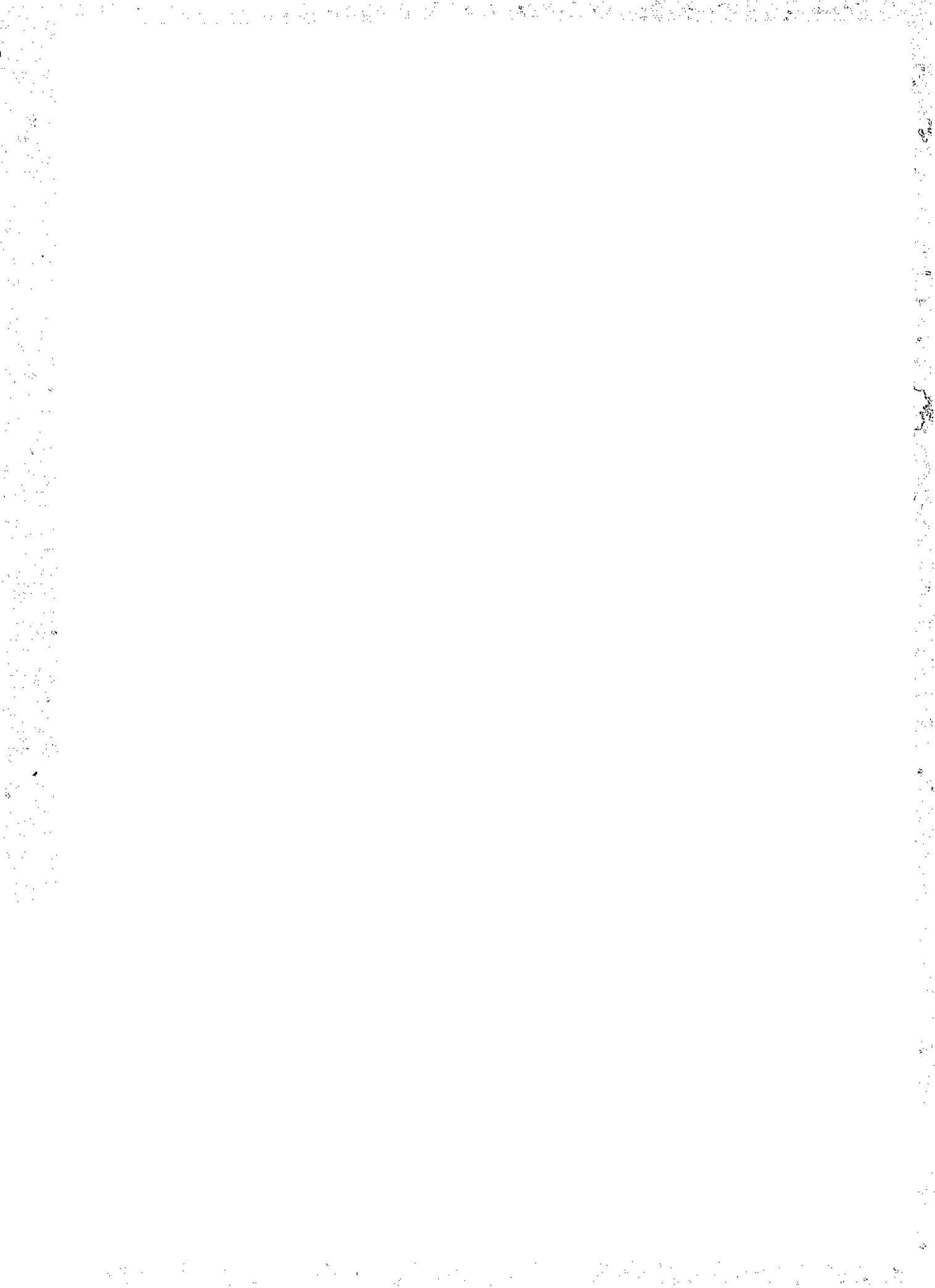
Van der Jagt, D.L., Wilson, S.P., Dean, V.L. and Simons, P.C. (1982) Bilirubin binding to rat liver ligandin (glutathione S-transferase A and B), *J. Biol. Chem.* 257, 1997-2001.

Vessey, D.A. and Boyer, T.D. (1984) Differential activation and inhibition of different forms of rat liver glutathione S-transferase by the herbicides 2,4-dichloro phenoxyacetate (2,4-D) and 2,4,5-trichlorophenoxyacetate (2,4,5-T), *Toxicol. Appl. Pharmacol.* 73, 492-499.

Vessey, D.A. and Boyer, T.D. (1988) Characterization of the activation of rat liver glutathione S-transferase by phenoxyherbicides, *Toxicol. Appl. Pharmacol.* 93, 275-280.

- Wackett, L.P., Logan, M.S.P., Blocki, F.A. and Bao-li, C. (1992) A mechanistic perspective on bacterial metabolism of chlorinated methanes, *Biodegradation*, 3, 19-36.
- Wackett, L.P. (1994) Dehalogenation in environmental biotechnology, *Curr.Op.in Biotech.* 5, 260-265.
- Walker, J., Crowley, P., Moreman, A.D. and Barrett, J. (1993) Biochemical-properties of cloned glutathione S-transferase from *Schistosoma Mansoni* and *Schistosoma Japonicum*, *Mol.Biochem.Parasit.* 61, 255-264.
- Wang, R.W., Newton, D.J., Huskey, S.E., McKeever, B.M., Pickett, C.B. and Lu, A.Y.H. (1992) Site-directed mutagenesis of glutathione S-transferase YaYa. Important roles of tyrosine 9 and aspartic acid 101 in catalysis, *J.Biol.Chem.* 267, 19866-19871.
- Warholm, M., Guthenberg, C., Mannervik, B. and von Bahr, C. (1980) Purification of a new glutathione S-transferase (transferase μ) from human liver having a high activity with benzoapyrene-4,5-oxide, *Biochem.Biophys.Res.Comm.* 98, 512-519.
- Widersten, M. Kolm, R.H., Bjornestedt, R. and Mannervik, B. (1992) Contribution of five amino acid residues in the glutathione-binding site to the function of human glutathione S-transferase P1-1, *Biochem.J.* 285, 377-381.
- Wilce, M.C.J. and Parker, M.W. (1994) Structural and function of glutathione S-transferase, *Biochem Biophys Acta.* 1205, 1-18.
- Wilce, M.C.J., Board, P.G., Feil, S.C. and Parker, M.W. (1995) Crystal structure of a theta-class glutathione transferase, *EMBO.J.* 14, 2133-2143.
- Zimniak, M., Nanduri, B., Pikula, S., Bandorowicz-Pikula, J., Singhal, S.S., Srivastava, K., Awasthi, S and Awasthi, Y.C. (1994) Naturally occurring human glutathione S-transferase GST P1-1 isoforms with isoleucine and valine in position 104 differ in enzyme properties, *Eur.J. Biochem.* 224, 893-899.





Author: Chen Chien Yu.

Name of thesis: Biochemical analysis of the W28F mutant of human class Pi glutathione S-transferase.

PUBLISHER:

University of the Witwatersrand, Johannesburg

©2015

LEGALNOTICES:

Copyright Notice: All materials on the University of the Witwatersrand, Johannesburg Library website are protected by South African copyright law and may not be distributed, transmitted, displayed or otherwise published in any format, without the prior written permission of the copyright owner.

Disclaimer and Terms of Use: Provided that you maintain all copyright and other notices contained therein, you may download material (one machine readable copy and one print copy per page) for your personal and/or educational non-commercial use only.

The University of the Witwatersrand, Johannesburg, is not responsible for any errors or omissions and excludes any and all liability for any errors in or omissions from the information on the Library website.